

UNIVERSIDADE FEDERAL FLUMINENSE
INSTITUTO DE GEOCIÊNCIAS
DEPARTAMENTO DE GEOLOGIA E GEOFÍSICA
PROGRAMA DE PÓS-GRADUAÇÃO EM DINÂMICA DOS OCEANOS E DA TERRA

DANILO JOTTA ARIZA FERREIRA

**ADVANCED TECHNIQUES FOR 3D RESERVOIR
CHARACTERIZATION: MODELS FOR THE BUZIOS FIELD,
SANTOS BASIN**

NITERÓI
2022

DANILO JOTTA ARIZA FERREIRA

ADVANCED TECHNIQUES FOR 3D RESERVOIR
CHARACTERIZATION: MODELS FOR THE BUZIOS FIELD,
SANTOS BASIN

Thesis submitted to the Programa de Pós-Graduação em Dinâmica dos Oceanos e da Terra of Universidade Federal Fluminense in partial fulfillment of the requirements for the degree of Doctor in Science - Geology and Geophysics.

Advisor: Prof. Dr. Wagner Moreira Lupinacci

NITERÓI - RJ
2022

Ficha catalográfica automática - SDC/BIG
Gerada com informações fornecidas pelo autor

F383a Ferreira, Danilo Jotta Ariza
Advanced Techniques for 3D Reservoir Characterization:
Models for the Buios Field, Santos Basin / Danilo Jotta Ariza
Ferreira ; Wagner Moreira Lupinacci, orientador. Niterói,
2022.
115 f. : il.

Tese (doutorado)-Universidade Federal Fluminense, Niterói,
2022.

DOI: <http://dx.doi.org/10.22409/PPGDOT.2022.d.14382625742>

1. Presalt carbonates. 2. 3D reservoir characterization. 3.
Machine Learning. 4. 4D sedimentary modeling. 5. Produção
intelectual. I. Lupinacci, Wagner Moreira, orientador. II.
Universidade Federal Fluminense. Instituto de Geociências.
III. Título.

CDD -

ADVANCED TECHNIQUES FOR 3D RESERVOIR
CHARACTERIZATION: MODELS FOR THE BUZIOS FIELD,
SANTOS BASIN

DANILO JOTTA ARIZA FERREIRA

Thesis submitted to the Programa de Pós-Graduação em Dinâmica dos Oceanos e da Terra of Universidade Federal Fluminense in partial fulfillment of the requirements for the degree of Doctor in Science - Geology and Geophysics.

Approved by the Committee on January 26, 2022.

Committee:

Ph.D. Antonio Fernando Menezes Freire (GIECAR/GGO/UFF and INCT-GP)

Ph.D. João Paulo Rodrigues Zambrini (Emerson)

Ph.D. Karen Maria Leopoldino Oliveira (UFC)

Ph.D. Leonardo Márcio Teixeira da Silva (Petrobras)

Ph.D. Marcílio Castro de Matos (SISMO)

Ph.D. Wagner Moreira Lupinacci - Orientador (GIECAR/GGO /UFF and INCT-GP)

Acknowledgments

I dedicate this thesis to my late aunt Katia Ariza Ferreira who was my aunt, my friend and my second mother. I know you are enlightening us, guiding us and sending us love at all times. The acknowledgments that I make here will be eternally incomplete considering the countless help I received throughout my academic life until this achievement. These acknowledgments are not limited only to the professional help, but mainly the psychological, spiritual and motivational help that brought me here. I thank God and all Spirituality for having constantly supported me throughout my career and for always being on my side in this daily fight that we call life and in the evolutionary process of our Souls. To my husband, companion, best friend, Dr. Jonathan Gonçalves de Oliveira for the countless advices, reviews, suggestions during this academic period, for the daily coexistence, affection, and Love. I hope you never forget your eternal contributions to my personal and professional life. To my beloved parents Mirtes Jotta Ferreira and Márcio Ariza Ferreira, my brother Vitor Jotta Ferreira, my grandparents Marly Ariza Ferreira and Luiza Jotta dos Anjos and my aunt Maristela Jotta Vaz who always created ways to support and motivate me, even when daily socializing was not possible. This thesis would be possible without them. To my advisor, Prof. Dr. Wagner Moreira Lupinacci, who has always provided me with invaluable knowledge, advice, guidance, and opportunities in my academic and professional life. May you be responsible for enlightening the careers of many other geoscience professionals throughout your life. They will be lucky to have your guidance. To my friends, especially Thais Mallet, Henrique Dutra, Marcelo Alvarenga, José Caparica, Julio Kosaka, Raquel Macedo, Suelen Gouvea, Alessandra Peçanha, Lidia Calonio, Lívia Spagnuolo, Ingra Martins, Igor Neves, Carla Barros, Rafaella Reis, Brenno Barros, Brunno Barros, Reginaldo Reis and Eloá Barros, among many others who shared this journey with me, especially during the difficult times we have been through in the last two years of the pandemic. To the members of the committee for accepting the invitation to participate in this very special moment for me and for evaluating this thesis. To the companies ANP and Schlumberger for having given me the opportunity to carry out this study and publish papers related to it, making the data available and providing access to its entire educational resources. To CAPES, CNPq and National Institute of Science and Technology of Petroleum Geophysics (INCT-GP) for providing all the funding that makes all research in this country possible. Long live the democratization of education! It is the only possible future. To the Universidade Federal Fluminense and the Universidade do Estado do Rio de Janeiro, places where I had the privilege of studying to become the researcher and professional I am today.

Abstract

This thesis aims to build workflows using innovative 3D reservoir characterization techniques that have the capacity of provide robust, automatized, and with fair predictability lithological facies and petrophysical properties models from well data and secondary data can honor the heterogeneities for complex reservoirs, such as the presalt Aptian carbonates in the Brazilian marginal basins. First, I applied for the first-time an integrated approach between 4D sedimentary modeling and geostatistical modeling for facies reconstruction for presalt reservoirs from Barra Velha Formation within the Buzios Field located in the Santos Basin. The results from this first study demonstrate that this methodology makes it possible for the geomodeler to incorporate its conceptual geological knowledge about the facies paleoenvironment to be modeled in a more precise manner and the integration with geostatistics allows proper matching of the facies model with well data. For the second study, I used of a neural network algorithm for a multi-attribute unsupervised seismic facies classification. My results from this study showed that this technique allows the automatized creation of a 3D seismic facies model that can be further associated with the porosity and permeability distributions from well data for a qualitative inference of the reservoir properties. The third study present in this thesis approaches also for the first-time the use of a pre-commercial and innovative machine learning methodology that implements geostatistical concepts for supervised estimation of petrophysical reservoir properties from multiple secondary variables called EMBER. The results from this study allowed the quantitative evaluation of the reservoirs from Barra Velha Formation through the creation of effective porosity and permeability 3D models also helping to address the uncertainties related to effective porosity distribution. Before this research, two of those methodologies had never been applied for carbonate rocks characterization or presalt Aptian reservoir modeling. Finally, I hope that those standardized methodologies and the results discussions from this thesis can help the presalt studies to build a better understanding of these reservoirs origins diminishing complexity and provide alternatives for the classical reservoir characterization approaches which not always can properly provide robust results impacting the future of oil and gas exploration and production.

Keywords: Presalt carbonates, 3D reservoir characterization, Machine Learning, 4D Sedimentary Modeling.

Resumo

Esta tese tem como objetivo construir fluxos de trabalho usando técnicas inovadoras de caracterização de reservatórios 3D que tenham a capacidade de fornecer modelos de fácies e propriedades petrofísicas robustos, automatizados e com previsibilidade razoável a partir de dados de poços e dados secundários, honrando as heterogeneidades de reservatórios complexos como os carbonatos Aptianos do pré-sal brasileiro. Inicialmente neste trabalho, foi aplicada pela primeira vez uma abordagem integrada entre modelagem sedimentar 4D e modelagem geoestatística para a reconstrução de fácies para reservatórios de pré-sal da Formação Barra Velha do Campo de Búzios localizado na Bacia de Santos. Os resultados deste estudo demonstraram que esta metodologia possibilita a incorporação do conhecimento geológico conceitual paleoambiental as fácies a serem modeladas de forma precisa e sua integração com a geoestatística para correspondência adequada do modelo com dados de poços. No segundo estudo, foi utilizado um algoritmo de rede neural para classificação de sismofácies multiatributos não-supervisionada para a mesma área. Os resultados deste trabalho mostraram que esta técnica permite a criação automatizada de um modelo de sismofácies 3D que pode ser posteriormente associado as porosidade e permeabilidade de perfis de poços para uma inferência qualitativa das propriedades do reservatório. O terceiro estudo presente nesta tese, também pela primeira vez publicado, aborda o uso de uma metodologia pré-comercial e inovadora de aprendizado de máquina que implementa conceitos geoestatísticos para estimativa supervisionada de propriedades de reservatórios petrofísicos a partir de múltiplas variáveis secundárias denominada EMBER. Os resultados deste estudo permitiram a avaliação quantitativa dos reservatórios da Formação Barra Velha através da criação de modelos 3D de porosidade efetiva e permeabilidade e auxiliando na avaliação das incertezas relacionadas à distribuição efetiva da porosidade. Antes desta tese, duas dessas metodologias nunca haviam sido aplicadas para caracterização de rochas carbonáticas ou modelagem de reservatórios Aptianos do pré-sal. Finalmente, espera-se que essas metodologias padronizadas e as discussões dos resultados desta tese possam ajudar na construção de um melhor entendimento das origens desses reservatórios, reduzindo a complexidade e fornecendo alternativas para as abordagens clássicas de caracterização de reservatórios que nem sempre podem fornecer resultados robustos impactando no futuro da exploração e produção de petróleo e gás.

Keywords: carbonatos do pré-sal, caracterização de reservatórios 3D, aprendizagem de máquina, modelagem sedimentar 4D.

Table of Contents

Preface	12
1. Introduction	16
2. Geological Process Modeling and Geostatistics for Facies Reconstruction of Presalt Carbonates	22
Abstract.....	22
2.1. Introduction	23
2.2. Geological Setting	25
2.3. Method.....	28
2.4. Results	39
2.5. Discussion.....	47
2.6. Conclusions	50
3. Seismic Pattern Classification Integrated with Permeability-Porosity Evaluation for Reservoir Characterization of Presalt Carbonates in the Buzios Field, Brazil.....	52
Abstract.....	52
3.1. Introduction	53
3.2. Method.....	56
3.3. Results and Discussions	64
3.4. Conclusions	73
4. Geostatistics assisted by machine learning for reservoir property modeling: A case study in presalt carbonates of Buzios Field, Brazil.....	75
Abstract.....	75
4.1. Introduction	76
4.2. Method.....	80
4.3. Results and Discussion	87
4.4. Conclusions	94
6. Final Considerations.....	96
7. References	100

List of Figures

Figure 1: Location of the Búzios Field within the Santos Basin.	25
Figure 2: Structural map of the Base of Salt of the Búzios Field. The arbitrary sections presented in this study are shown as red lines, black circles represent the well locations and the stippled blue line represents extent of the seismic volume.	29
Figure 3: Simplified chronostratigraphic chart for the Santos Basin. The Base of Salt and Pre-Alagoas unconformities respectively define the top and base of the studied interval, the Barra Velha Formation. Modified from Wright and Barnett (2015) after Moreira et al. (2007).	30
Figure 4: Lithological and Compressional Slowness (DTCO) logs for selected wells from the Búzios Field.	31
Figure 5: Absolute lake level curve a) and relative lake level b) for the Barra Velha Formation paleoenvironment constructed using the compressional slowness log from the ANP-1 well.	32
Figure 6: a) Initial lake topography. b) Final lake topography. c) Tectonic subsidence rate used for the Barra Velha Formation geological process modeling in the Búzios Field area.	33
Figure 7: a) Schematic sediment succession for the Barra Velha Formation used in this study and b) proposed growth depth multiplier per simulated sediment depending on relative lake level.	34
Figure 8: Shrubs sediment lake area growth scaling.	35
Figure 9: Diffusion multiplier by relative lake base level.	37
Figure 10: Seismic (patterns) facies identified in the Búzios Field area: a) Carbonate Build-ups architecture; b) Debris flow seismic facies; c) Aggradational or progradational carbonate platforms seismic facies; d) Lake bottom facies.	37
Figure 11: Integrated workflow for the geological process and facies reconstruction modeling.	39
Figure 12: Results represented across arbitrary section line AB1 (location shown in Figure 2) for a) interpreted seismic section, b) carbonate geological process modeling and c) facies reconstruction using truncated Gaussian simulation with sediment proportion volumes as trends and lithology logs from wells (RWD – reworked sediments, SHR – shrubs, SPH – spherulites and FGM – fine-grained muds).	40

Figure 13: Results represented across arbitrary section AB2 (location shown in Figure 2) for a) interpreted seismic amplitude volume, b) carbonate geological process modeling and c) facies reconstruction using truncated Gaussian simulation with sediment proportion volumes as trends and lithology logs from wells (RWD – reworked sediments, SHR – shrubs, SPH – spherulites and FGM – fine-grained muds).	41
Figure 14: Results represented across arbitrary section AB3 (location shown in Figure 2) for a) interpreted seismic amplitude volume, b) carbonate geological process modeling and c) facies reconstruction using truncated Gaussian simulation with sediment proportion volumes as trends and lithology logs from wells (RWD – reworked sediments, SHR – shrubs, SPH – spherulites and FGM – fine-grained muds).	42
Figure 15: Geological process modeling results at a) 125 Ma, b) 121 Ma, c) 117 Ma and d) 113 Ma. Mean model (sediment) thicknesses for each time-step are: b) 104 m, c) 108 m and d) 258 m.	43
Figure 16: Results for facies reconstruction modeling in map view over the Base of Salt surface in the Búzios Field. White circles represent the well locations.	45
Figure 17: Results for facies reconstruction in 3D sliced view for the Búzios Field. Black lines represent the well traces.	46
Figure 18: Location of the Buzios Field within the Santos Basin.	56
Figure 19: Map view of the base of salt interpreted seismic horizon (depth contours) across the Buzios Field (black polygon) with the coverage of the 3D Seismic data shown by the green rectangle and well locations shown by black circles. The red lines show the location of the arbitrary seismic lines (AB1 and AB2) presented in this study.	57
Figure 20: Simplified methodology flowchart.	58
Figure 21: Preconditioning to remove random and structurally oriented noise effects. a) Original seismic data; b) Preconditioned seismic data.	59
Figure 22: Principal seismic patterns identified within the Barra Velha Fm. interval - Typical seismic amplitude for a) carbonate build-ups (IL4710), b) debris and c) aggradational/progradational carbonate platforms as observed within IL4710, XL3804 and IL4186 respectively. Note: IL - Inline, XL - crossline. Selected seismic attributes for the same seismic patterns: local flatness in d), e) & f); rms amplitude in g), h) & i); principal dip component in j), k) & l), and acoustic impedance in m) n) & o).	61

Figure 23: Seismic trace expression for each of the selected attributes used as input for the unsupervised neural network seismic facies classification. The seismic trace was extracted along the ANP-1 well trajectory within the Barra Velha Fm. interval. From left to right, preconditioned seismic trace, local flatness, rms amplitude, principal dip component and acoustic impedance..... 62

Figure 24: Preconditioned seismic section (a) from the 3D seismic volume along arbitrary line 1 (AB1) with the values of b) the local flatness attribute c) the rms amplitude attribute; d) the principal dip component; e), the acoustic impedance attribute for the Barra Velha Formation; f) results of the seismic facies classification of the Barra Velha Fm overlain on the filtered seismic data. Well paths are shown by the yellow or white lines and faults by the black lines. As can be noted, build-ups are mostly concentrated on the footwall side of normal faults and are laterally associated with the debris seismic facies which tend to occur on the hanging wall side of faults. 65

Figure 25: Preconditioned seismic section (a) from the 3D seismic volume along arbitrary line 2 (AB1) with seismic attributes shown for the Barra Velha Formation interval: b) local flatness attribute; c) rms amplitude attribute; d) principal dip component attribute; e) acoustic impedance attribute and f) the results of the seismic facies classification for the same interval. Faults are shown by black lines and well paths by the yellow or white lines. It should be noted that the aggradational/progradational carbonate platforms are the dominant seismic facies in stable areas of structural highs away from their faulted margins. 66

Figure 26: The results of the seismic facies classification presented in map view over the base of the salt unconformity (top of the Barra Velha Fm.) shown. Well locations are represented by the white circles and the black polygon shows the limits of Buzios Field..... 67

Figure 27: Sliced 3D view of the results of the seismic facies classification across the study area. Well paths are shown by the black lines. The build-up and debris seismic facies are more common within the western part of the Buzios Field associated with major faulting..... 68

Figure 28: Seismic facies proportion maps within the Barra Velha Fm. interval for a) build-ups, b) aggradational/progradational carbonate platforms, c) debris seismic facies and d) a zonation map created from these proportion maps for the Buzios Field. 70

Figure 29: Comparison between the results of seismic facies classification and the total porosity and permeability logs for five wells within the Barra Velha Formation interval. The high heterogeneity of the interval makes it difficult to establish a direct correlation between the

petrophysical logs and seismic facies. Nonetheless a general decrease in porosity towards the top of the Barra Velha Formation was observed in the majority of the wells.....	72
Figure 30: Porosity and permeability distribution histograms and cross-plots between the two parameters for carbonate build-ups a.1), a.2) and a.3); aggradational/progradational carbonate platforms b.1), b.2) and b.3); and for the debris seismic facies c.1), c.2) and c.3). The debris and build-up seismic facies display better permeability and porosity. The correlation coefficients between permeability and porosity are high for all the seismic facies.....	73
Figure 31: Location of the Buzios Field within the Santos Basin.....	80
Figure 32: Map view of the base of salt interpreted seismic horizon (depth contours) across Buzios Field (black polygon) with the coverage of the 3D seismic data shown by the dashed blue rectangle and well locations shown by black circles. The red lines show the location of the arbitrary seismic lines (AB1 and AB2) presented in this study.....	81
Figure 33: Arbitrary section 1 (AB1) with a) original seismic volume with Barra Velha Formation top and bottom unconformities, base of salt and pre-Alagoas, respectively, and secondary variables chosen for EMBER porosity modeling: b) facies model from Ferreira et al. (2021a), c) local flatness attribute, and d) acoustic impedance attribute from Dias et al. (2019).	83
Figure 34: Arbitrary section 2 (AB2) with a) original seismic volume with Barra Velha Formation top and bottom unconformities, base of salt and pre-Alagoas, respectively, and secondary variables chosen for EMBER porosity modeling: b) facies model from Ferreira et al. (2021a), c) local flatness attribute, and d) acoustic impedance attribute from Dias et al. (2019).	84
Figure 35: Expression for each of the secondary variables used for effective porosity EMBER modeling and effective porosity and permeability upscaled logs along the ANP-1 well trajectory within the Barra Velha Formation interval. From left to right, facies model, local flatness attribute, acoustic impedance attribute, and effective porosity and permeability well logs.....	85
Figure 36: The resulting EMBER 3D property modeling volume along arbitrary line 1 (AB1) for a) effective porosity and b) permeability and along the arbitrary line 2 (AB2) for c) effective porosity and d) permeability. Well paths are shown by the white lines, except for ANP-1 well used as a blind test, which is presented with a yellow line and with the associated upscaled property.....	89

Figure 37: The results EMBER 3D property modeling presented in map view for a) effective porosity and b) permeability over the base of salt surface (top of the Barra Velha Formation) and restricted to the main structural highs. Well locations are represented by the white circles, and the black polygon shows the limits of the Buzios Field. 90

Figure 38: Comparison between the effective porosity and permeability upscaled well logs (black lines) and EMBER simulation results (red lines) for those properties are presented in a). In b) and c), effective porosity and permeability upscaled well log distributions (green histograms) and results distributions (blue histograms) are shown, respectively. 93

Figure 39: Illustrations at the arbitrary section 2 (AB2) for effective porosity P10 (a) and P90 (b) conditional distributions and uncertainty (c). Blind test ANP-1 well is represented by the yellow line, and its associated upscaled effective porosity well log is illustrated on the right side of the well trajectory. 94

List of Tables

Table 1: Maximum sediment growth rate per millimeter per year used for the geological process modeling.	34
Table 2: Grain diameter used for the diffusion process for each simulated sediment.....	36

Preface

Why geosciences? Why geological modeling?

One of the most important phrases for history and science is without a doubt the famous “You have to know the past to understand the present” from Carl Sagan. During my academic career in geosciences, I could notice that I had become a history researcher of Earth’s history which is longer and more complex than human history. However very much alike to the advocated by Sagan, it is essential the comprehension of the origin and dynamics of older rock formations for the understanding of present geology and its evolution. Although, several times in geosciences the contrary logic is also true where understanding the present is necessary to support the unraveling of the geological history of the past.

These premises are the basis for geological modeling which is a technique greatly applied by the oil and gas industry, one of the economic sectors most important to society. This sector is responsible for proving not only energy but also feedstock for other sectors. Specifically, geological modeling is a tool that allows the creation of tridimensional models of rock in the subsurface and, applied to the hydrocarbon exploitation, supports the inference of reservoir characteristics for production planning and optimization.

My academic career started, like the ones from many other geological modeling researchers, applying a specific rock physics methodology to characterize a sedimentary environment from a hydrocarbon reservoir and try to predict the changes that would occur to it during production.

Advised by professor and Ph.D. Sergio Bergamaschi from the Universidade do Rio de Janeiro (UERJ) and the co-advisership of researcher and Ph.D. Sergio Sacani from Halliburton, I performed the 1D fluid substitution modeling using the Gassmann-Biot equations as a 4D feasibility study for the siliciclastic Paleocene reservoirs from the South Viking Graben in the North Sea. This study was my bachelor’s monography in 2015 and my first contact and contribution for the geoscience’s academic environment in the reservoir characterization field.

After the conclusion of the geology bachelor, I started still in 2015 as a *latu sensu* post-grad at the Seismic Stratigraphic Interpretation course, also at UERJ sponsored by the company Statoil, current Equinor. In that environment, I had the opportunity to get in

contact with most of the reservoir interpretation and characterization techniques from seismic interpretation and well log analysis to geostatistical modeling and seismic inversion. It was also during this course that with a group of colleagues I made my second contribution to the geoscience's academic research sector with the conclusion study in 2016: Prospective study in the NE sector of the Oliva Field, Santos Basin.

In the same year, I joined the Universidade Federal Fluminense (UFF) as a master's degree candidate in the *stricto sensu* post-graduation program Dinâmica dos Oceanos e da Terra having as an advisor the professor and PhD. Wagner Moreira Lupinacci. The master's degree project I worked on the application of seismic acoustic inversion associated with geostatistical modeling for the facies and petrophysical properties of the Albian carbonate platform of the Pampo Field located at the Campos Basin. The results from my master's project in the first year allowed the publication of my first academic paper (Ferreira and Lupinacci, 2018) at the AAPG Bulletin journal.

During this period, I was able to contribute as a technical support for two other studies that applied the same methodology for reservoir characterization for the Albian and Aptian carbonates from the Linguado Field, Campos Basin. Also I co-authored the two outcome papers from these studies (Peçanha et al., 2019; Lupinacci et al., 2020) published at the Journal of Petroleum Science and Engineering and Brazilian Journal of Geology, respectively.

Still during my master's degree period in the second year, I started working as a researcher in a research and development project at UFF focused on the salt layer and presalt reservoirs characterization at the Santos Basin sponsored by the company Galp Energia. Our research group was focused on a presalt field where I had the opportunity to learn and make contributions related to the use of innovative machine learning methodologies for reservoir characterization. More specifically, I applied the workflow of unsupervised seismic facies classification using several seismic attributes as inputs in a self-organizing maps algorithm and the results of this study allowed me to author the publication of the paper Ferreira et al. (2019) at the AAPG Bulletin journal.

Also in the same research team, I had the opportunity to co-author and participate in several other papers related to interpretation and discussions regarding (i) the paleogeography of the Brazilian presalt carbonate reservoirs in Neves et al. (2019) at the Interpretation journal, (ii) the impacts of halokinesis in seismic interpretation in Lupinacci

et al. (2019) at the Brazilian Journal of Geophysics and (iii) the application of spectral decomposition, pre-stack inversion and machine learning techniques to reduce exploratory risks for siliciclastic reservoirs in Jesus et al. (2020) at the AAPG Bulletin journal.

I concluded my master's degree in 2018 and, in the same year, I joined again the post-graduation *stricto sensu* course Dinâmica dos Oceanos e da Terra at UFF as a Ph.D. candidate continuing the advisership with the professor and Ph.D. Wagner Moreira Lupinacci. Initially, the proposed theme for my Ph.D. project was to apply the developed workflow in Galp Energia project for seismic facies unsupervised classification using seismic attributes for other presalt fields. The goal was the standardization of this technique that automatizes and facilitates the reservoir characterization of these carbonate rocks that are complex in genesis and facies distribution and, consequently, petrophysical properties such as porosity and permeability. For this project, we required as a dataset the seismic and well data in the area of the Buzios Field, located in the Santos Basin, for the ANP (Agência Nacional de Petróleo, Gás Natural e Biocombustível). This field is currently one of the most important producing presalt fields in the national scenario.

Nevertheless, at the beginning of my Ph.D., I started working as a geologist at Schlumberger company where I had contact with another innovative reservoir characterization methodology. This method was based on 4D sedimentary modeling which allowed the modeling of sedimentation through geological time considering the paleoenvironmental dynamics, basically acting as a digital sedimentary laboratory. Therefore, envisioning to obtain a more conceptual understanding of the sedimentary origin of the presalt carbonate reservoirs, I applied this technique integrated to geostatistical modeling for facies reconstruction of the Barra Velha Formation at the Buzios Field, which became my first academic paper during the Ph.D. in Ferreira et al. (2021a) at Marine and Petroleum Geology journal.

After this study, I came back to the initial scope of the Ph.D. project which was related to the application of machine learning techniques for unsupervised seismic facies characterization. I applied neural networks algorithms on the Barra Velha Formation carbonates in the Buzios Field to achieve that objective and associated the results with porosity and permeability well data to infer qualitatively about the properties of these reservoirs. The outcome from this work allowed the publication of the second paper

during the Ph.D. in Ferreira et al. (2021b) at the Journal of Petroleum Science and Engineering.

In the final phase for the Ph.D. in 2021, I had the opportunity to get involved in a project within Schlumberger to test an innovative and cloud-based pre-commercial machine learning approach that was developed to integrate geostatistical concepts for reservoir property modeling called EMBER. I applied this technology to the Barra Velha Formation in the Buzios Field to model effective porosity and permeability aiming a quantitative evaluation of the reservoir properties of these carbonates using as input for the algorithm seismic attributes and the facies model build in the 4D sedimentary modeling integrated with geostatistics paper (Ferreira et al., 2021a). This final study allowed the integration between the two innovative reservoir characterization technologies applied during the Ph.D. as well as allowed the publication of the last paper from my Ph.D. (Ferreira et al., 2021c) at the Leading Edge journal in the Latin America Special Edition.

Finally, I hope that the academic contributions here described can help to promote the knowledge of new techniques developed for reservoir characterization and geological modeling amongst new professionals in the geosciences sector looking for a career in the oil and gas industry as well as providing one more piece on the puzzle of the presalt Brazilian carbonate reservoir complexity and property distribution behavior.

1. Introduction

Reservoir characterization is a process that consists of the tridimensional determination of seismic patterns, structures, and rock properties of a field. The main objective is to build a geological model that can incorporate all the gathered information in the available data which allows prediction, monitoring, and production optimization of the hydrocarbons present in the lifespan of a field (Sancevero et al., 2006).

This process can become especially more difficult the more complex is the origin, depositional dynamics, and compositional heterogeneity of the rocks to be characterized. And such is the case for the presalt Brazilian carbonate reservoirs which usually required its analysis, interpretation, and modeling to be sustained by a deep conceptual geological knowledge of the modeler as well as the use of advanced reservoir characterization techniques (Johann et al., 2012; Johann, 2013; Bruhn et al., 2017).

The presalt reservoirs are currently the most important oil and gas producers in Brazilian production. In 2021, they were responsible for the expressive oil production of 2.1 Mbbo/d and gas production of 90.000 Mm³/d accounting for approximately 72% of the total Brazilian hydrocarbon production (ANP, 2021).

According to Riccomini, Sant'Anna e Tassinari (2012), the main petroleum systems for the Brazilian presalt have as reservoirs: the carbonate rocks of alkaline and lacustrine origins, such as the Barra Velha Formation in the Santos Basin (Moreira et al., 2007), the biologically sedimentation controlled carbonate coquinas and fractured igneous rocks (Chang et al., 2008). All of these reservoirs were formed during the rift and sag formation phases of the marginal Brazilian basins (Moreira et al., 2007; Wright and Barnett, 2015).

Still, according to these authors, the seal and source rocks components of these petroleum systems are composed of, respectively, lacustrine shales of high organic content deposited during the rift phase of the Brazilian marginal basin development, and the seals are represented both by the salt layers and the very source shales.

As stated by Wright (2012), perhaps the most complex and the biggest source of interest and uncertainty reservoir in the presalt petroleum exploration context are the alkaline lacustrine origin carbonates developed during rift and sag evolution phases of the marginal Brazilian basins initially described as travertines/microbialites (Moreira et al.,

2007; Terra et al., 2010; Azerêdo et al., 2011; Buckley et al., 2015). The uncertainty related to these reservoirs comes from the lack of publications and, consequently, investigations of the origin of carbonate rocks in a lacustrine environment.

One of the first studies that compile the possible formation contexts of these types of lithologies in a sedimentary lacustrine environment is from Porta Della (2015). However, as stated by Wright (2012), Wright & Barnett (2015), and Szatmari & Milani (2016), it is most probable that the sedimentary dynamics which controlled the formation of these presalt carbonates acted by the interaction between the lixiviation of elements from the volcanic terrains around the lakes and hydrothermalism. This synergy saturated these lakes with alkalis that together with the paleoweather conditions controlled the carbonate factory mainly by chemical precipitation.

We can also find a few lithological formations already studied that can be considered analogs for some of the processes that occurred during the presalt lacustrine carbonates precipitation. Some examples are the carbonate facies described in the great US lakes, such as the Mono Lake (Council and Bennett, 1993) and the Great Salt Lake (Chidsey et al., 2015), the carbonate rocks from Shark Bay in Australia (Logan et al., 1970), the lacustrine carbonates from the east African rift (Cerling, 1994), and the alkaline lacustrine carbonates with volcanic interaction from East Kirkton in Scotland (Mercedes-Martín et al., 2017; Rogerson et al., 2017).

However, it is important to cite that not all studies consider that the dynamics for the origin of the presalt lacustrine carbonates are dominated by chemical precipitation. Several authors such as Terra et al. (2010), Muniz and Bosence (2015) and Saller et al. (2016) suggest that these carbonate rocks may have a biologically controlled precipitation similar to the ones observed in microbialites.

It is a fact that none of these analogs can be fully considered a proper sedimentary model for the presalt lacustrine carbonates from Brazil. Therefore, due to its origin high complexity until recently the geoscientist still find difficulties of conformity in the creation of depositional models that can justify the physical-chemical and biological dynamics present during the sedimentation or possible precipitation of these reservoirs. This is the reason there are several models proposed in literature such as the ones from Wright and Barnett (2015), Sabato Ceraldi and Green (2016), Farias et al. (2019), Gomes et al. (2020), amongst others.

The challenging theoretical understanding and knowledge uniformity regarding the paleoenvironment and depositional controls for these lacustrine reservoirs, consequently, translate themselves into high complexities in the 3D characterization process of these facies in the oil and gas scenario. Thus it is not uncommon to find in the literature the use for advanced geological modeling purposes of several machine learning methodologies (Ferreira et al., 2019a; Ferreira et al., 2019b; Jesus et al., 2019), inversion methods for the inference of petrophysical properties (Dias et al., 2019; Figueiredo et al., 2019; Penna et al., 2019; Penna and Lupinacci, 2020; Penna and Lupinacci, 2021), as well as stratigraphic forward modeling (Liechoscki de Paula Faria et al., 2017; Ferreira et al., 2021a).

The high importance of these reservoirs is counterbalanced with the lack of knowledge and certainty regarding its origin and most proper 3D reservoir characterization methodologies for the presalt alkaline lacustrine Brazilian reservoirs. Therefore, in this thesis, my objective was to evaluate, investigate and characterize the Barra Velha Formation, one of these reservoir representatives deposited during the upper rift and sag phases from the Santos Basin in the opening of the South Atlantic Ocean (Moreira et al., 2007; Wright and Barnett, 2015).

It is important to highlight that the most prolific hydrocarbon producer basin in Brazil from the presalt reservoirs in the Santos Basin. The Buzios Field is its most productive oil and gas field, operated by Petrobras, responsible for 27% of the basin total production with more than 30 billion barrels of light oil of estimated reserves with 27° API (ANP, 2016, 2021). Due to its importance in the national oil and gas scenario this field is the study area of this thesis.

My motivation for this thesis was to build and standardize using innovative 3D reservoir characterization techniques workflows that can provide robust, automatized, and fair predictability modeling results for lithological facies and petrophysical properties for the Barra Velha Formation respecting its heterogeneities. The input data would be well data and secondary data and the results from these methodologies would help to provide a better understanding regarding this complex geological Formation settings.

To achieve these objectives and fulfill the proposed motivation, this thesis was subdivided into the application of three innovative and advanced reservoir characterization techniques in the Barra Velha Formation from the Buzios Field area that

originated as outcomes three already published papers in several journals. In chronologic order, the first study and article refer to the first-time published application of an integrated approach between 4D sedimentary modeling and geostatistical modeling for the facies reconstruction for presalt reservoirs at the Marine and Petroleum Geology journal.

The 4D sedimentary modeling or geological process modeling or forward stratigraphic modeling is a revolutionary technology that allows the creation of digital conceptual sedimentary models based on the simulation of the physical and chemical mechanisms which control sedimentation and diagenesis through geological time (Merriam and Davis, 2001; Tetzlaff et al., 2014; Huang et al., 2015; Lanteaume et al., 2018; Borgomano et al., 2020; Ferreira et al., 2021a).

The outputs from this methodology can be associated with geostatistical modeling algorithms as sedimentary models for each facies present in the wells as secondary variables to make it possible for the geomodeler to incorporate its conceptual geological knowledge about the facies paleoenvironment to be modeled in a more precise manner into the chosen interpolation and extrapolation algorithm. This association between these modeling techniques was fundamental in my study for the reconstruction of a geological facies model for the Barra Velha Formation Buzios Field due to the possibility of incorporation of conceptual dynamics of the complex geology of these reservoirs for modeling honoring well data.

The second study and article from this thesis, published at Journal of Petroleum Science and Engineering, used the application of a neural network algorithm for unsupervised seismic facies classification also for the Barra Velha Formation having as inputs a group of seismic attributes (Ferreira et al., 2021b). The neural networks method proposes to establish its machine learning dynamics and neuron architecture based on the organization and functioning of human neurons for pattern recognition aiming at data classification or estimation (McCulloch and Pitts, 1943).

The results of the application of this technique allowed the quick and automatized creation of a 3D seismic facies model for the study area and reservoir interval and these outputs were further associated with the porosity and permeability distributions from well data per classified seismic facies for a qualitative inference of its reservoir properties.

The third paper and study in this thesis, published at The Leading Edge journal, approached for the first time the application of a pre-commercial and innovative machine learning methodology that implements geostatistical concepts for supervised estimation of petrophysical reservoir properties from multiple secondary variables called EMBER developed by Daly (2020a). This innovative technique automatizes 3D reservoir modeling processes and aims to overcome a few of the premises and limitations from conventional geostatistical algorithms such as stationarity and required high linear correlation between primary and secondary variables when co-kriging is used (Ferreira et al., 2021c). Also, it allows the use of several secondary variables for modeling the primary variable unlike several conventional geostatistical methods (Hirsche et al., 1998).

EMBER is a non-stationary spatial modeler that allowed then the use of several secondary variables for effective porosity and permeability modeling Buzios Field combining geostatistics and the quantile random forest machine learning algorithm. It is important to highlight that one of the secondary variables used for the petrophysical modeling in this study was the output facies reconstruction 3D model from the first paper from this thesis allowing a link between the two studies.

As result of this last study (Ferreira et al., 2021c), effective porosity and permeability 3D models allowed the quantitative evaluation of the modeled reservoirs as well as to address the uncertainties related to the distribution of effective porosity.

All the methodologies applied in the three studies and papers have their advantages and disadvantages and its appropriate application scenario depending on the detail required and available time for the geological modeling process. However, it is undeniable that all those techniques and workflow have their robustness when applied to high complex geological environments such as the case for the presalt carbonate Brazilian reservoirs.

It is important to highlight that in thesis it is the first time that both the integrated approach between 4D sedimentary modeling and geostatistical modeling for the facies reconstruction for presalt reservoirs, first paper, nor the application of EMBER technology for carbonate reservoir quantitative characterization, third paper, has been performed, standardized and published.

Finally, this thesis is structured in the presentation of each of the above-cited published papers in detail. Nonetheless, at the end of this thesis, final considerations of

these studies and future expectations for the tridimensional reservoir characterization area are discussed.

2. Geological Process Modeling and Geostatistics for Facies Reconstruction of Presalt Carbonates

Article published in

Marine and Petroleum Geology, volume 124, 2020

Impact factor: 4.348

Authors: Danilo Jotta Ariza Ferreira, Henrique Picorelli Ladeira Dutra, Thais Mallet de Castro and Wagner Moreira Lupinacci.

Abstract

The presalt reservoirs of the Barra Velha Formation are complex and heterogeneous. Their deposition was controlled by a mixture of physical and chemical processes, which consequently affected the distributions of facies and variations in porosity and permeability. In this paper we present a presalt facies reconstruction of reservoirs within the Barra Velha Formation of the Búzios Field. This was achieved through the use of an innovative workflow that integrates geological process modeling with a truncated Gaussian simulation geostatistical algorithm with trends. Our results show that the structural highs are dominated by carbonate build-ups/mounds architecture seismic patterns which are dominated by spherulites and its intercalation with shrub sediments culminating in spherulitites and shrubby carbonate lithologies. Reworked sediments and facies are concentrated in regions dominated by debris seismic patterns and lake bottom seismic facies corresponding to laminites also occur within the study area. In chronostratigraphic terms the Barra Velha is muddier at the base transitioning to in-situ carbonates in the middle section, before becoming muddier again at the top. The western portion of the Búzios Field is mostly composed by shrubby carbonates and reworked facies whilst spherulitities are more abundant to the east intercalated with shrubby carbonates. Some uncertainties remain in relation to the parameters used in the proposed methodology. Nonetheless, the proposed workflow was effective for facies reconstruction of the presalt carbonates allowing not only a better understanding of sedimentological processes but also accurately distributing facies throughout the study area.

2.1. Introduction

Geological process modeling is a technique of 4D reservoir characterization that allows the construction of conceptual sedimentary models based on the simulation of physical and chemical mechanisms, which control sedimentation and diagenesis through time (Merriam and Davis, 2001; Tetzlaff et al., 2014; Huang et al., 2015; Lanteaume et al., 2018; Borgomano et al., 2020). This approach has been successfully used for carbonate sedimentary modeling of the Triassic Esino Limestones in the Alps (Berra et al., 2016), the Miocene limestones from the Marion Plateau in Australia (Guerra, 2016), the Aptian carbonate platform in Abu Dhabi (Lanteaume et al., 2018), as well as for a number of Cenozoic, Mesozoic and Paleozoic carbonate platforms (Whitaker and Frazer, 2018) and the Lower Cretaceous Urgonian platform in France (Borgomano et al., 2020). Geological process modeling has also been applied to clastic sedimentation in deep water turbidite systems from offshore Brazil (Acevedo et al., 2016; Høyve et al., 2016; Madhoo et al., 2016). This modeling simplifies the exploration phase and optimizes reservoir characterization, allowing a better comprehension of sedimentary evolution and dynamics as it requires detailed (user) input of tectonic and eustatic parameters as well as rates of erosion and sediment transport.

Geostatistical methods for determining petrophysical properties and reservoir characterization of facies are widely used, with an extensive bibliography (Ziegel et al., 1998; Lantuéjoul, 2002; Caers, 2005; Pyrcz and Deutsch, 2014; Azevedo and Soares, 2017). These methods have been successfully applied to the characterization of both post salt (Ferreira and Lupinacci, 2018) and presalt (Peçanha et al., 2019) Brazilian carbonate reservoirs.

Aptian presalt reservoirs of Brazil's marginal basins are amongst the most challenging for oil and gas production due to their geological complexity related to the heterogeneity of their lacustrine carbonate facies (Pereira et al., 2013; Szatmari and Milani, 2016; Farias et al., 2019; Gomes et al., 2020). For their characterization, a good understanding of sedimentological, depositional and post-depositional processes needs to be coupled with advanced 3D reservoir characterization techniques leading to accurate positioning of wells (Bruhn et al., 2017).

The majority of published and successful advanced characterization workflows applied to Brazilian presalt carbonates involve either the classification of seismic facies

by neural networks based on seismic attributes (Ferreira et al., 2019a; Ferreira et al., 2019b; Jesus et al., 2019) or the use seismic inversion methods for petrophysical inference (Dias et al., 2019; Figueiredo et al., 2019; Penna et al., 2019). However, these approaches are very dependent on seismic data and lack a connection with sedimentological dynamics which limits their capacity for accurate facies modeling due to the similar seismic responses obtained for several presalt carbonate lithologies. Geological process modeling addresses these limitations as this technique can be integrated with geostatistical modeling and takes into account sedimentological mechanisms and is not overly dependent on seismic data.

The Búzios Field within the Santos Basin (Figure 1) is a supergiant presalt field and is currently the second largest producing field in Brazil, accounting for 26% of total presalt productivity and approximately 17% of total national production (ANP, 2021). It has a total area of 852.2 km² and contains an estimated 29 Bbo of reserves, producing light oil with 28 gAPI (ANP, 2016). For the first time, this study presents a facies reconstruction for the Barra Velha Formation within the Búzios Field. An innovative workflow was used that involved the construction of a conceptual sedimentary model with the aid of geological process modeling. This conceptual model was then used as a secondary input for geostatistical facies modeling. Our objective was to characterize the faciological distribution of the Barra Velha Formation across the study area by taking into account a conceptual geological model for the sedimentary dynamics that govern presalt lacustrine deposition and not relying solely on sparse well data and seismic information.

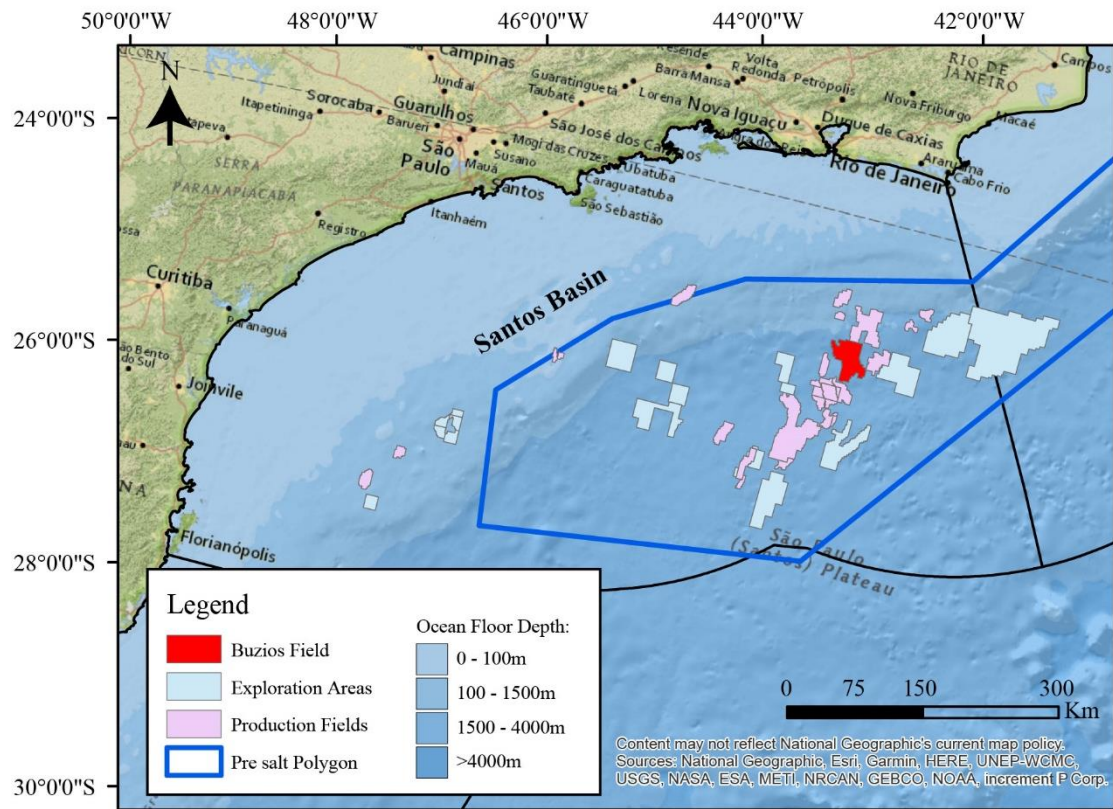


Figure 1: Location of the Búzios Field within the Santos Basin.

2.2. Geological Setting

The Barra Velha Formation represents the end of the rift and sag phases of the Santos Basin, which formed during the opening of the South Atlantic ocean during the Aptian (Wright and Barnett, 2015). This Formation was first described by Moreira et al. (2007) as a shallow lacustrine sequence characterized by intercalations of microbial carbonates, stromatolites and laminites in its proximal portion and distal facies of finer grained carbonates and shales. The proximal facies were described as being commonly reworked into grainstones and packstones containing fragments of stromatolites and associated bioclasts. Ephemeral volcanic activity was also present leading to the intercalation of mafic igneous rocks with these aforementioned lithologies.

The structural setting for the development of the paleoenvironment of the Barra Velha Formation consisted of a series of distal, N-S to NE-SW rift fault shoulders uplifted during the Barremian which led to shallow carbonate sedimentation due to the scarcity of siliciclastic sediment input (Gomes et al., 2002, 2008). Mean basin subsidence was around 600 m during the Aptian, according to Contreras et al. (2010).

Szatmari and Milani (2016) suggested that the faults acted as pathways for hydrothermal fluids as well as for volcanic activity which together with meteoric waters from the continent supplied the shallow lacustrine waters with alkalis such as Ca, Mg and SiO₂ (Boyd et al., 2015). This favored the deposition of non-marine carbonate facies, such as Mg-rich authigenic shales, travertines, stromatolites, grainstones, spherulitic packstones and mudstones. In addition, there is evidence of eventual subaerial exposure and erosion by wave action.

The core-based cyclothem succession proposed for the Barra Velha Formation is inferred to be controlled by tectonics, lake water level, lake geochemistry and erosional processes (Wright, 2012; Wright and Barnett, 2015; Wright and Tosca, 2016). The succession consists of an evaporitic/shallowing upwards sequence with basal facies of predominantly detrital laminated carbonate muds with the occasional presence of spherulites and shrub fragments. These laminated carbonate grade into shallow water spherulitic carbonates and stevensite rich lithologies and finally shrub-like carbonate facies, all which show evidence of microbial influenced precipitation (Wright, 2012; Wright and Barnett, 2015; Wright and Tosca, 2016).

Farias et al. (2019) analyzed core samples from the upper Barra Velha Formation and proposed slightly different facies with a shallowing upwards succession that began with freshwater flooding and, therefore a high water table leading to the deposition of laminites over a calcite crust from previous cycles. These facies grade into shrub-like carbonate deposition, formed in an evaporative phase with a lowered lake water table, followed by the deposition of spherulites and stevensite in a desiccation phase with the water table below the surface. Stevensite can also occur in protected and evaporative shallow lake conditions with high Mg/Si ratio, salinity and pH forming directly from water column (Pozo and Calvo, 2018), causing its eventual preservation in some sectors as demonstrated by several authors (Saller et al., 2016; Herlinger et al., 2017; de Castro and Lupinacci, 2019).

Gomes et al. (2020) proposed a new facies classification for carbonates of the Barra Velha Formation, as well as two facies succession schemes with reservoir rocks, deposited on paleo highs, and non-reservoirs rocks deposited basinward. The first facies succession scheme is defined by an upward increase in shrub grains, similar to Wright and Barnett (2015), suggesting a shallowing upwards cycle in a humid to arid climate

with fluctuating lake levels. In this succession, the reservoir rocks initially contain an abundance of spherulite grains, but they become increasingly dominated by shubs towards the top of the sequence, all with insignificant mud content. The non-reservoir rocks show a similar pattern, but they are dominated by mud at the base with increasing spherulite grains towards the middle of the succession, followed by increasing shubs at the top of the sequence. The second scheme, similar to Farias et al. (2019), is characterized by an upward trend of increasing spherulite content associated with a semi-arid to arid climate with only minor fluctuations in lake levels. Within this context the non-reservoir rocks consist of muds with shubs grading into spherulite-rich muds followed by solely muds abundance at the top of the sequence. For the reservoir rocks, the proposed succession begins with shub grains at the base and grades to spherulites at the top of the sequence with little or no mud.

As shown by Gomes et al. (2020), Muniz and Bosence (2015) and Neves et al. (2019), the basal part of the Barra Velha Formation is dominated by finer-grained facies with increasing in-situ carbonate grains towards the top. Generally muddier rocks are found at the top of the formation and they represent the Lula marker (V Paul Wright and Barnett, 2017; Neves et al., 2019a). These muddier facies were encountered in some of the wells drilled across the Búzios Field (Castro and Lupinacci, 2019).

A number of different authors (Terra et al., 2010; Pereira et al., 2013; Muniz and Bosence, 2015; Rezende and Pope, 2015; Wright and Barnett, 2015; Saller et al., 2016; Farias et al., 2019; Gomes et al., 2020) have made observations about the variation in grain size between different facies of the Barra Velha Formation. The average grain size of shub grains is 2 to 5 mm but they can also reach up to 20 mm in size. Spherulite grains are commonly less than 2 mm in size but can also grow to 15 mm. Carbonate muds and stevensite usually have grain sizes of less than 125 μm . Dorobek et al. (2012) suggested that carbonate deposition rates could have varied from 200 μm to 5 mm per year for the Barra Velha Formation.

At a regional scale, the seismic facies associated with the lacustrine Barra Velha Formation carbonates or their African analogs are: (1) carbonate platforms located on the flexural margins of faulted blocks and on structural highs with parallel to sub-parallel reflectors; (2) mound/build-up shaped reflectors located along the borders of these structural highs or on isolated highs; (3) debris or reworked seismic facies with lobate

geometries located within structural lows adjacent to border faults and (4) deep-water, distal, lacustrine facies within structural lows which display parallel to sub-parallel or absent reflectors (Buckley et al., 2015; Ferreira et al., 2019a; Jesus et al., 2019; Kattah and Balabekov, 2015; Neves et al., 2019; Saller et al., 2016; Zalán et al., 2019) . Some of these seismic facies were previously identified in the Búzios Field by Ferreira et al. (2019b).

Saller et al. (2016) observed that that shrubby boundstones and spherulitic grainstones with intraclasts are the most common lithologies within the presalt sequence of the Kwanza Basin occurring as carbonate platforms and fault-aligned carbonate build-ups. Isolated carbonate build-ups are dominated by microbial boundstones whilst deep-water lacustrine facies consist of mudstones with or without the presence of spherulites. Liechoski de Paula Faria et al. (2017) proposed conceptual sedimentological process models for the late sag interval of the Barra Velha Formation for an exploration area within the Santos Basin. The most successful model was obtained by using a constant tectonic subsidence of 0.05 mm/y, a carbonate depositional rate of 0.08 mm/y, and a maximum oscillation of around 100 m in the lake level over a period of 2.4 My. This model predicted the precipitation of lacustrine carbonate facies laminites, grainstones, shrubs/stromatolites, spherulites and the deposition of mudstones. They concluded that for the study area and simulated time, a 100-meter interval of sediments were deposited within the context of an arid climate with carbonate precipitation, and that the creation of accommodation was mostly controlled by fluctuations in the water level of the lake.

2.3. Method

The dataset used in this study consisted of 1036 km² of 3D post-stack depth migrated seismic (PSDM), in addition to well data and lithological logs from 6 wells located within the Búzios Field. The well locations and the seismic lines represented in this study are shown in Figure 2, as well as the structural contour of the Base of Salt which represents the top of the Barra Velha Formation.

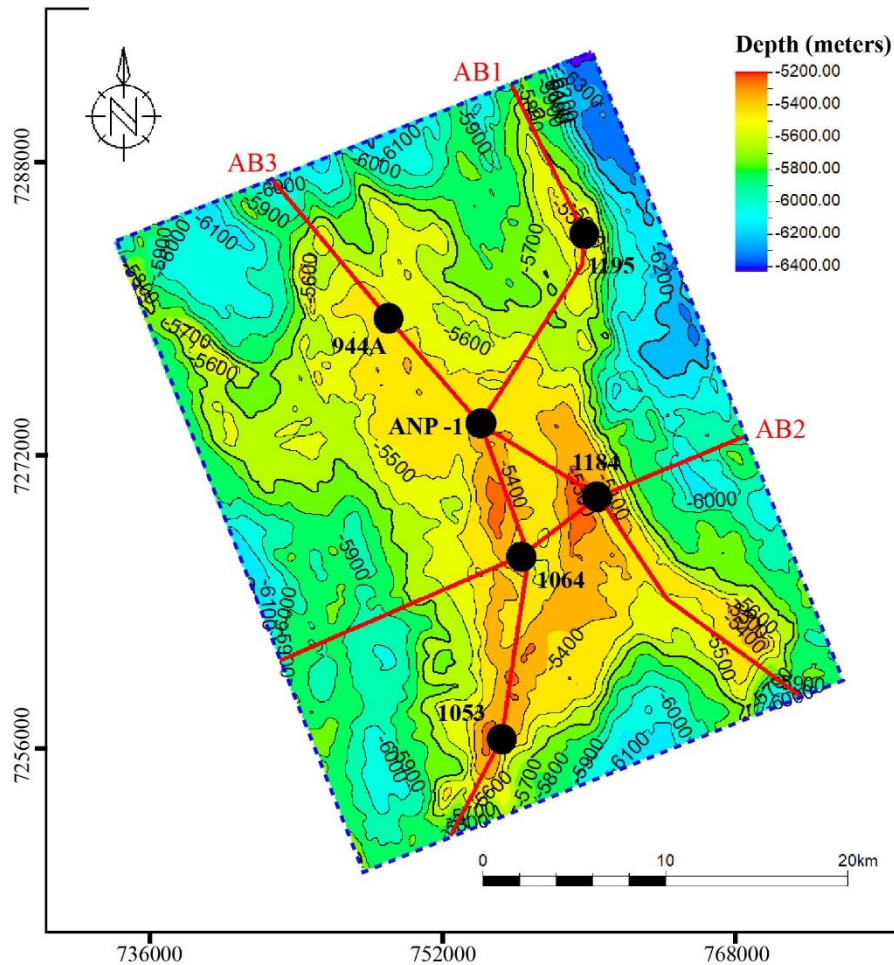


Figure 2: Structural map of the Base of Salt of the Búzios Field. The arbitrary sections presented in this study are shown as red lines, black circles represent the well locations and the stippled blue line represents extent of the seismic volume.

Carbonate geological process modeling is a methodology that consists of an iterative loop where the inputs are: (1) the simulated time interval, (2) an initial and final paleotopography that dictates tectonic activity during deposition, (3) a base level curve during sedimentation that coupled with the paleotopographic evolution, controls the creation of accommodation during the simulation, (4) a carbonate growth rate per year for each simulated sediment type which is controlled by lake depth and position and (5) modeled sediment properties such as grain size and diameter. The results of the simulation are then compared with observed seismic facies (patterns) within the modeled interval and the inputs are modified until there is reasonable match between them (Lanteaume et al., 2018). The algorithm used for geological process modeling (GPM) is available in the Petrel software from Schlumberger and was first developed by Tetzlaff (1987) with later modifications by Hill et al. (2009), Tetzlaff and Priddy (2001) and Tetzlaff et al. (2014).

A time interval of 12 My was used in the simulation, which corresponds approximately to the interval over which the Barra Velha Formation was deposited according to Wright and Barnett (2015) after Moreira et al. (2007) (Figure 3). Initial and final paleotopography and lake base level curve were constructed by applying the iterative loop methodology and respecting the Barra Velha Formation lithological trend (Figure 4). The basal lithologies are indicative of a flooded lake phase that evolved into a shallower phase towards the middle of the formation, followed by another flooding phase at the top of the formation (Muniz and Bosence, 2015; de Castro and Lupinacci, 2019; Neves et al., 2019a; Gomes et al., 2020).

Time (Ma)	Period	Age	Unconformities	Formation	Tectonic Evolution
110	CRETACEOUS	Albian		Guarujá	Drift
				Ariiri	SAG + Upper Rift
120		Aptian	Base of Salt	Barra Velha	
130		Barremian	Pre-Alagoas	Itapema	Early Rift
				Piçarras	
		Hauterivian	Basalt	Camboriú	

Figure 3: Simplified chronostratigraphic chart for the Santos Basin. The Base of Salt and Pre-Alagoas unconformities respectively define the top and base of the studied interval, the Barra Velha Formation. Modified from Wright and Barnett (2015) after Moreira et al. (2007).

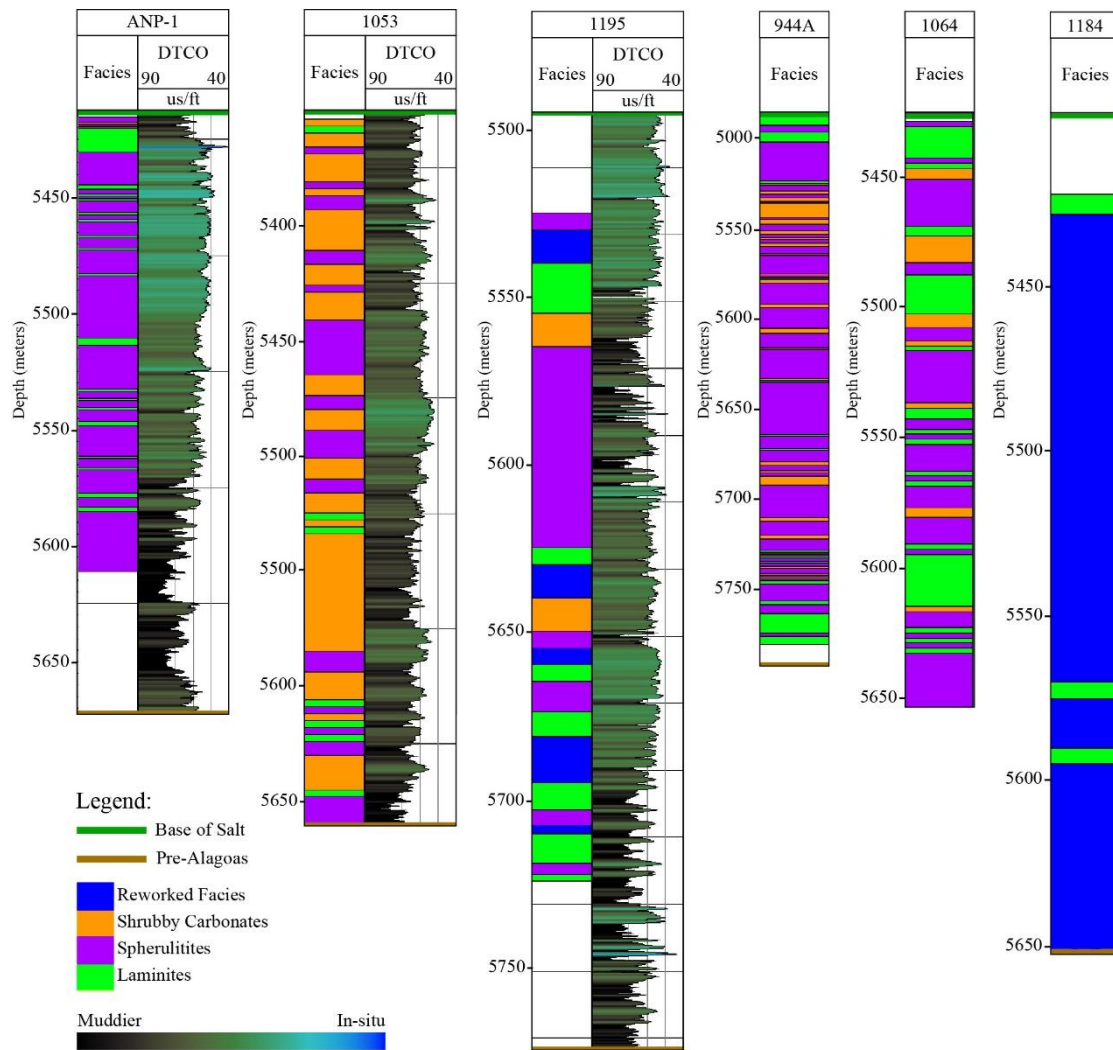


Figure 4: Lithological and Compressional Slowness (DTCO) logs for selected wells from the Búzios Field.

The lake base level curve (Figure 5a) was created by a normalization followed by multiplication by tectonic operator of compressional slowness (DTCO) log from the ANP-1 well. This operator guaranteed a fall in the lake level of 0.05 mm/y in accordance with the subsidence rate proposed by Contreras et al. (2010). The initial base level of the lake was set at 0 m since our modeling considers the beginning of deposition of the Barra Velha Formation as a reference for younger ages. The DTCO log was chosen due to its good correlation with lithological variations and consequently with the paleoenvironmental tendencies of the Barra Velha Formation. Higher slowness values were observed in the basal and uppermost portions of the formation which correlates with the prevalence of finer sediments, whilst lower values in the middle of the formation can be correlated with dominantly in-situ sedimentation (Figure 4). The high frequency variations in slowness values reflect high-order fluctuations in lake levels.

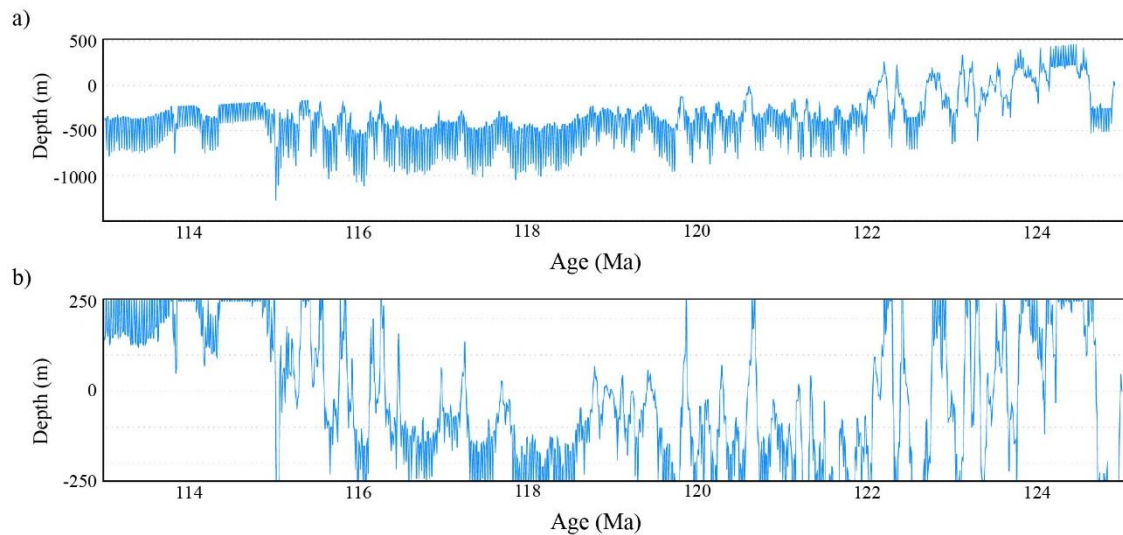


Figure 5: Absolute lake level curve a) and relative lake level b) for the Barra Velha Formation paleoenvironment constructed using the compressional slowness log from the ANP-1 well.

Seismic interpretation was undertaken of the 3D seismic volume with mapping of principal faults and of the top and bottom of the Barra Velha Formation represented by the Base of Salt and Pre-Alagoas unconformities, respectively. Initial and final lake paleotopographies were constructed to represent the geomorphology changes during deposition of the Barra Velha Formation. This was achieved by using concomitantly the lake base level curve and through normalization of the two mapped seismic horizons. The Base of Salt unconformity was adjusted by between -210 and -930 m (Figure 6a), for creation of initial topography, and the Pre-Alagoas (Figure 6b) unconformity was shifted of +5140 m, for creation of final topography, to resemble actual lake bottom bathymetry variations during the Aptian. This was undertaken in accordance with a proposed tectonic subsidence rate of between 0 to 0.06 mm/y for the Búzios Field (Figure 6c). A relative lake level curve was then (or can be) estimated (Figure 5b) which demonstrated that the relative lake level varied from between -250 to 250 m. Higher lake levels occurred at the beginning and end of the modeled interval of 12 My whilst the lake was lower for intermediate ages.

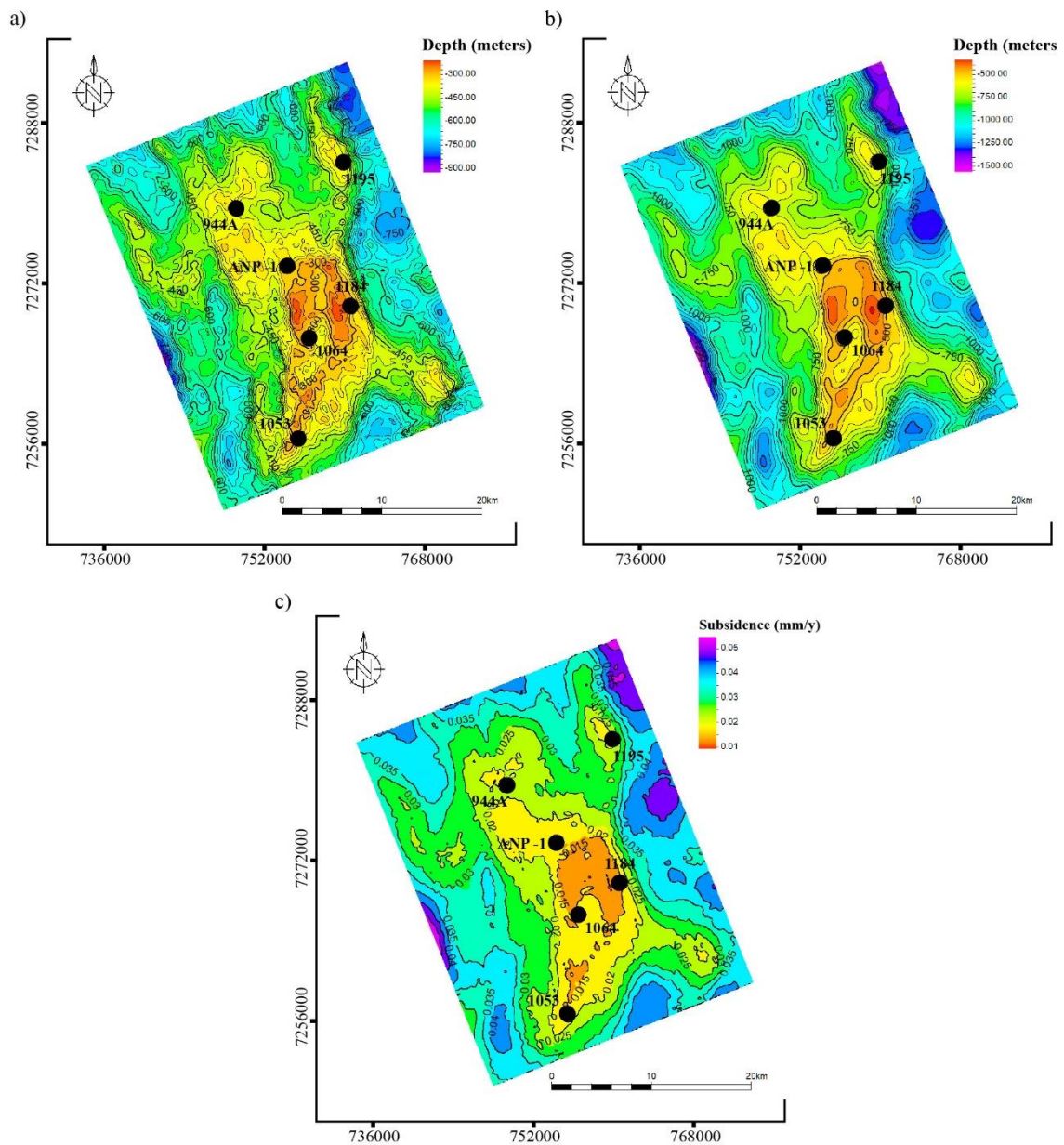


Figure 6: a) Initial lake topography. b) Final lake topography. c) Tectonic subsidence rate used for the Barra Velha Formation geological process modeling in the Búzios Field area.

Four sediment types were simulated during the geological process modeling in accordance with the carbonate facies succession proposed by Wright and Barnett (2015). Stevensite precipitation in shallow waters was also taken into consideration as proposed by Pozo and Calvo (2018). As such, the proposed succession moving from shallower to deeper lake waters: Mg-rich clays (stevensite), shrubs, spherulites and fine-grained carbonate muds (Figure 7a). The first three sediments occur in up to 20 m deep water whilst in the deeper/distal portions of the lake only fine-grained carbonate mud sedimentation would take place. The proposed sediment growth multipliers, depend on

the relative lake level, used for modeling are shown in Figure 7b and Table 1, and display the maximum sediment growth rates of millimeters per year.

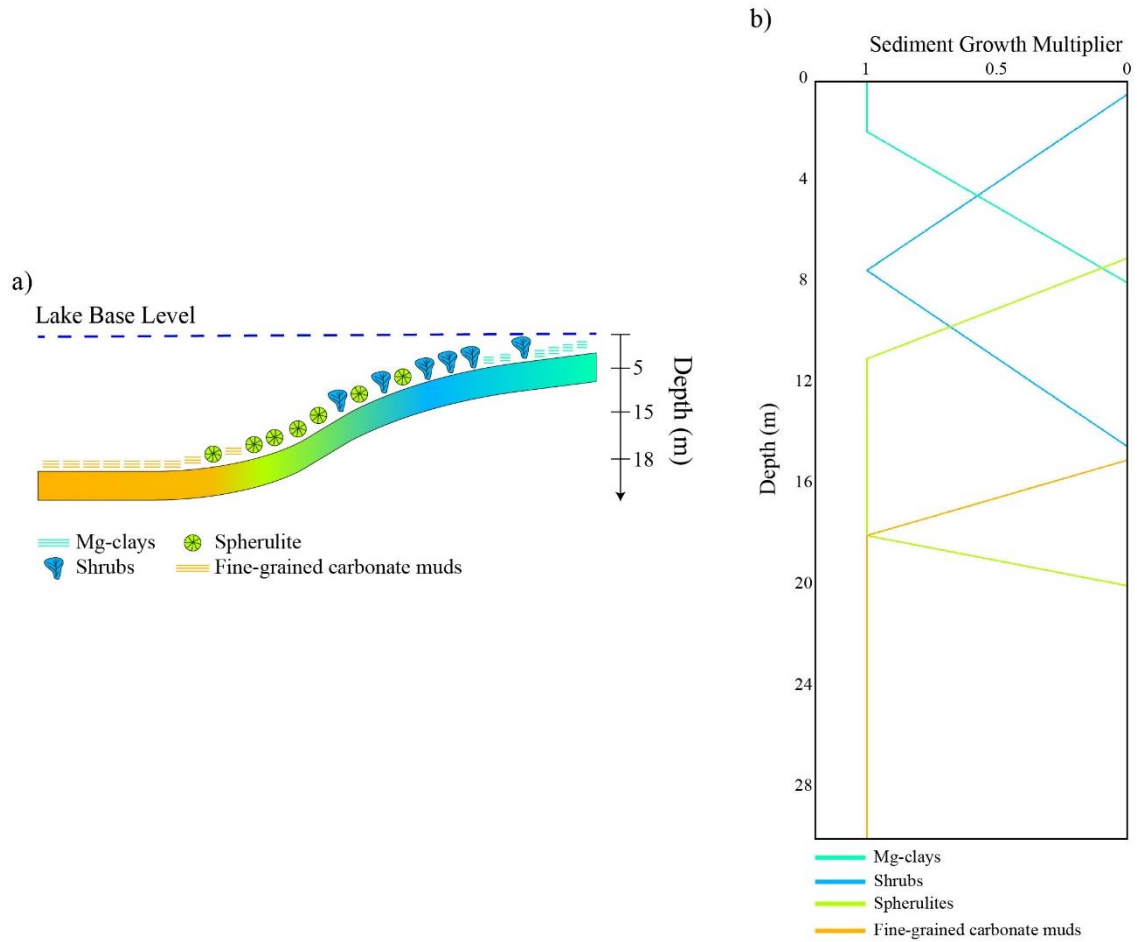


Figure 7: a) Schematic sediment succession for the Barra Velha Formation used in this study and b) proposed growth depth multiplier per simulated sediment depending on relative lake level.

Table 1: Maximum sediment growth rate per millimeter per year used for the geological process modeling.

Maximum sediment growth rates (mm/y)	
Shrubs	0.35
Spherulites	0.25
Fine-grained carbonate muds	0.05
Mg-clays	0.04

We also used an areal carbonate sediment growth scaling for the shrubs, due to their inferred dominance in areas where both the Base of Salt and Pre-Alagoas unconformities present steeper dips. This dip variation in the seismic horizons occurs at the vicinity of faults and where carbonate build-ups architecture seismic facies are more present, which may be associated with hydrothermal activity (Figure 8).

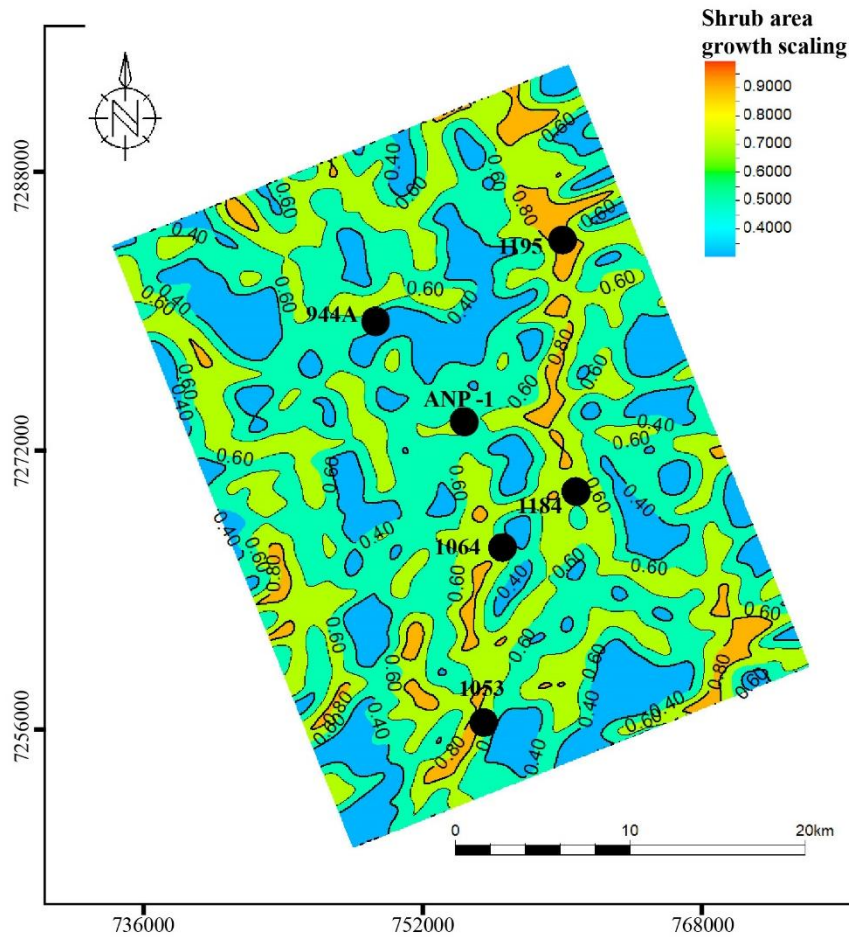


Figure 8: Shrubs sediment lake area growth scaling.

Sediment growth for each simulated time step is a function of the depth dependent growth multiplier, areal scaling in the case of shrubs sediment, and maximum sediment growth rate. Therefore, each cell from the geological process modeling grid will have a mixture of all sediments that could have been deposited simultaneously (Hill et al., 2009). Consequently, one of these modeled sediment types would prevail for each lithology encountered in the wells from the Búzios Field. That is, laminites contain the highest quantities of Mg-rich clays or fine-grained carbonate muds, shrubs are the dominant sediment in shrubby carbonates, and spherulite grains are at their most abundant in spherulitites.

Geomorphological evolution is controlled by erosion and downslope sediment transport. These processes were modeled as diffusion processes as proposed by Tetzlaff and Schafmeister (2007) and are dependent on a global diffusion coefficient for the paleoenvironment, sediment grain diameter and a diffusion multiplier that is a function of local depth at the time of deposition. The global diffusion coefficient used for the simulation was 0.005 m²/y. The grain diameter for each sediment type is given in Table 2, whilst Figure 9 illustrates the diffusion multiplier by relative lake base level. The highest values for the diffusion multiplier are located close to the lake relative base level of 0 m, where it can be inferred that wave-action erosion and transport take place. However, high values also occur below the relative lake level possibly representing the activity of deep water currents, whilst higher values above 0 m represent the action of weathering and wind¹. When diffusion affects the shrubs or spherulite sediments, they become a fifth type of sediment referred to as “reworked sediments” in the simulation.

Table 2: Grain diameter used for the diffusion process for each simulated sediment.

Sediment grain diameter (mm)	
Shrubs	2
Spherulites	1
Fine-grained carbonate muds	0.002
Mg-clays	0.001

¹ The high diffusion multiplier peaks both above and below 0 meters were placed randomly.

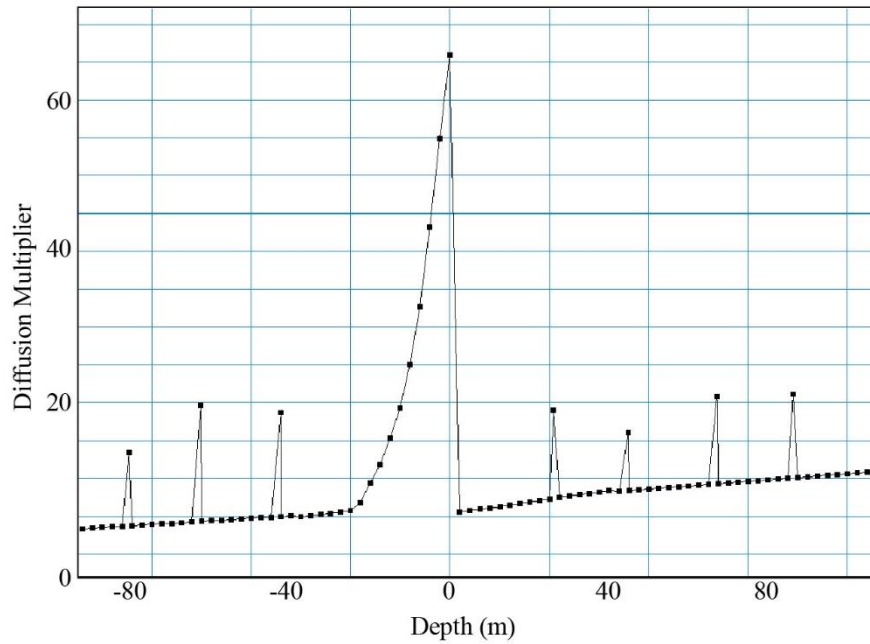


Figure 9: Diffusion multiplier by relative lake base level.

After sedimentary geological process modeling, a comparison was made with the four main seismic facies patterns identified within the interval spanning the Barra Velha Formation: carbonate build-ups architecture seismic facies, debris flow seismic facies, aggradational or progradational carbonate platforms and lake bottom seismic facies (Figure 10)². The conceptual sediment distribution model was then adjusted to its current depth range and thickness, using a depth-depth conversion model to fit it to the depth interval between the Base of Salt and Pre-Alagoas unconformities.

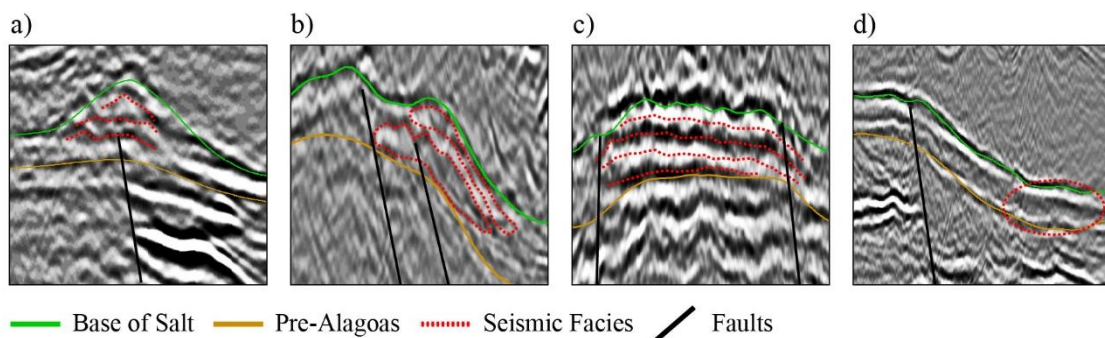


Figure 10: Seismic (patterns) facies identified in the Búzios Field area: a) Carbonate Build-ups architecture; b) Debris flow seismic facies; c) Aggradational or progradational carbonate platforms seismic facies; d) Lake bottom facies.

² The comparison between the results from the sedimentary geological process modeling and the seismic facies was performed manually for the entire seismic cube within the Barra Velha Formation interval.

Facies reconstruction modeling was undertaken using the geostatistical method of truncated Gaussian simulation (Pyrcz and Deutsch, 2014; Beucher and Renard, 2016; Ferreira and Lupinacci, 2018; Peçanha et al., 2019). Sediment proportion volume cubes were estimated from the results of the geological process modeling and applied as trends for each facies described in the wells. It is important to highlight that sediment proportion volumes for the finer simulated sediments were merged since they are represented in the lithological logs by the same rock type, laminites.

The first step in this process was the upscale of lithological logs to a grid with a cell size of 100x100x5 m (x, y, z) constructed between the Base of Salt and Pre-Alagoas surfaces. A unique experimental Gaussian semi-variogram in the N-S direction was created with 8000 and 3000 m as the major and minor horizontal ranges, and a vertical range of 10 m. Sediment proportion volume cubes were inserted as secondary variables for each facies and geostatistical modeling was performed.

The sediment proportion volumes used as trends for geostatistics contribute in the following manner; a global facies probability of occurrence for each modeled facies at each grid cell is calculated by multiplying the values of sediment proportion used for that specific facies with the global facies fraction estimated from the upscaled lithological well logs, and then dividing this value by the mean value of the sediment proportion volume related to that facies.

Well 944A was excluded from the modeling process so that it could be used as quality control for the facies reconstruction results. The proposed workflow for the geological process modeling and facies reconstruction modeling is illustrated in Figure 11.

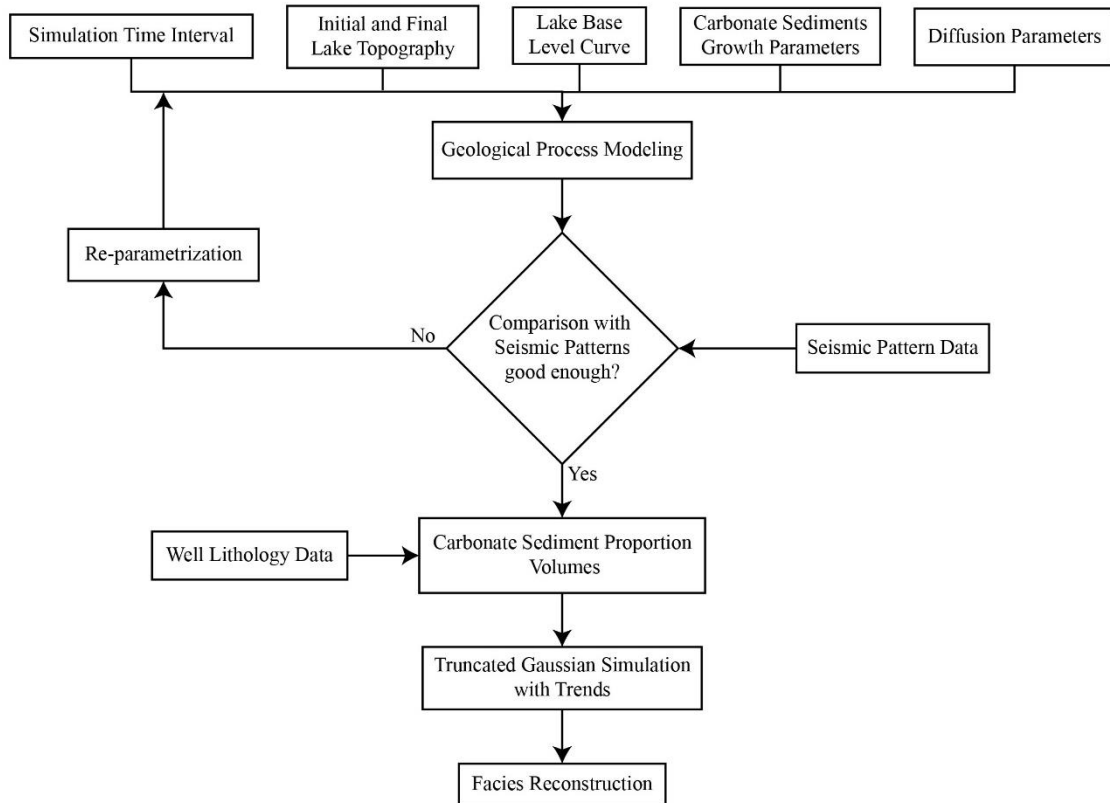


Figure 11: Integrated workflow for the geological process and facies reconstruction modeling.

2.4. Results

Seismic sections were used to make comparisons between the observed seismic patterns, the results of the carbonate geological modeling process and the results of the facies reconstruction using geostatistics (Figure 132-Figure 14). Figure 12 presents a N-S oriented seismic section which is sub-parallel to the principal direction of syn-rift faulting of the Santos Basin. An E-W orientated seismic section, perpendicular to faulting, is presented in Figure 13, and Figure 14 shows a NW-SE orientated seismic section, also sub-parallel to faulting. Figure 15 shows a 3D view of the results of the geological process modeling for four-time steps taken from the modeled 12 My time interval.

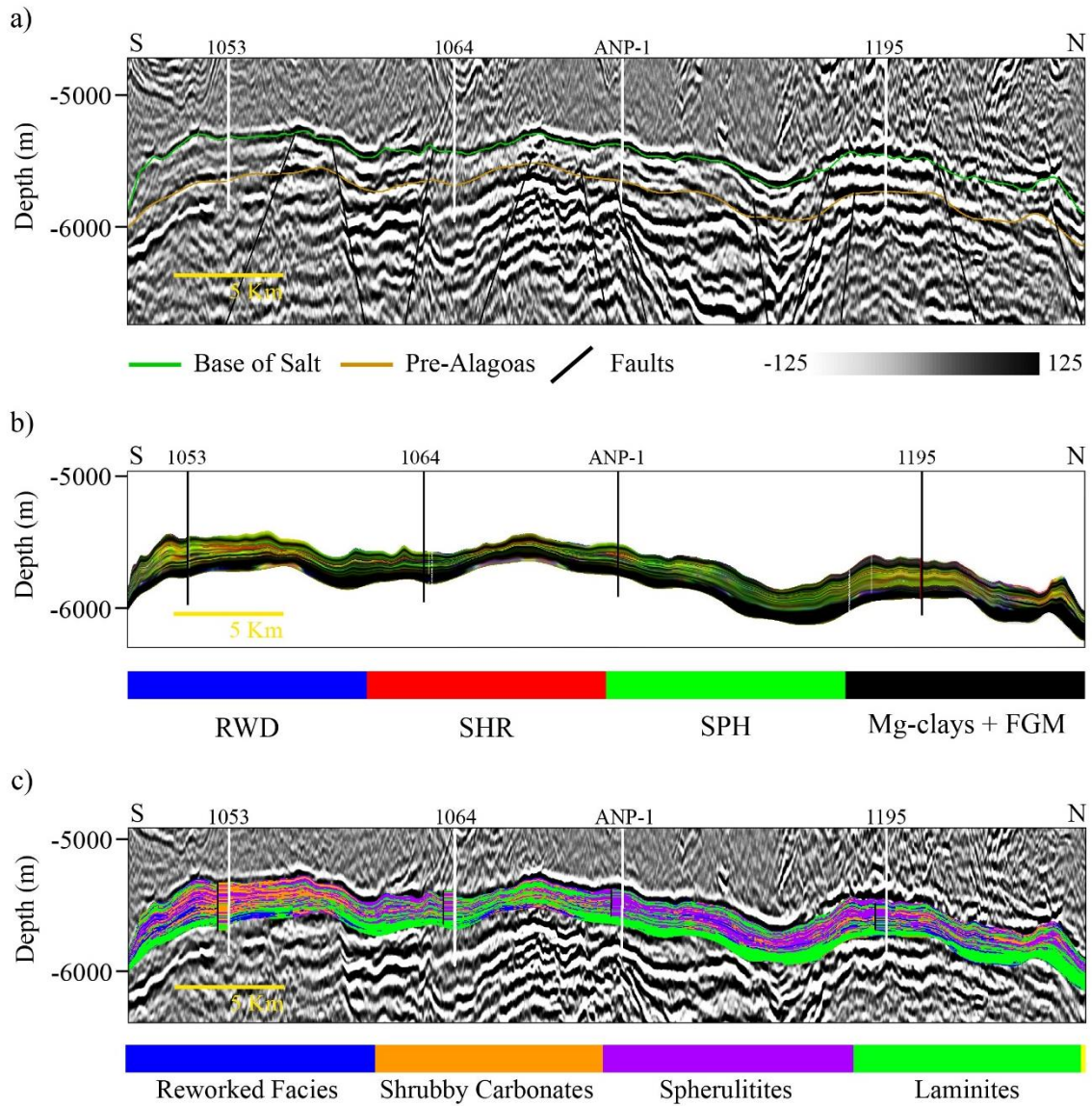


Figure 12: Results represented across arbitrary section line AB1 (location shown in Figure 2) for a) interpreted seismic section, b) carbonate geological process modeling and c) facies reconstruction using truncated Gaussian simulation with sediment proportion volumes as trends and lithology logs from wells (RWD – reworked sediments, SHR – shrubs, SPH – spherulitites and FGM – fine-grained muds).

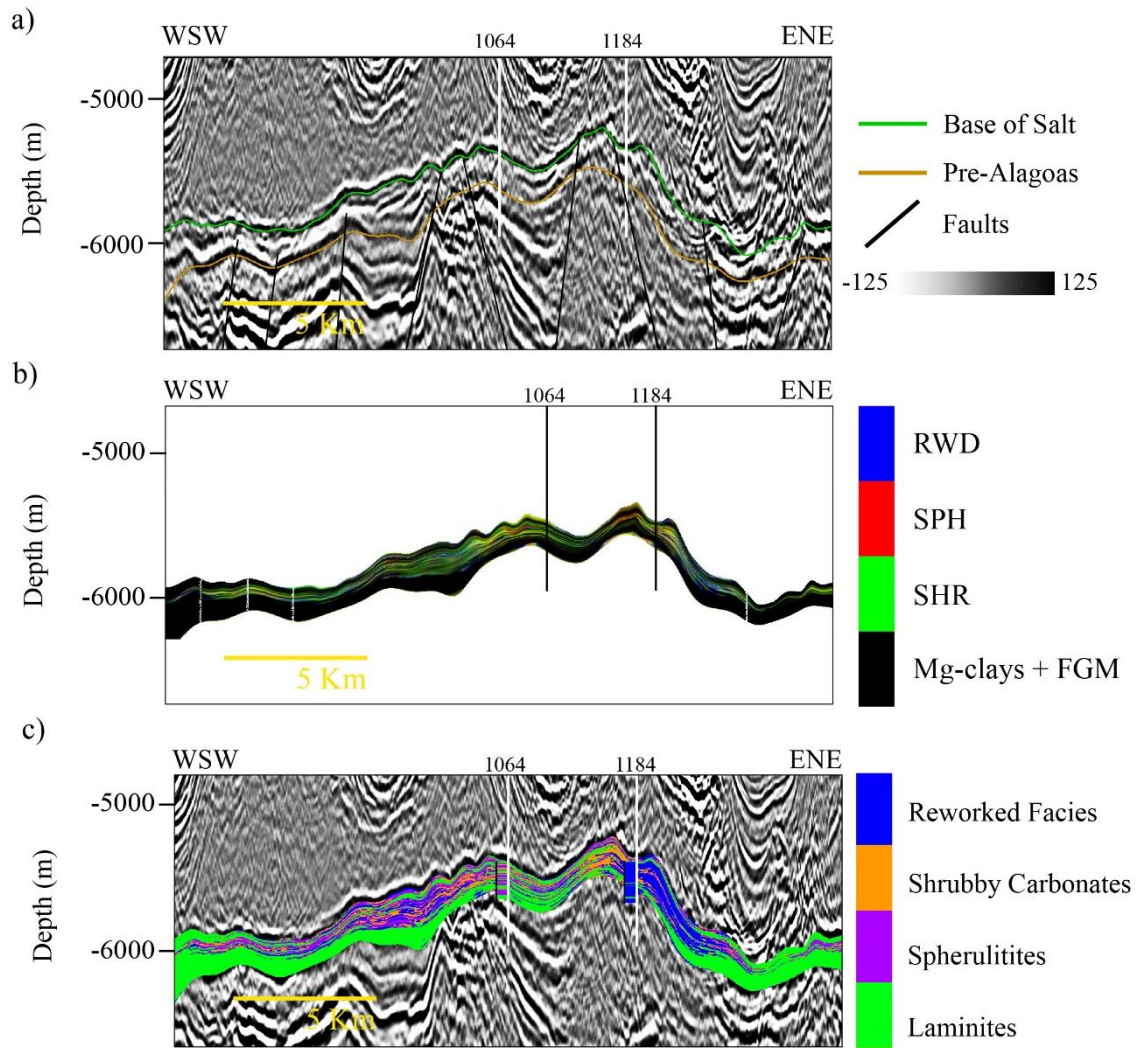


Figure 13: Results represented across arbitrary section AB2 (location shown in Figure 2) for a) interpreted seismic amplitude volume, b) carbonate geological process modeling and c) facies reconstruction using truncated Gaussian simulation with sediment proportion volumes as trends and lithology logs from wells (RWD – reworked sediments, SHR – shrubs, SPH – spherulites and FGM – fine-grained muds).

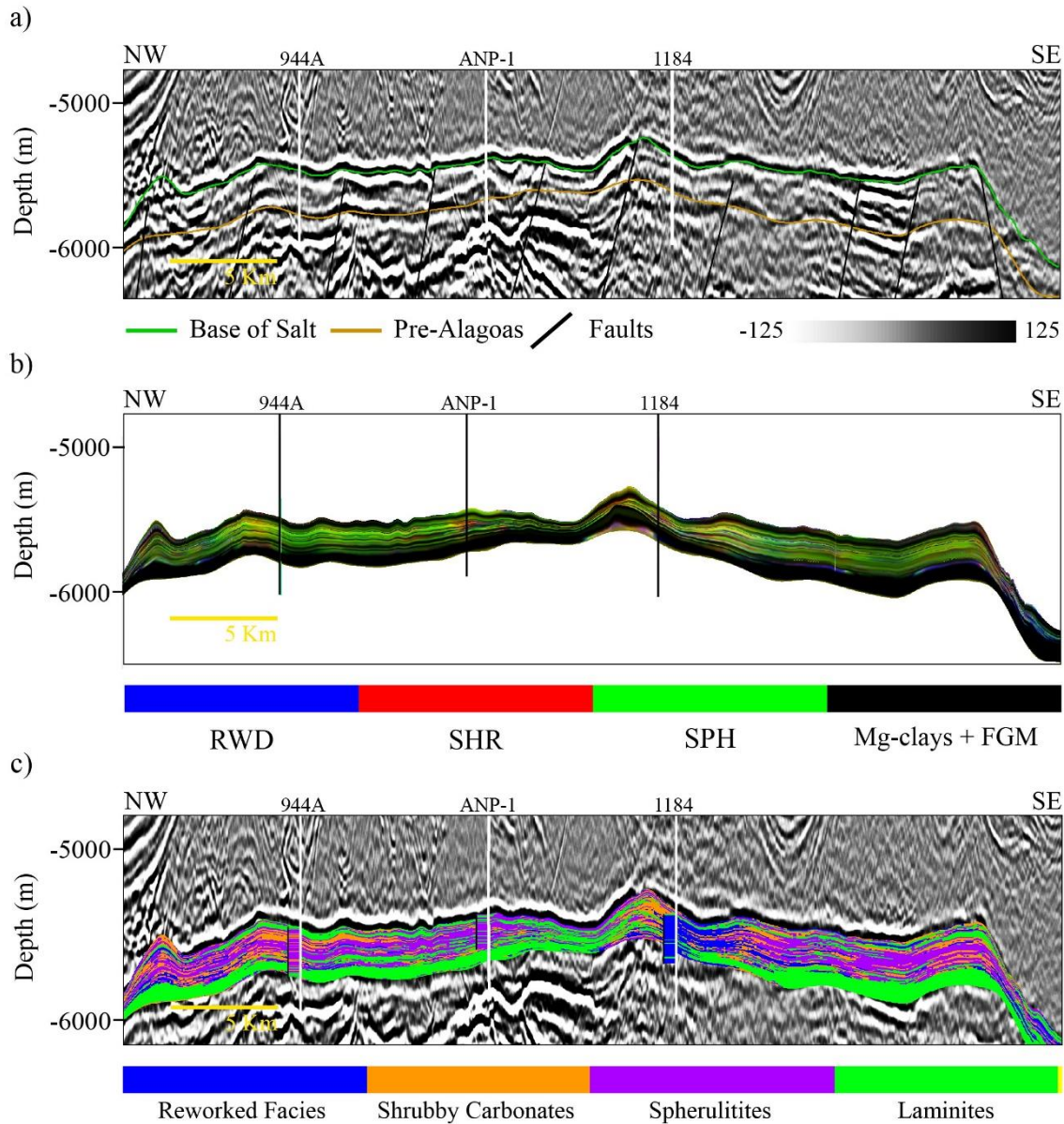


Figure 14: Results represented across arbitrary section AB3 (location shown in Figure 2) for a) interpreted seismic amplitude volume, b) carbonate geological process modeling and c) facies reconstruction using truncated Gaussian simulation with sediment proportion volumes as trends and lithology logs from wells (RWD – reworked sediments, SHR – shrubs, SPH – spherulites and FGM – fine-grained muds).

The carbonate geological process modeling in the sections (Figure 12b, Figure 13b and Figure 14b) and 3D view (Figure 15) show the predominance of fine-grained carbonate mud sediments, both in both the basal and uppermost portions of the Barra Velha Formation. In contrast the middle of the formation is dominated by in-situ carbonate sedimentation, with shrubs and spherulites. This corroborates with the high relative lake levels at the top and bottom of the simulated depositional interval, and the lower lake levels in the middle of the interval. This suggests that the creation of

accommodation and style of sedimentation were mostly governed by the fluctuations in lake level rather than by tectonic subsidence.

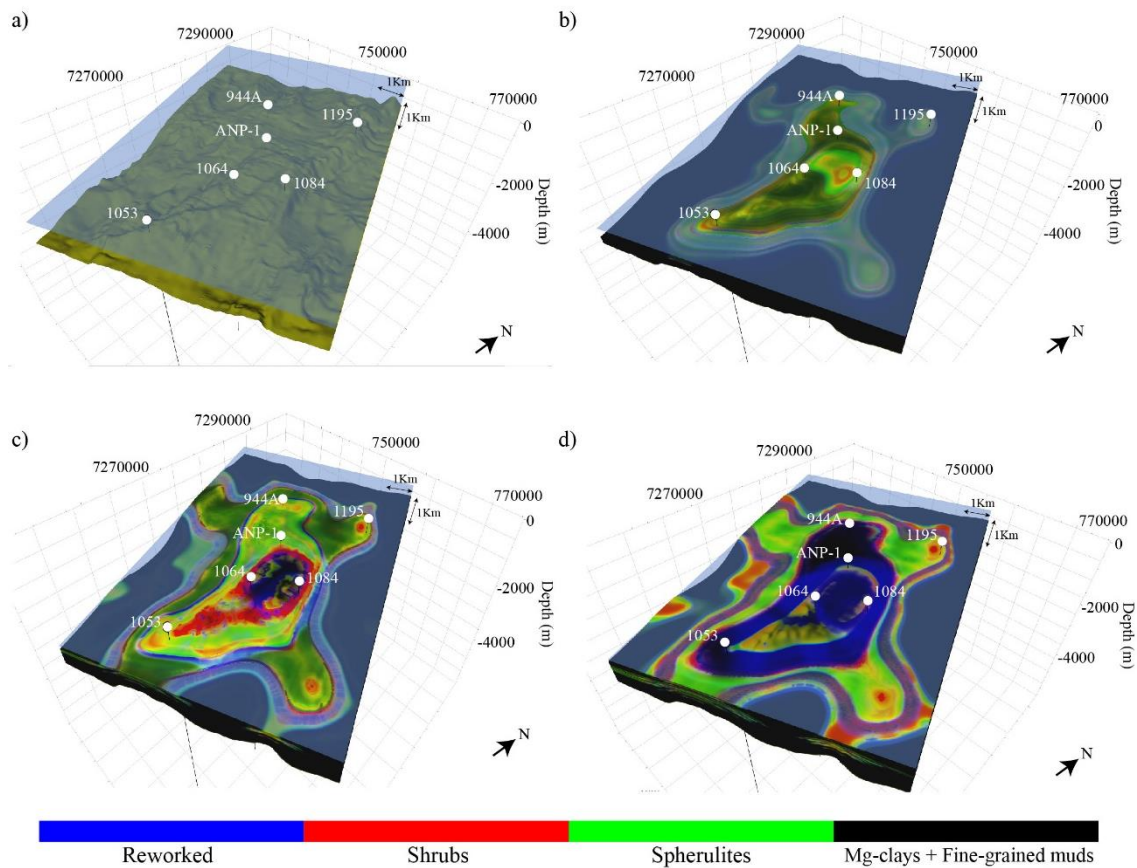


Figure 15: Geological process modeling results at a) 125 Ma, b) 121 Ma, c) 117 Ma and d) 113 Ma. Mean model (sediment) thicknesses for each time-step are: b) 104 m, c) 108 m and d) 258 m.

The seismic patterns observed in the seismic sections (Figure 12a, Figure 13a and Figure 14a) indicate that aggradational or progradational carbonate platforms are common on the flat or gently-dipping ramps of the structural highs. The most abundant sediments in these areas are either spherulites or intercalations of spherulites and shrubs. Spherulite and shrub sediments are also observed on the edges of the structural highs or in local highs, where domed-shape carbonate build-ups architectures are common or where the presence of clinoforms indicates the progradation of carbonate platforms. A greater proportion of shrubs sediments are present in the western portion of the Búzios Field. Reworked sediments, the product of diffusion, are also common especially in the structural lows near the fault borders where they are probably the result of the collapse of carbonate platforms and build-ups or wave erosion. The volume of reworked sediments

was underestimated by the geological process modeling especially when considering their common occurrence in wells such as well 1184 (Figure 4).

Muddier sedimentation, especially in the uppermost part of the formation, could be related to the deposition of Mg-rich clays in isolated structural lows within the main structural high of the study area. On the other hand, the muddier sediments found in the connected structural lows, where lake bottom seismic facies are also observed, were predominantly fine-grained carbonate muds. The carbonate geological process modeling indicates that the sediments at the well the locations are mostly spherulites with, less abundant intercalations of shrub sediments; a result that correlates well with the lithological logs shown in Figure 4.

The results of the truncated Gaussian simulation for facies reconstruction are presented in sections (Figure 12c, Figure 13c and Figure 14c) as a projection over the Base of Salt unconformity (Figure 16) and in a sliced 3D view (Figure 17). We used the sediment proportion volumes obtained from the carbonate geological process modeling as trends for facies reconstruction modeling. It is important to note that the upscaled lithological log from well 994A which was used as quality control, had a good Spearman correlation of 74% with the results of facies reconstruction along the well's trajectory.

Spherulites are the dominant lithology at structural highs and in places are intercalated with shrubby carbonates, especially in the western part of the study area. This corroborates with the conceptual sedimentary modeling and, consequently with the expected rock types for each seismic pattern observed in the study area. Also, in accordance with the geological process modeling, laminites are dominant in the basal portion of the formation in both the structural highs and lows. However, the muddier sediments present in the upper section are not as thick in the facies reconstruction, except in isolated lows within the structural highs which are possibly related to the deposition of Mg-rich clays.

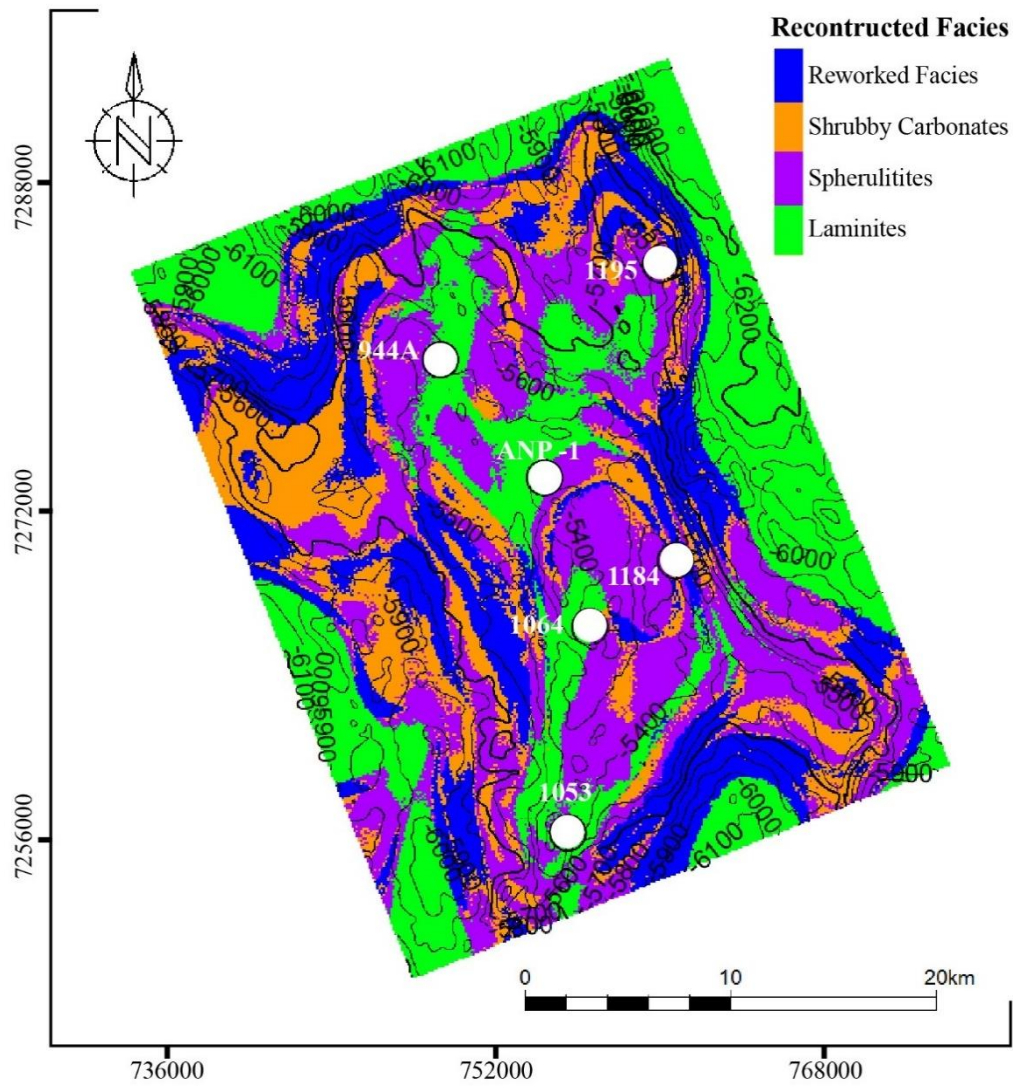


Figure 16: Results for facies reconstruction modeling in map view over the Base of Salt surface in the Búzios Field. White circles represent the well locations.

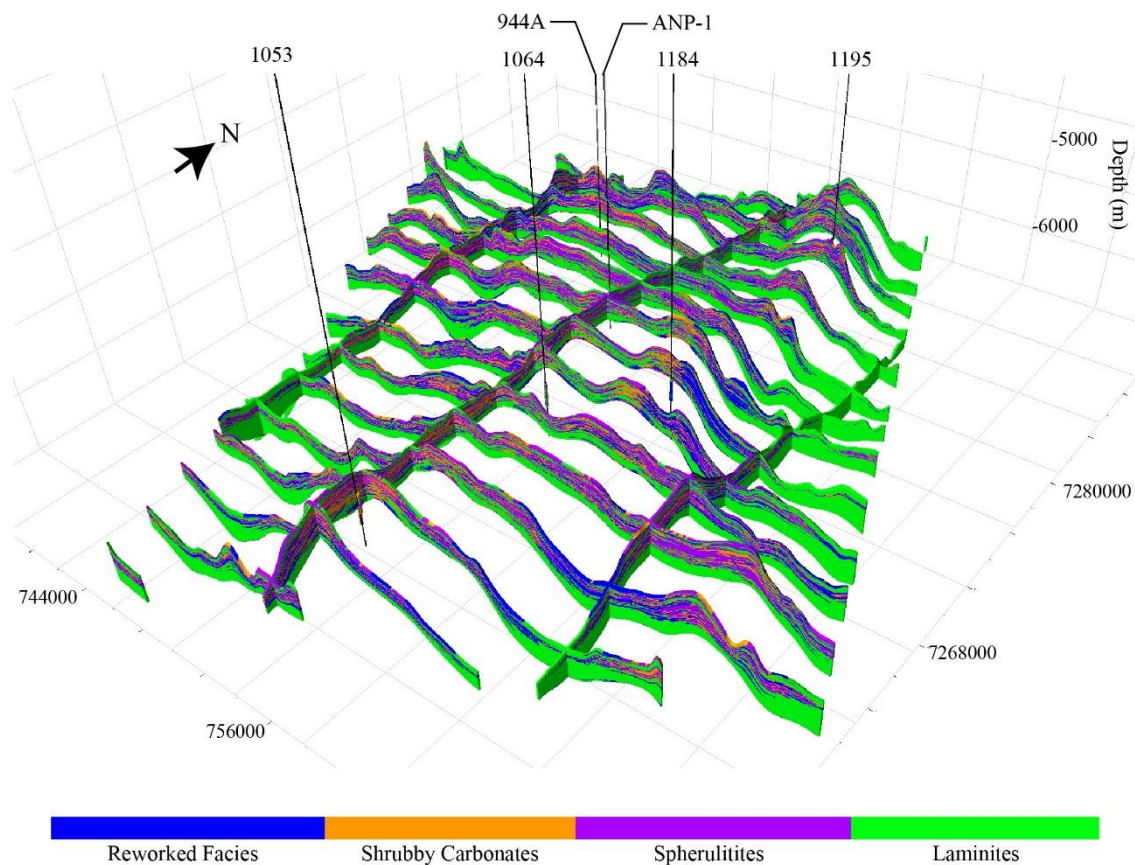


Figure 17: Results for facies reconstruction in 3D sliced view for the Búzios Field. Black lines represent the well traces.

The facies reconstruction shows high volumes of reworked sediments within structural lows near faults especially in western portion of the study area. This is possibly due to the use of the lithological logs from wells 1184 and 1195 as inputs for the geostatistics. However, in general the presence of reworked sediments was underestimated in the results of the geological process modeling. It is important to mention that the majority of the wells were sited in structural highs and both the lithological logs and the results facies reconstruction indicate that at those locations spherulitites intercalated with shrubby carbonates predominate, except for well 1184 which was drilled in a fault border where reworked facies predominate. The Barra Velha Formation facies succession is very well represented throughout the whole study area by the facies reconstruction results which show a shallowing upwards cycle from laminites at the base, transitioning to spherulitites followed by shrubby carbonates and culminating with laminites again.

2.5. Discussion

As stated by Della Porta (2015), there is still a lack of knowledge regarding the sedimentary processes that govern non-marine carbonate precipitation. Since they occur as a variety of types which are intrinsically related to the environment in which they form, they usually have specific geomorphological, geochemical and hydrologic characteristics. These unique genetic characteristics make them very different from marine carbonates in terms of origin and sedimentary dynamics (Alonso-Zarza and Tanner, 2010).

Consequently, it would not be productive to compare our results to forward stratigraphic modeling studies of marine carbonates such as the ones developed by Berra et al. (2016), Guerra (2016) and Lanteaume et al. (2018). One of the main reasons for this is the use of global sea level curves, such as Haq (2014), as the base level curve for these studies. Global sea level curves cannot be used for lacustrine environments since their base level is mostly influenced by variations in rainfall, surface flow and groundwater levels rather than sea level changes (Gierlowski-Kordesch, 2010).

Therefore, we can only compare our results with the work of Liechoscki de Paula Faria et al. (2017), which presented sedimentary models constructed for the upper section of the Barra Velha Formation at another presalt field in Santos Basin. It should be highlighted that any stratigraphic forward model is a simplification of the real geological environment, so no model can be regarded as a definitive statement on the dynamics of a depositional system (Burgess, 2006). The first point of comparison is methodological since Liechoscki de Paula Faria et al. (2017) did not integrate forward stratigraphic modeling with geostatistics for facies reconstruction of the presalt carbonates, as was undertaken in our study. Liechoscki de Paula Faria et al. (2017) used sedimentary 4D modeling solely and specified a constant subsidence rate for tectonic control across the whole area, as well as a single maximum growth rate of for all of the modeled carbonate facies with a growth multiplier per depth for the in-situ carbonate facies down to a depth of 80 m. The methodology presented in this study increases the level of complexity for the application of forward stratigraphic modeling to presalt carbonates since it is integrated with geostatistics permitting greater correlation with well lithological data. The forward stratigraphic modeling undertaken in this study is more complex in a number of aspects as parameters were introduced that take into consideration variations in tectonic activity across the Búzios Field, different maximum growth rates for carbonate deposition

for each of the modeled sediments as well as the addition of an areal growth scaling map as input for shrub precipitation to address its occurrence in the vicinity of faulting where hydrothermal activity is higher.

For the schematic sediment succession, we also considered that in-situ carbonate sediment precipitation is limited to shallower depths down to only 18 m. Our lake base level curve was derived from the DTCO well log for well ANP-1, whereas in the work of Liechoscki de Paula Faria et al. (2017) the lake level oscillation curves were derived from the carbonate lithological succession described in the wells.

The results obtained in this study can be compared with the best-fit model for their study area as selected by Liechoscki de Paula Faria et al. (2017). Their model and our proposed model are similar for the upper section of the Barra Velha Formation with both indicating the dominance of shrubby carbonates, presented as a stromatolite facies in their work. These carbonates mostly occur along the edge of structural highs associated with reworked sediments, which were presented as grainstones in their work. Fine grained laminite facies are dominant at the top of the formation, possibly related to occurrence of the Lula marker (V Paul Wright and Barnett, 2017; Neves et al., 2019a).

Our study is the first to forward model the entire Barra Velha Formation, which allowed us to analyze the paleoenvironmental evolution across the entire depositional interval. We observed that muddier facies dominate the lower section of the formation whilst the middle section is mainly dominated by in-situ carbonate rocks. Another contrast with Liechoscki de Paula Faria et al. (2017) is the occurrence in their model of spherulitic carbonates as deeper and low energy facies. This result reflects that in their study it was considered that the spherulites precipitate in the range from 25 to 80 m deep. In our results, laminites predominate in the deeper regions since we considered spherulite precipitation to only occur in shallower conditions³ ranging from 7 to 20 m.

Other advanced 3D reservoir characterization workflows have previously been applied to the Barra Velha Formation with evaluation based mostly on seismic attribute data and machine learning approaches such as those presented by Ferreira et al. (2019a), Ferreira et al. (2019b) and Jesus et al. (2019). These studies were successful in

³ It is important to note that the lower range for the precipitation of in-situ carbonate sediments in our study may be overestimating the predominance of laminites in the basal part of both our 4D sedimentary and facies reconstruction models.

discriminating presalt seismic facies such as carbonate build-ups/mounds, carbonate platforms and debris seismic facies. However, they could only infer the relationship of these seismic facies with lithological facies. This limitation is addressed in our modeling as we were able to not only correlate seismic facies with lithological facies but also with the dominant sediment types. Other limiting factors for these previous studies are the inherent difficulties in differentiating seismic facies associated with muddier lithological facies, as well as the poor resolution since seismic based methodologies are restricted by seismic resolution.

All modeling processes are attempts to reproduce the factual geology and as such they are always uncertain to some extent. In our geological process modeling results, it is inferred that sediment production was mainly controlled by water depth with only minor tectonic influence. This was the case for all sediment types except for shrub grains, for which an areal growth scaling map was also used as input for the simulation. This addressed the possible influence of hydrothermal activity in the vicinity on the production of shrub grains as suggested by Wright (2012), Wright and Barnett (2015), Wright and Tosca (2016), Saller et al. (2016) and Szatmari and Milani (2016).

A number of these aforementioned authors (e.g., Wright and Barnett, 2015, 2020; Szatmari and Milani, 2016), proposed that water geochemical dynamics played an important role in carbonate sediment precipitation in the presalt lacustrine paleoenvironment. However, this type of modeling was still not available in the algorithm used in this study for forward sedimentary modeling and consequently has not been considered in our modeling results. Nonetheless it is again worth noted that the areal scaling of shrub precipitation was included in the modeling process to account for differences in salinity or temperature caused by the interaction of hydrothermal fluids with the lake waters.

In addition, we acknowledge that there are some uncertainties related to the parameters used in the geological process modeling, especially for the lake base level curve and diffusion. It is difficult to calculate the real range and behavior of the lake base level curve and as such it could only be inferred after several simulation trials⁴. This is

⁴ Also, we would like to knowledge that there is some level of uncertainty associated to the used of the DTCO curve having as perspective that it correlates with the lithology logs from the available wells since the compressional slowness can also be affected by diagenetic effectes interfering on its used to derive a lake base level curve that should be related to the sedimentary process solely.

also the case for the diffusion parameters which relates to the erosion and transport of sediments. Intuitively, this parameter should be higher at the water-air interface but not as high for deep lake currents and windy layers, however the depths of occurrence of these latter processes are difficult to estimate. For that reason, they were randomly placed as high value peaks in the diffusion multiplier both above and below water surface (0 m).

Regarding the results of facies reconstruction, it was only possible to infer where laminites are composed mainly of deep water, fine-grained carbonate muds or of shallow water Mg-rich clays. This was because there is no differentiation between deep water and shallow water laminites in the lithological logs. Finally, we can infer from our results that greater wave action and hydrothermal activity in the western portion of the Búzios Field can be correlated with greater quantities of reworked facies in the structural lows and shrubby carbonate facies near faulted borders, respectively.

2.6. Conclusions

The application of an innovative integrated workflow of geological process modeling combined with geostatistical facies reconstruction by using a truncated Gaussian simulation to characterize the presalt carbonates of the Barra Velha Formation in the Búzios Field proved to be very effective. We achieved a better understanding of the sedimentological processes that govern the distribution of lithological facies within the Barra Velha Formation.

The correlation of seismic data with the integrated analysis of the geological process modeling and the results of the facies reconstruction successfully explained: 1) the seismic pattern of carbonate build-ups architecture, which occur at structural highs near fault borders or on isolated highs and are composed by in-situ carbonate grain sediments namely spherulites and shrubs leading to the intercalation of spherulitites and shrubby carbonate lithofacies; 2) the aggradational/progradational carbonate platform seismic pattern, which is observed on flat or gently dipping ramps of the structural highs and for which the dominant sediment type is spherulites as well as intercalation of those with shrubs in parts; 3) the debris facies seismic pattern, which occurs at the structural lows near fault borders and is dominated by reworked sediments and facies and 4) the lake bottom seismic facies which occurs within both connected and isolated structural

lows associated with dominantly fine-grained carbonate muds or Mg-rich clays forming laminite deposits.

The Barra Velha Formation chronostratigraphic lithological trend consists of a muddier basal succession that develops into a middle succession with the predominance of in-situ carbonates that becomes muddier towards the top of the formation. The results of the geological process modeling also suggest that oscillation of the lake base level curve had a greater influence than tectonic activity on sedimentation within the Barra Velha Formation. The western portion of the Búzios field presents greater quantities of shrubby carbonates on the structural highs, with reworked facies in the structural lows near fault borders. In contrast, the eastern portion is dominated by spherulitites often intercalated with shrubby carbonates.

The geological process modeling underestimated the impact of diffusion on the transport and reworking of sediments. However, this limitation was resolved during facies reconstruction through the use of lithological data from well logs. Facies reconstruction could only infer whether laminite facies were associated with Mg-rich clays or fine-grained carbonate muds as these sediment types were not differentiated in the lithological logs. Spherulitites, shrubby carbonates and reworked sediments were the most common lithologies encountered in wells and the facies reconstruction was able to satisfactorily represent the lithologies encountered in the quality control well 944A. Finally, we acknowledge the limitations of the proposed approach with a number of uncertainties identified in relation to modeling of water geochemical dynamics in addition to the estimation of the lake base level curve and diffusion parameters.

3. Seismic Pattern Classification Integrated with Permeability-Porosity Evaluation for Reservoir Characterization of Presalt Carbonates in the Buzios Field, Brazil

Article published in

Journal of Petroleum Science and Engineering, volume 201, 2021

Impact factor: 4.346

Authors: Danilo Jotta Ariza Ferreira, Raquel Macedo Dias and Wagner Moreira Lupinacci.

Abstract

This paper presents the application of an unsupervised neural network to classification of seismic facies based on a unique combination of stratigraphic and structural seismic attributes. This classification was integrated with statistical analysis of the porosity and permeability of the seismic facies which permitted the advanced reservoir characterization of the presalt carbonate reservoirs of the Barra Velha Formation in the Buzios Field, Santos Basin. This advanced approach is required due to the high degree of heterogeneity and complexity these reservoirs, which directly impacts on their porosity and permeability. Preconditioning of the seismic data was essential for filtering random and structurally oriented noise prior to the generation of seismic attributes. Four seismic attributes: acoustic impedance, rms amplitude, local flatness and principal dip component, were selected as the inputs for the unsupervised classification based on their capacity for differentiating between the observed seismic patterns within the Barra Velha Formation. Principal component analysis was then performed to decrease redundancy of the input seismic attribute data prior to classification. The analysis of amplitude seismic features as well as of the classification results allowed the identification of three different seismic patterns within the study area: build-ups, debris and aggradational/progradational carbonate platforms. The seismic attribute of principal dip component proved to be crucial for distinguishing between carbonate build-ups and debris seismic facies. Our results demonstrated that the build-up and debris seismic facies are commonly occur aligned

with faults, display higher porosity and permeability and as such they are inferred to be the best reservoirs.

3.1. Introduction

In recent years, the presalt carbonates from marginal Brazilian basins have gained worldwide recognition due their importance as the principal reservoirs of a number of giant fields. As of August 2020, these reservoirs were producing 2.2Mbo/day which represents 98% of the production from the Santos Basin, the most prolific Brazilian oil and gas basin (ANP, 2021).

The Barra Velha Formation represents the uppermost section of the presalt carbonates within the Santos Basin and was deposited within an alkaline-lacustrine paleoenvironment during the late rift and sag phases of the Aptian (Moreira et al., 2007; Wright and Barnett, 2015). Carbonate precipitation occurred mainly controlled by chemical processes (Wright, 2012; Wright and Barnett, 2015; Wright and Tosca, 2016; Wright and Barnett, 2017) and rift faults, that acted as paths for hydrothermal vents, as well as meteoric water, that lixiviated the surrounding basaltic terrains, both fed the lacustrine waters with alkalis and CO₂ (Szatmari and Milani, 2016).

The Barra Velha Formation (Fm.) is typically composed of varying proportions of different sediments: shubs, spherulites, carbonate muds and Mg-rich clays. Lithotype classification varies depending on the origin and composition of the component sediments but lithotypes can be divided into three main groups: mudstones, in situ carbonates and reworked carbonates (Terra et al., 2010; Pereira et al., 2013; Rezende and Pope, 2015; Wright and Barnett, 2015; Farias et al., 2019; Gomes et al., 2020). In situ carbonate rocks represent the proximal lacustrine facies and are represented by shrubby carbonates, spherulitic carbonates and laminites which may all be reworked into grainstones. Mudstones represent the distal (deep water) facies of the Barra Velha Formation. It should also be highlighted that volcanic rocks occur in places intercalated with these lacustrine lithologies (Fornero, Marins, Lobo, Freire, and E.F. de Lima, 2019; Penna and Lupinacci, 2020).

The seismic patterns associated with the lacustrine carbonates of the Barra Velha Fm. are: (1) carbonate platforms on structural highs with parallel to sub-parallel reflectors; (2) carbonate build-ups with convex-up concordant internal reflections either along the footwalls of normal faults or on isolated highs, (3) debris or reworked seismic

facies on the hanging wall side of normal faults characterized by clinoform geometries and (4) deep lake facies within the structural lows with weak parallel to sub-parallel or absent reflectors (Buckley et al., 2015; Kattah and Balabekov, 2015; Saller et al., 2016; Ferreira et al., 2019a; Jesus et al., 2019; Neves et al., 2019; Zalán et al., 2019).

Due to the complex depositional history and compositional heterogeneity of the Barra Velha Fm., advanced techniques are required for reservoir characterization combined with robust analysis and interpretation sustained by an in-depth understanding of conceptual depositional models (Johann et al., 2012; Johann, 2013; Bruhn et al., 2017). An effective and promising advanced technique for the characterization of seismic facies within presalt carbonate reservoirs is unsupervised classification by a multi-attribute neural network. Johann et al. (2012) proposed a methodology based on self-organized maps with the use of seismic attributes as inputs for the unsupervised classification of seismic facies in a presalt reservoir area. Their results indicated a good correlation between the best classified facies and well placement.

Jesus et al. (2019) also adopted a similar approach through the use of a neural network to undertake unsupervised seismic classification which resulted in the effective mapping of individual geobodies representing the carbonate mounds within a presalt field. These authors also employed a self-organizing maps methodology with the inputs being the seismic attributes of coherence, curvature and hybrid spectral decomposition within the Barra Velha Formation interval. Ferreira et al. (2019a) used a k-means clustering approach with envelope and acoustic impedance as stratigraphic attributes and high resolution eigen coherence as a structural attribute for unsupervised seismic facies classification in a presalt field located on the Outer high of the Santos Basin. Their results allowed the differentiation and mapping of aggradational/progradational carbonate platforms, carbonate build-ups and debris seismic patterns throughout the study area. The carbonate build-up seismic facies were inferred as having the highest porosity and permeability with well information.

The Buzios Field is a giant oil field operated by Petrobras is the second largest Brazilian oil field and is located within the Santos Basin (Figure 18). This field accounts for 26% of the total production from the Santos Basin, with total estimated oil reserves of approximately 30 Bbo (ANP, 2016, 2021). Castro and Lupinacci (2019) performed a petrophysical evaluation of reservoirs within the Barra Velha Fm. and the Itapema Fm

encountered within a well drilled in the Buzios Field. They highlighted the presence of fine grains intercalated with carbonate rocks that have a negative impact on reservoir quality. They proposed a division of the Barra Velha Formation sag phase into a lower and upper sag with the lower section being characterized by a greater stevensite clay content. They established that the mean effective porosity for the Barra Velha Fm. was around 8% in the studied area.

Dias et al. (2019) performed an acoustic inversion of both the Barra Velha and Itapema Formations across the Buzios Field aiming to infer the relationship between acoustic impedance and porosity. They identified, a strong correlation between these two properties for the Barra Velha Formation, however two main trends were observed. One for the upper sag and upper rift sections, and another for the lower sag section, due to the presence of stevensite clays in the lower interval.

Ferreira et al. (2019b) proposed a multi-attribute, unsupervised neural network classification of the Barra Velha Formation interval within the Buzios Field. They were able to individualize carbonate build-ups and aggradational/progradational carbonate platform seismic patterns. However, the debris facies could not be discriminated from the other seismic facies using the selected seismic attributes.

In this paper, we propose the use of an unsupervised artificial neural network algorithm to perform seismic facies classification based on a unique combination of stratigraphic and structural seismic attributes. This classification is then integrated with porosity and permeability logs from the Barra Velha Fm. to improve the efficiency of reservoir characterization within the Buzios Field. By doing so, we aimed to effectively identify and individualize three seismic patterns – build-ups, carbonate platforms and debris – and also assess their reservoir potential without the need for geostatistical modeling.

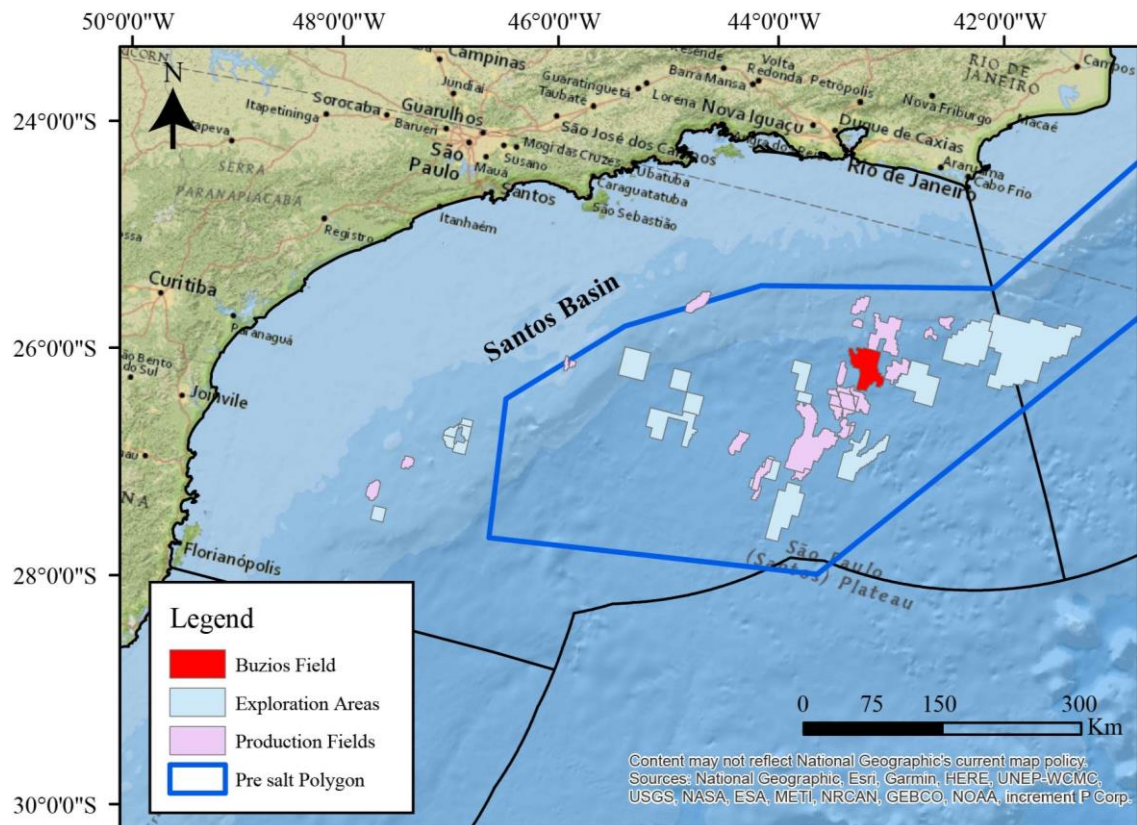


Figure 18: Location of the Buzios Field within the Santos Basin.

3.2. Method

The data available for this study consists of 770 km² of 3D post-stack depth migrated seismic (PSDM) and porosity and permeability well logs from 15 wells within the Buzios Field. We mapped the base of salt (upper Aptian age) and the Pre-Alagoas (lower Aptian age) unconformities – that represent, respectively, the top and bottom of the Barra Velha Fm. interval. The main faults were also mapped across the study area. Figure 19 shows the data coverage across the study area including well location, depth contours of the base of salt unconformity and the location of the seismic sections are presented in this study.

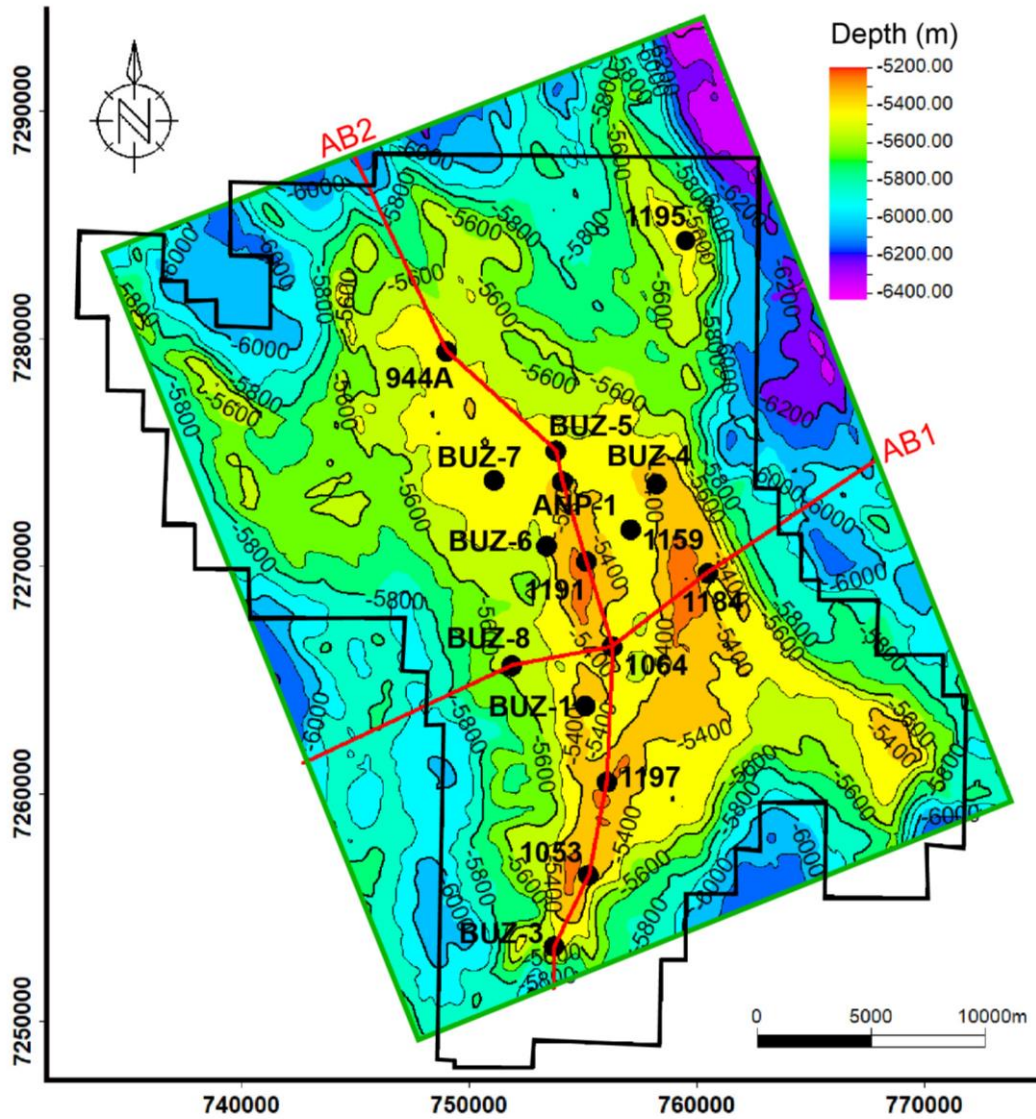


Figure 19: Map view of the base of salt interpreted seismic horizon (depth contours) across the Buzios Field (black polygon) with the coverage of the 3D Seismic data shown by the green rectangle and well locations shown by black circles. The red lines show the location of the arbitrary seismic lines (AB1 and AB2) presented in this study.

Our methodology can be divided into two stages: (1) identification of the principal seismic patterns and selection of the seismic attributes to be used as input for the (2) neural network unsupervised seismic facies classification and integration with permeability-porosity evaluation. A simplified methodology flowchart is presented in Figure 20.

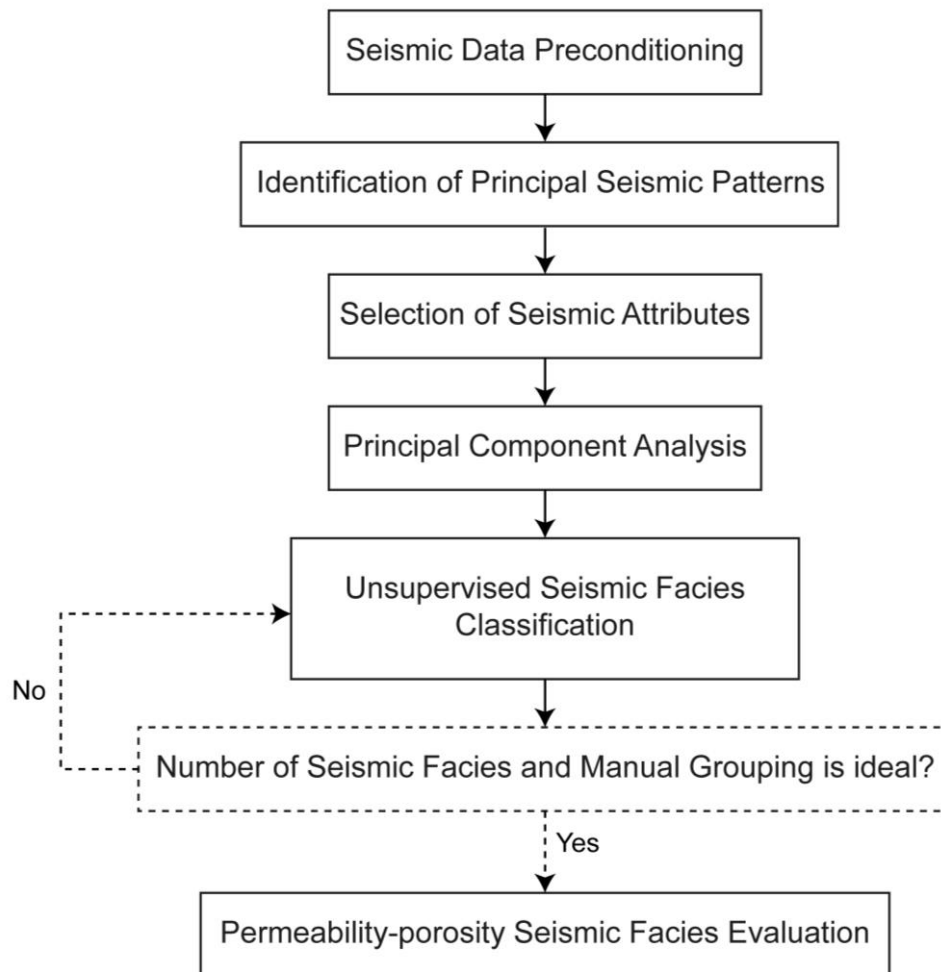


Figure 20: Simplified methodology flowchart.

Identification of the principal seismic patterns and selection of seismic attributes

Prior to the identification of the main seismic patterns and selection of the seismic attributes to be used as inputs for the neural network classification, preconditioning of the seismic data was undertaken. This was achieved through the use of a structural smoothing filter (Hale, 2009) to reduce the influence of structurally oriented noise followed by a median filter (Huang et al., 1979) to reduce random noise. The resulting combination of these two filters was effective for partial removal of both oriented and random noise thus increasing the signal-to-noise ratio (Figure 21).

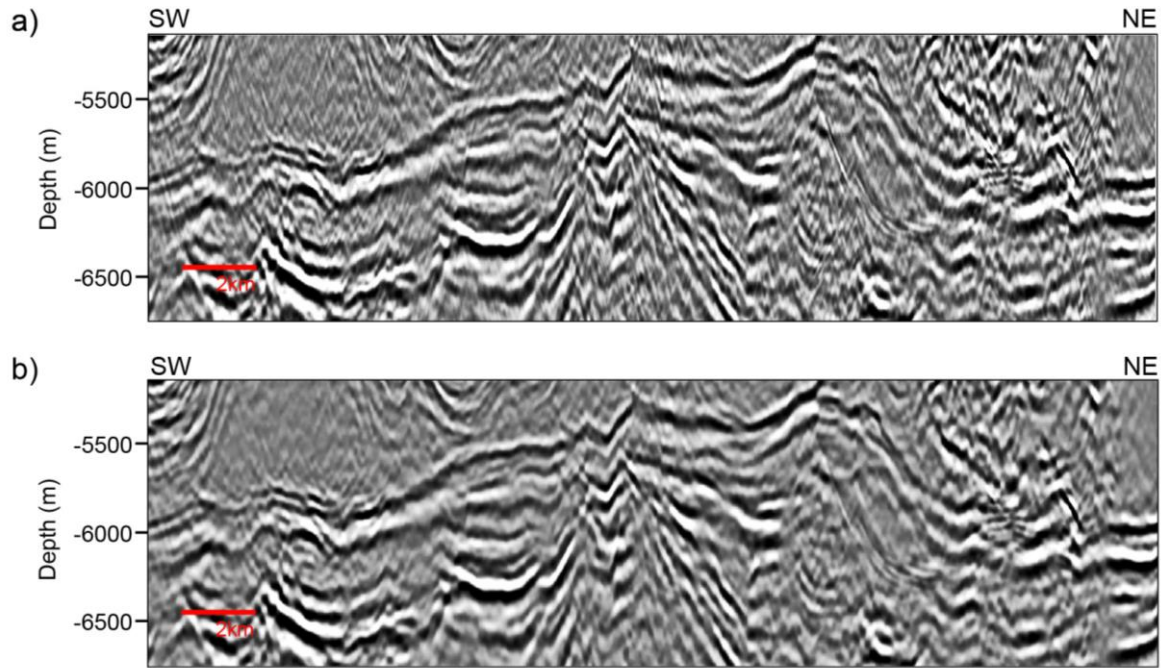


Figure 21: Preconditioning to remove random and structurally oriented noise effects. a) Original seismic data; b) Preconditioned seismic data.

Carbonate build-ups, debris and aggradational/progradational carbonate platforms are the principal seismic patterns identified within the Barra Velha Fm. in the study area. Their characteristics were analyzed in the original seismic volume to build a conceptual geological model which was used to guide later interpretation of the seismic facies obtained by the unsupervised neural network classification (Figure 22).

We analyzed the response of several seismic attributes⁵ as extracted from the preconditioned seismic data based on amplitude, phase and frequency or a combination of these components to identify stratigraphic and structural characteristics that could be used to differentiate and map the seismic patterns in the study area, as proposed by Ferreira et al. (2019a); Ferreira et al. (2019b) and Jesus et al.(2019).

We chose two stratigraphic seismic attributes and two structural seismic attributes as inputs for the unsupervised classification:

⁵ The seismic attributes that had their feasibility analyzed for this study included coherence, 3D curvature, chaos, spectral decomposition, relative acoustic impedance, consistent dip, amongst others. However, we chose the ones cited in the thesis and published paper based on their qualitative capacity to discriminate the seismic facies identified in the original amplitude volume. It is also important to highlight that many of the tested seismic attributes somewhat correlated to one of the ones for the analysis.

- Acoustic impedance stratigraphic attribute, which usually correlates well with lithological signatures and was obtained using the inversion algorithm proposed by Russell and Hampson (1991, 2006) and Barclay et al. (2008);
- Rms amplitude stratigraphic attribute, extracted using the method proposed by Taner et al. (1979) and which is sensitive to abrupt changes in acoustic impedance;
- Local flatness structural attribute that maps the flatness of reflectors, that are not necessarily horizontal, thus revealing vertical anomalies (Randen and Sønneland, 2005; Pereira, 2009);
- Principal dip component structural attribute (Randen et al., 2000) that calculates the principal eigenvector normal to the local dip, thus revealing a smoothed dip gradient of reflectors.

The stratigraphic and structural characteristics highlighted by the seismic attributes for each of the identified seismic patterns is shown in Figure 22. The expression of these attributes along an individual seismic trace extracted along the trajectory of the ANP-1 well, is shown in Figure 23.

Carbonate build-ups are characterized by domical shaped reflectors and chaotic internal reflectors with high local flatness values highlighting internal discontinuities. The carbonate build-ups present low to intermediate rms amplitude values related to the intercalation of a few high amplitude internal reflectors. This corroborates with acoustic impedance which usually presents low to intermediate values for this seismic pattern. The principal dip component shows a variation between high and low dips, probably related to internal chaoticity.

The debris seismic pattern displays a clinoformal shape in the seismic amplitude volume and can often display chaotic internal reflectors. This pattern is characterized by high local flatness values whilst the values for rms amplitude and acoustic impedance are low, indicating only minor intercalation of lithologies. Intermediate to high values are obtained for the principal dip component attribute as expected for a dipping seismic pattern which occurs in faulted areas.

In the seismic amplitude volume, the aggradational/progradational carbonate platforms are characterized by an intercalation of parallel to sub-parallel reflectors with onlap and downlap truncation where progradations occur. Low local flatness values indicate good reflector continuity. Both the rms amplitude and acoustic impedance

attributes display an intercalation of high and low values, suggesting a reasonable degree of lithological variation. The principal dip component attribute shows very low values across carbonate platforms corroborating with the horizontal continuity observed in the seismic amplitude volume.

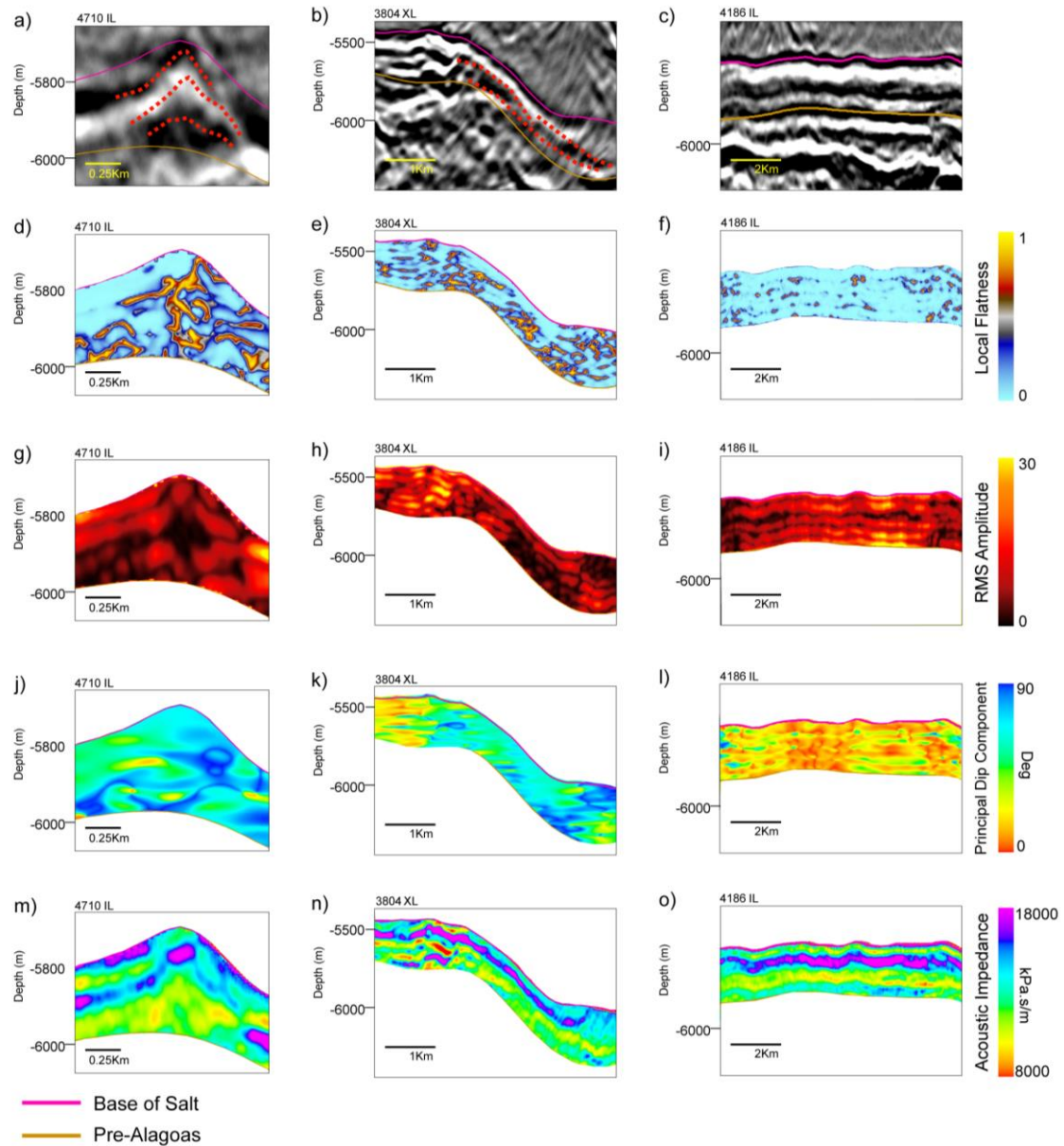


Figure 22: Principal seismic patterns identified within the Barra Velha Fm. interval - Typical seismic amplitude for a) carbonate build-ups (IL4710), b) debris and c) aggradational/progradational carbonate platforms as observed within IL4710, XL3804 and IL4186 respectively. Note: IL - Inline, XL - crossline. Selected seismic attributes for the same seismic patterns: local flatness in d), e) & f); rms amplitude in g), h) & i); principal dip component in j), k) & l), and acoustic impedance in m) n) & o).

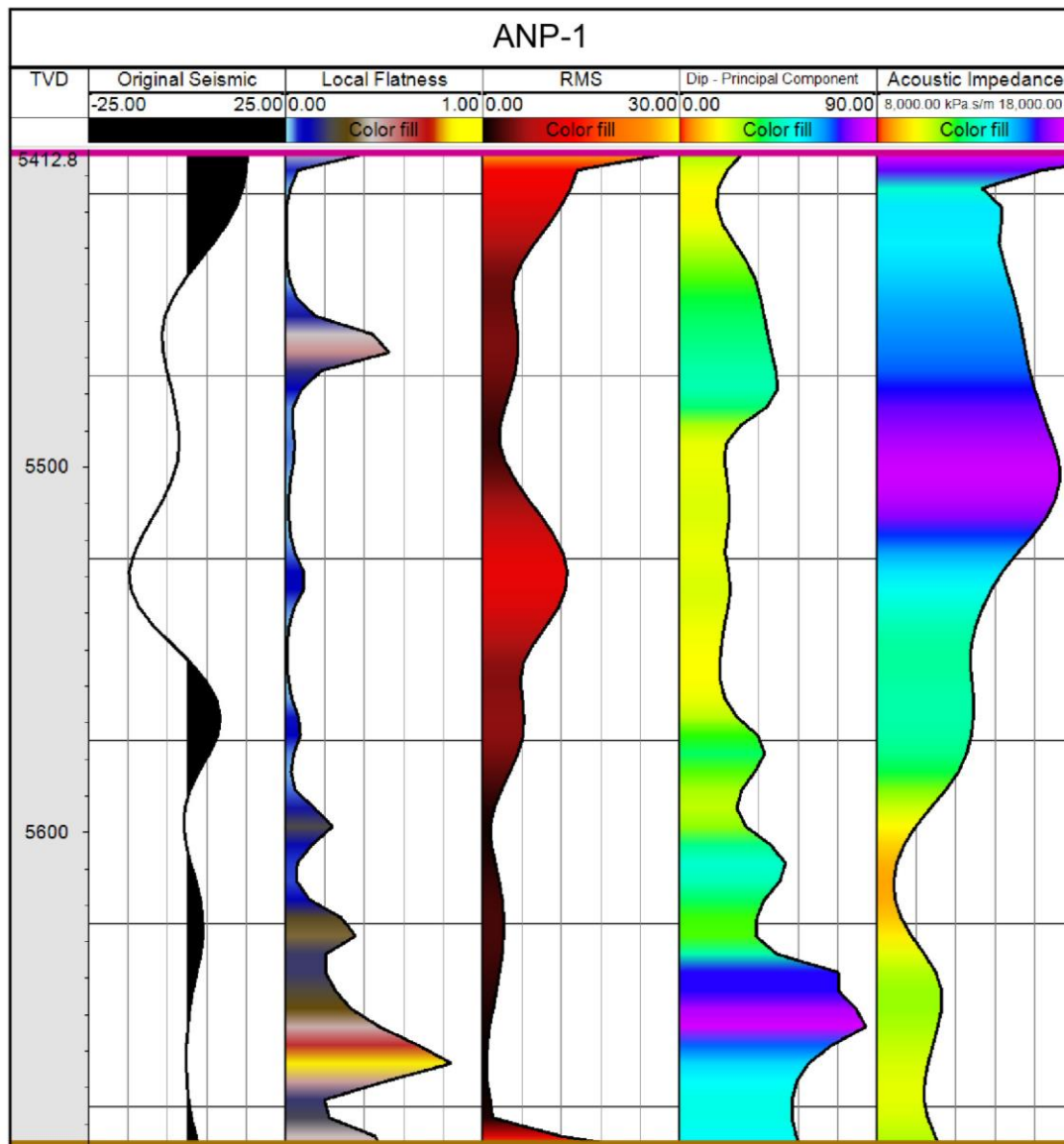


Figure 23: Seismic trace expression for each of the selected attributes used as input for the unsupervised neural network seismic facies classification. The seismic trace was extracted along the ANP-1 well trajectory within the Barra Velha Fm. interval. From left to right, preconditioned seismic trace, local flatness, rms amplitude, principal dip component and acoustic impedance.

Unsupervised Neural network seismic facies classification integrated with permeability-porosity evaluation

The neural network technique was first developed by McCulloch and Pitts (1943), based on the dynamics of brain learning process where the input of external stimulus activates a specific groups of neurons based on their affinity to that type of stimulus. As

defined by Du and Swamy (2014), the output of each neuron is given by the following equation:

$$y = \phi \left(\sum_{i=1}^{J_1} w_i x_i - \theta \right), \quad 4.1$$

where y is the output of a neuron, w_i is the link weight from the x_i input, θ is a threshold or bias, J_1 is the total number of inputs and $\phi(\cdot)$ is the activation function that is usually a continuous or discontinuous function between the interval of $(-1,1)$ or $(0,1)$.

Prior to the unsupervised classification, a principal component analysis was performed using the seismic attribute volumes as input. This linear transformation aims to create principal component volumes or major variance direction volumes to be used as inputs in the neural network, therefore reducing redundancy (Hotelling, 1933; Zhao et al., 2015). As defined by Zhao et al. (2015), the first principal component is extracted from the sample space composed of the seismic attribute volumes given as inputs and best represents the seismic attribute patterns. The first principal component is then subtracted from the original sample space and another principal component is extracted from the residual sample space. This process continues until the number of principal components generated from the sample space is equal to the dimensions of the original sample space. For our work we used all four principal component volumes generated from the selected seismic attributes sample space as inputs for the unsupervised neural network.

A multi-layered perceptron network with lateral connections for inhibition architecture and competitive learning method (Russell and Norvig, 2010; Du and Swamy, 2014) was used in this study to discriminate between the five different seismic facies. Competitive learning is based on the clustering principle, where input data is subdivided into a number of user defined clusters according to data similarity identified by the algorithm. We defined the ideal number of facies as 7 after a series of trial and error attempts with 3 to 10 facies.

The seismic facies classification volume was analyzed for greater geological understanding and the classified facies were then manually grouped into 3 classes (build-up, debris and aggradational/progradational carbonate platforms) in accordance with the seismic patterns identified in amplitude seismic data. The ideal number of facies and grouped facies classes was chosen based on the capacity of these two steps to differentiate

between facies and map the different seismic patterns identified by stratigraphic analysis of the original seismic data.

The unsupervised classification volume was then used to build probability of occurrence and zonation maps for the seismic patterns in the study area. These maps allowed the identification and delimitation of the most likely occurrences of each of the classified facies within the Barra Velha Fm. interval. Total porosity and permeability histograms and cross-plots were generated for each of the seismic facies based on the available well log information to qualitatively evaluate their reservoir potential within the Buzios Field.

3.3. Results and Discussions

The evaluation of the identified seismic patterns and the results of the seismic facies classification are presented as seismic sections in Figure 24 and Figure 25, in map view projected over the base of salt unconformity in Figure 26 and as a sliced 3D view in Figure 27.

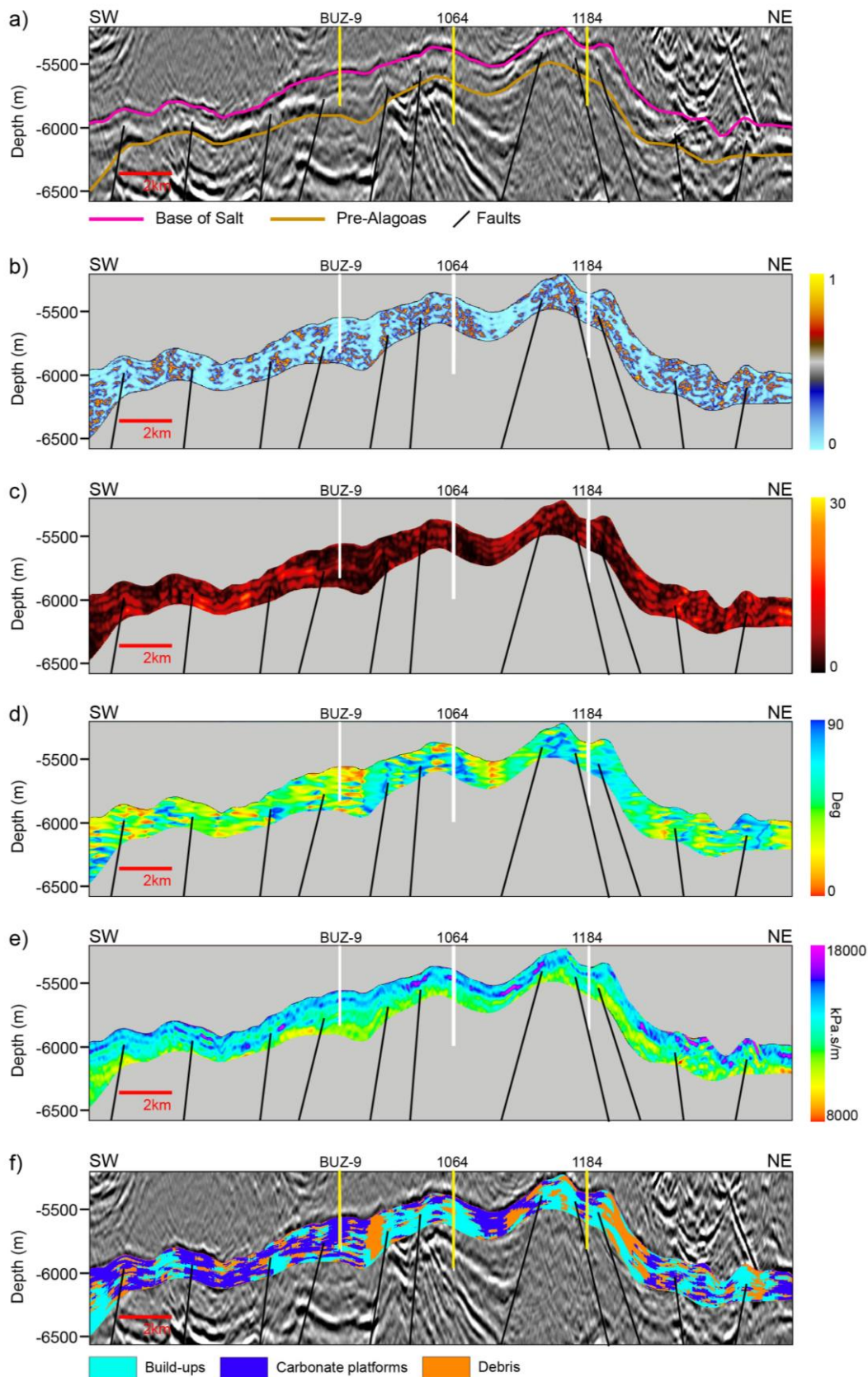


Figure 24: Preconditioned seismic section (a) from the 3D seismic volume along arbitrary line 1 (AB1) with the values of b) the local flatness attribute c) the rms amplitude

attribute; d) the principal dip component; e), the acoustic impedance attribute for the Barra Velha Formation; f) results of the seismic facies classification of the Barra Velha Fm overlain on the filtered seismic data. Well paths are shown by the yellow or white lines and faults by the black lines. As can be noted, build-ups are mostly concentrated on the footwall side of normal faults and are laterally associated with the debris seismic facies which tend to occur on the hanging wall side of faults.

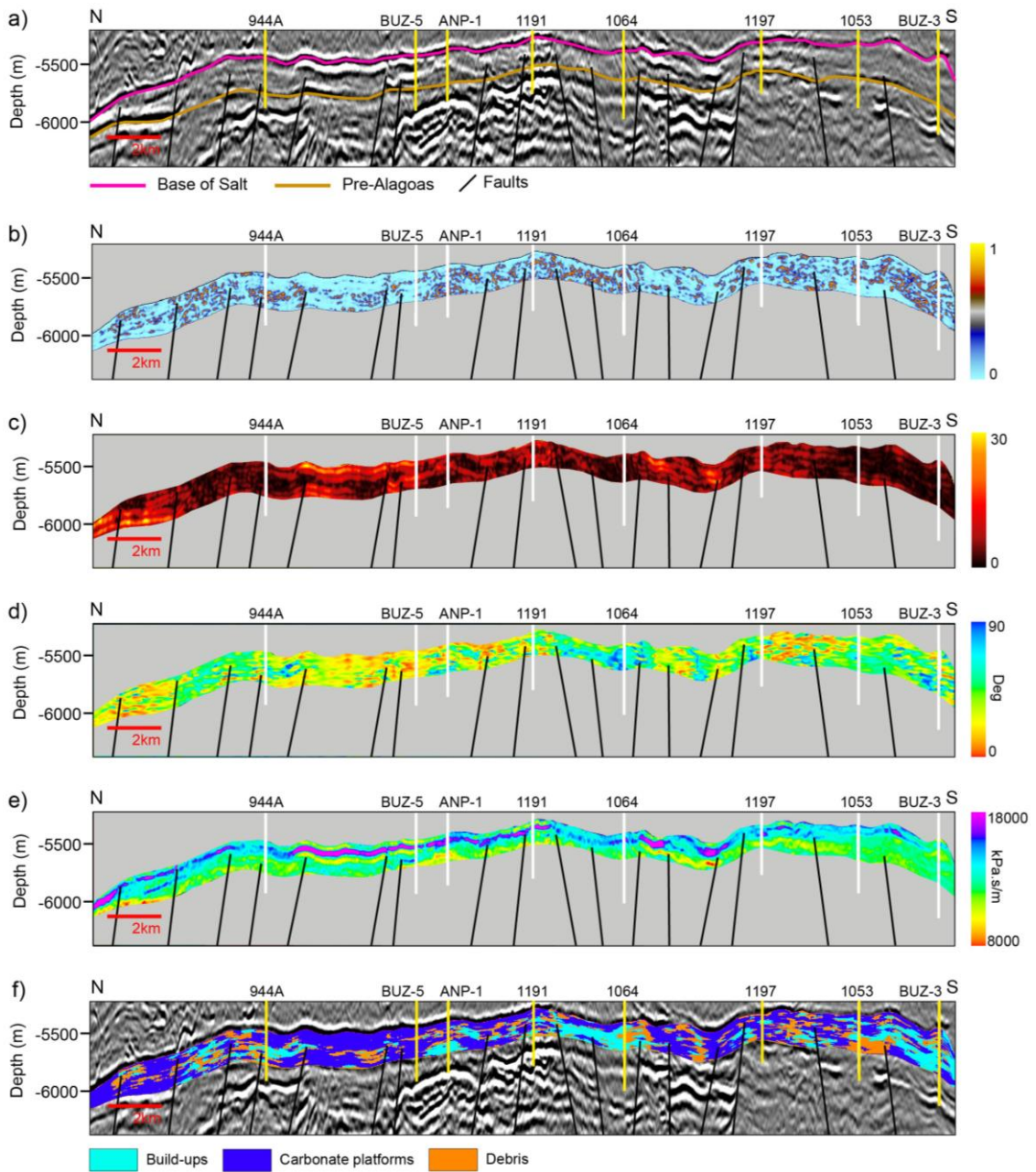


Figure 25: Preconditioned seismic section (a) from the 3D seismic volume along arbitrary line 2 (AB1) with seismic attributes shown for the Barra Velha Formation interval: b) local flatness attribute; c) rms amplitude attribute; d) principal dip component attribute;

e) acoustic impedance attribute and f) the results of the seismic facies classification for the same interval. Faults are shown by black lines and well paths by the yellow or white lines. It should be noted that the aggradational/progradational carbonate platforms are the dominant seismic facies in stable areas of structural highs away from their faulted margins.

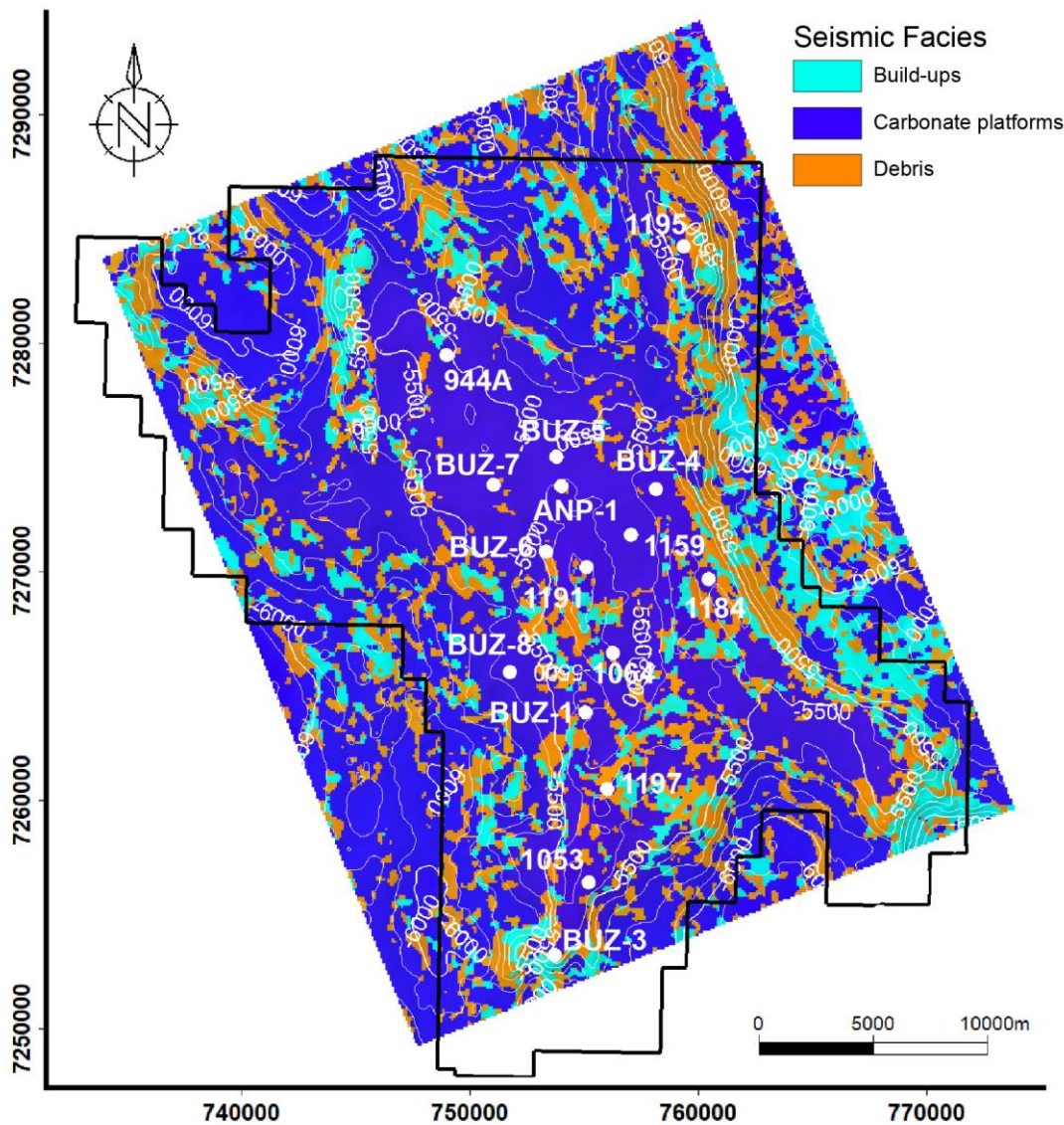


Figure 26: The results of the seismic facies classification presented in map view over the base of the salt unconformity (top of the Barra Velha Fm.) shown. Well locations are represented by the white circles and the black polygon shows the limits of Buzios Field.

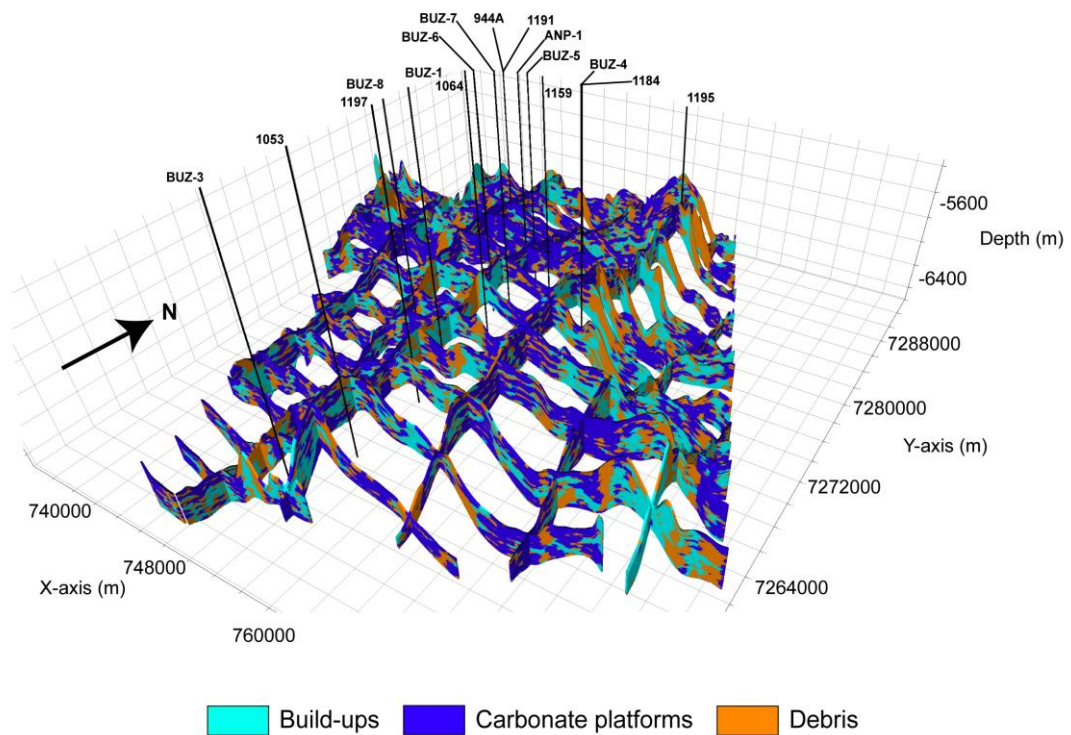


Figure 27: Sliced 3D view of the results of the seismic facies classification across the study area. Well paths are shown by the black lines. The build-up and debris seismic facies are more common within the western part of the Buzios Field associated with major faulting.

Aggradational/progradational carbonate platforms are the dominant seismic facies across the Buzios Field, in particular on structural highs away from faulted areas, within local structural lows and in the deeper portions of the study area. As expected, these seismic facies display high local flatness values related to subhorizontal reflectors and the intercalation of contrasting reflectors as evident in both the rms amplitude and acoustic impedance. These characteristics and associated seismic attributes were essential for the delimitation of this seismic facies by the unsupervised neural network.

We can infer that the carbonate platform seismic facies commonly contain intercalations of different lithologies; likely to be represented by low scale shrubby carbonates, spherulitic carbonates and laminites. It is expected that the shrubby and spherulitic carbonates would be more common on the structural highs, with laminites within local structural lows and in the deeper parts of the Barra Velha Formation.

Build-up seismic facies are less abundant in the study area and often occur as N-S aligned features subparallel to the main direction of faulting. The carbonate build-ups

are either located near faulted areas on the main structural highs or at local highs isolated by faulting within the deeper portions of the Barra Velha interval. These seismic facies display chaotic internal reflectors in original amplitude data and as such is associated with lower flatness (higher local flatness attribute values). Reflectors within these facies either display dips of greater than 80° or less than 45° . The carbonate build-ups consistently display intermediate to high impedance values and no response for the rms amplitude signal; characteristics which were important for their discrimination. A predominance of shrubby and spherulitic carbonates can also be inferred for these seismic facies related to hydrothermal activity as suggested by Wright (2012), Wright and Barnett (2015) and Zalán et al. (2019).

The debris seismic facies are generally laterally associated with carbonate build-ups and as such they also occur as N-S aligned features but on the hanging wall side of normal faults. The use of the principal dip component seismic attribute as input for unsupervised classification was essential for the differentiation of this seismic facies from the carbonate build-ups. The debris seismic facies display consistently intermediate to high dip values even where they presented similar values to the carbonate build-ups for the other seismic attributes. We infer that the debris seismic facies consist of reworked sediments in the form of grainstones with clasts sourced from the insitu carbonates. It is important to mention that since both the build-ups and the debris seismic facies are associated with chaotic seismic signals, their unsupervised classification results are often intertwined in some places or can be mistaken with noise in poorly illuminated areas. As such their occurrence may have been overestimated in the seismic volume that covers part of the Buzios Field

Figure 28 presents average proportion maps for each seismic facies as well as a zonation map of the study area that was created from these probability maps and which displays the most probable seismic facies within the Barra Velha Fm. interval. The zonation map (Figure 28d) indicates that the majority of the wells were drilled in places where either aggradational/progradational carbonate platforms or carbonate build-ups are the dominant seismic facies. There is a greater occurrence of the debris and carbonates build-ups seismic facies in the western portion of the study area.

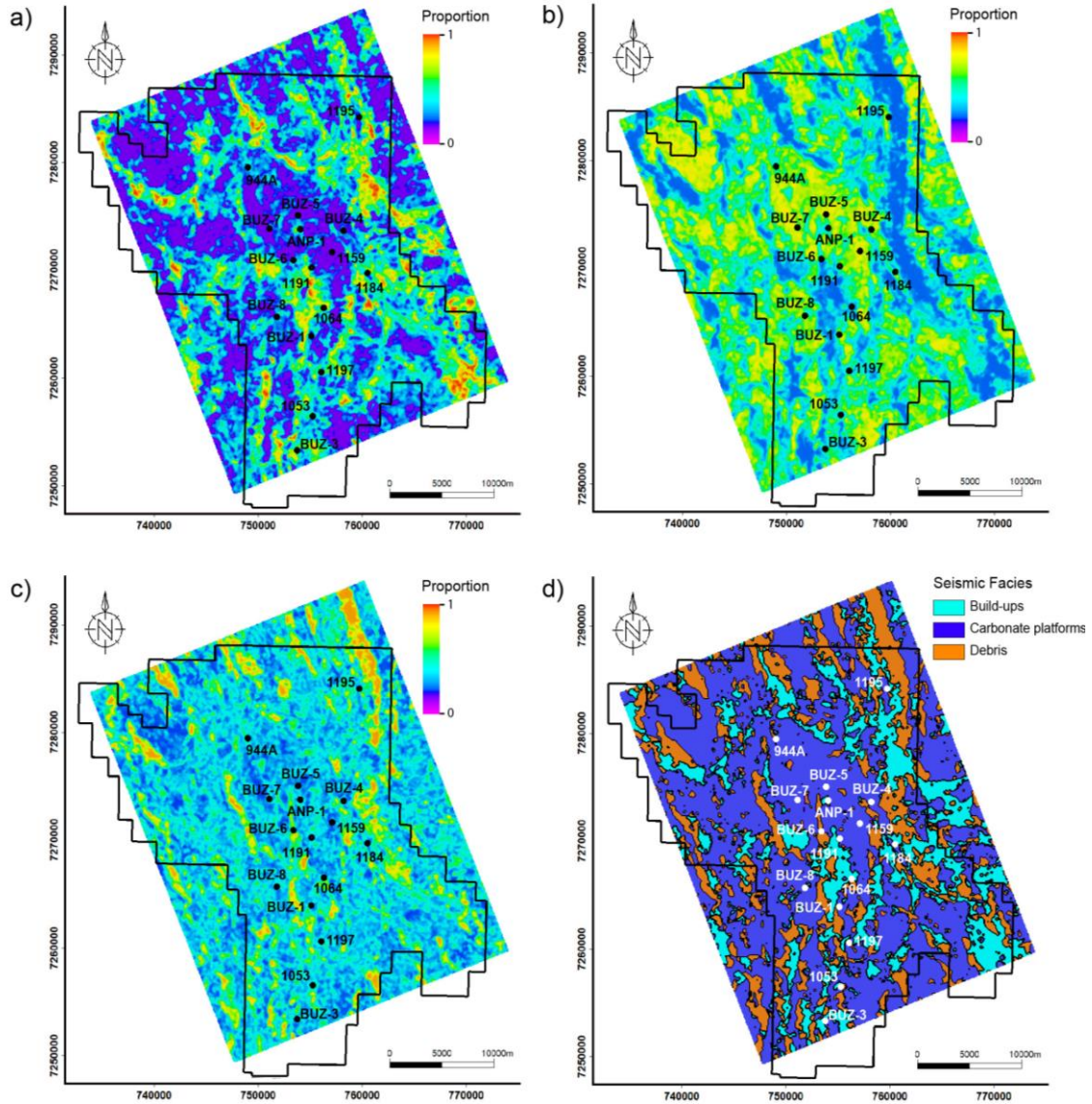


Figure 28: Seismic facies proportion maps within the Barra Velha Fm. interval for a) build-ups, b) aggradational/progradational carbonate platforms, c) debris seismic facies and d) a zonation map created from these proportion maps for the Buzios Field.

An evaluation of the reservoir potential of each of the seismic facies was done, we performed it by comparing available porosity and permeability log data with the mapped seismic facies for each well locations. A log view for five wells is illustrated in Figure 29 with an apparent trend of decreasing porosity and permeability towards the top of the Barra Velha Fm. However, due to the high heterogeneity of the formation it is difficult to observe any direct and marked correlation between the mapped seismic facies and petrophysical properties. Therefore, for a more statistical evaluation, porosity and

permeability histograms were constructed for each seismic facies as well as cross-plots between those properties (Figure 30).

Mean porosity is intermediate for all the seismic facies ranging from 0.10 to 0.12 whilst mean permeability is considerably high ranging from 156 to 704 mD. The correlation between these two petrophysical properties varies from 0.83 to 0.86⁶ for all the seismic facies and they can all be considered good reservoirs⁷. Permeability and porosity are higher for both the carbonate build-ups and the debris seismic facies thus we can infer that these seismic facies are the best reservoirs within the Buzios Field. However, it is important to note that the standard deviation in permeability is greater for these two seismic facies. Therefore, the carbonate build-ups and debris facies have greater heterogeneity leading to a possible reduction in reservoir quality in places. Finally, it is also important to highlight that these conclusions are based on information from wells drilled at structural highs, therefore caution should be used when using this well data to evaluate reservoir quality across the entire Buzios Field.

⁶ It is important to note that both the porosity and permeability well logs were acquired using the same well logging tool (NMR), therefore it is expected that those two petrophysical responses will present a high linear correlation. However, it is fair to assume that there is some uncertainty related to this correlation due to the acquisition tool.

⁷ We highlight that all the classified seismic facies have high porosity and permeability. However, since the porosity and permeability well logs were acquired from wells drilled at the structural highs and at the best target locations for drilling, the assumption that all the Barra Velha Formation interval for the area is composed solely of good quality reservoirs cannot be made.

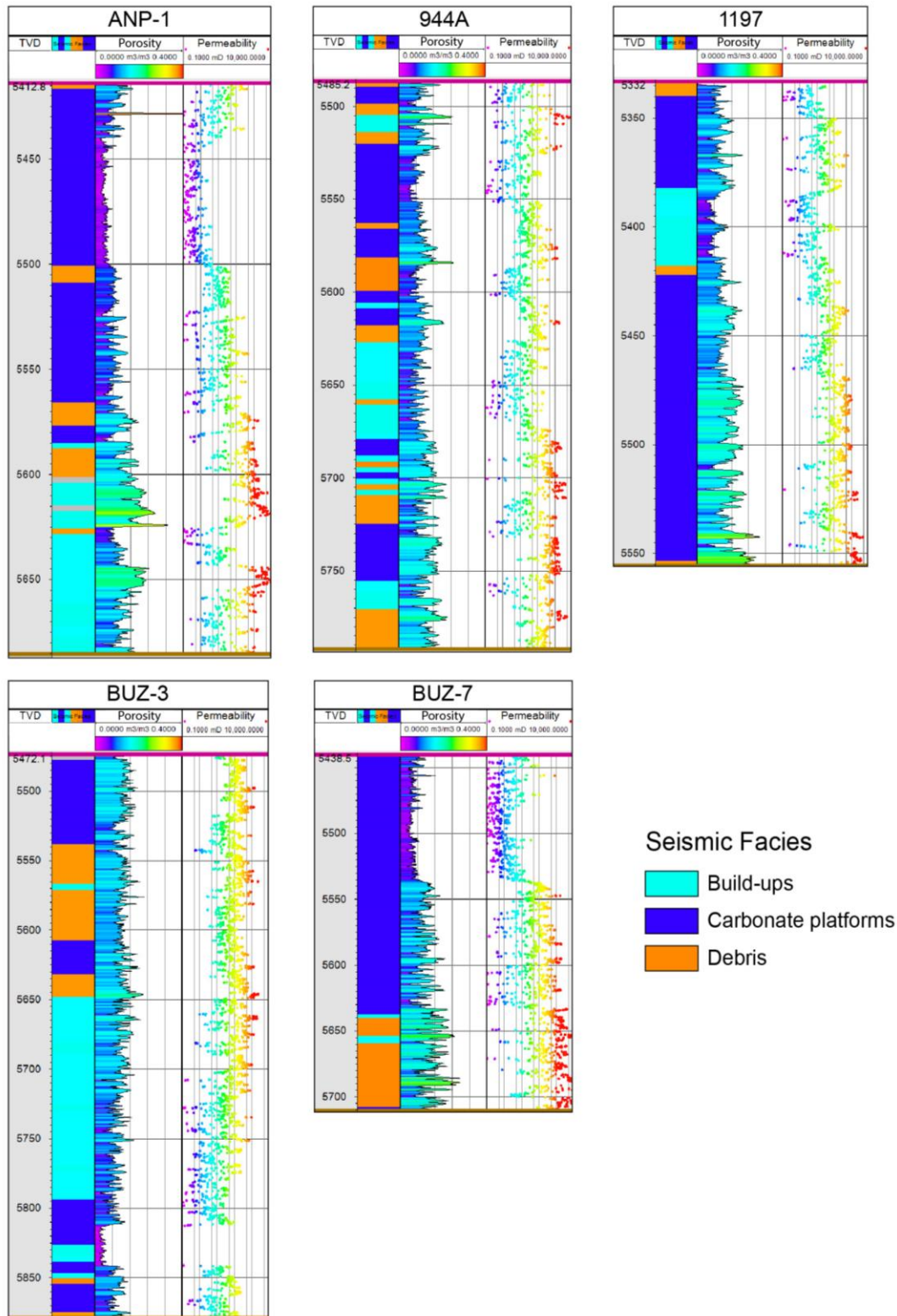


Figure 29: Comparison between the results of seismic facies classification and the total porosity and permeability logs for five wells within the Barra Velha Formation interval. The high heterogeneity of the interval makes it difficult to establish a direct correlation between the petrophysical logs and seismic facies. Nonetheless a general decrease in

porosity towards the top of the Barra Velha Formation was observed in the majority of the wells.

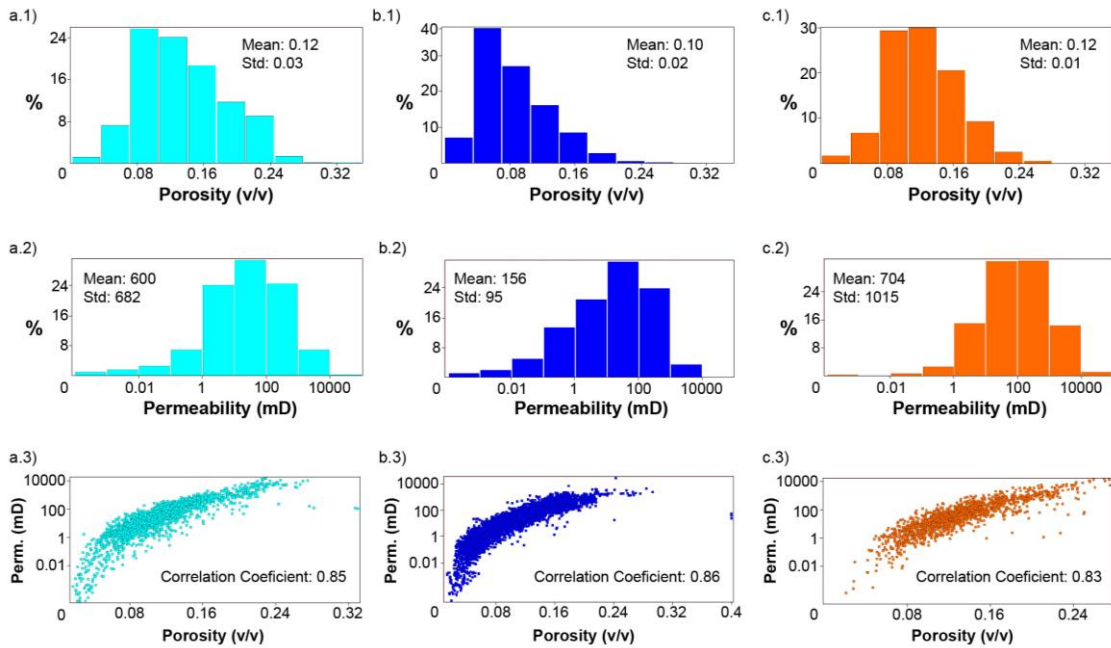


Figure 30: Porosity and permeability distribution histograms and cross-plots between the two parameters for carbonate build-ups a.1), a.2) and a.3); aggradational/progradational carbonate platforms b.1), b.2) and b.3); and for the debris seismic facies c.1), c.2) and c.3). The debris and build-up seismic facies display better permeability and porosity. The correlation coefficients between permeability and porosity are high for all the seismic facies.

3.4. Conclusions

The proposed workflow for classifying and mapping seismic facies within the Barra Velha Formation across the Buzios Field, through the use of an unsupervised neural network and integration with statistical analysis of porosity and permeability as an advanced reservoir characterization proved to be effective. The preconditioning of seismic data for noise attenuation through filtering and the selection of stratigraphic and structural seismic attributes, produced good quality data and enough signal diversity to be effectively used as the input for the unsupervised classification. Three seismic patterns were identified in the amplitude seismic data and were classified as seismic facies by the neural network: carbonate build-ups, aggradational/progradational carbonate platforms and debris. Build-ups are located mainly only the footwalls of normal faults whilst the debris seismic facies occur laterally on the hanging wall side of faults. These two seismic

facies are the most common in the western part of the study area. The principal dip component seismic attribute was fundamental for effectively differentiating between carbonate build-ups and the debris seismic facies during the unsupervised classification. The carbonate platforms are the dominant seismic facies across the Buzios Field and occur both on structural highs away from faulted areas and within the deeper portions of the studied interval. The carbonate build-ups and carbonate platforms are the most drilled seismic facies throughout the area but according to our statistical analysis the debris seismic facies and carbonate build-ups present the best porosity and permeability. The average porosity of these latter facies ranges from 0.11 to 0.12 and average permeability from 600 to 704 mD suggesting that carbonate build-ups and debris facies represent the best reservoirs within the Barra Velha Formation in the Buzios Field.

4. Geostatistics assisted by machine learning for reservoir property modeling: A case study in presalt carbonates of Buzios Field, Brazil

Article published in

The Leading Edge, volume 40, 2021

Impact factor: 1.535

Authors: Danilo Jotta Ariza Ferreira, Gabriella Martins Baptista de Oliveira, Thais Mallet de Castro, Raquel Macedo Dias and Wagner Moreira Lupinacci.

Abstract

An embedded model estimator (EMBER) petrophysical modeling algorithm has been applied to obtain effective porosity and permeability within the presalt carbonate reservoirs of the Barra Velha Formation in the Buzios Field, Santos Basin. This advanced methodology was used due to the heterogeneity and complexity of these reservoirs, which make modeling by conventional geostatistical methodologies hard. Effective porosity was modeled using as secondary variables one facies model; one stratigraphic seismic attribute, acoustic impedance; and one structural seismic attribute, local flatness. Permeability was modeled using as a secondary variable the best effective porosity simulation result. Our results demonstrate that average effective porosity and permeability were 0.10 v/v and 440 md, respectively, indicating good reservoir quality throughout the studied area. A vertical trend of high effective porosities and permeabilities for the basal and uppermost reservoir sections was identified in our results as well as a trend with lower values for these reservoir properties for the intermediate reservoir section. The lower section of the formation presented more continuity, and we infer to be the best reservoir interval. Also, two horizontal trends for these reservoir properties were observed at the formation top: one of higher values aligned to the north-south direction at the structural highs and another one of lower reservoir properties related to isolated structural lows within structural highs. Correlation between modeled results and the blind-test ANP-1 well upscaled properties was high, and upscaled well log property distributions were preserved in the EMBER simulations proving the predictive capacity of the used algorithm. Finally, conditional distributions analysis indicated that

the basal section of the Barra Velha Formation presents higher uncertainty for the estimation of effective porosity. Therefore, even though this interval is considered to have the best reservoir characteristics, decision making should be done with caution for this reservoir section.

4.1. Introduction

Presalt carbonates from marginal Brazilian basins represent the main reservoirs of several important fields. As of May 2021, these reservoirs were producing 2.6 million barrels of oil per day, which represents 98% of the production from the Santos Basin, the most prolific Brazilian oil and gas basin (ANP, 2021). The Buzios Field is an important oil field operated by Petrobras and the second largest Brazilian oil field located within the Santos Basin limits (Figure 31). This field accounts for 27% of the total production from the Santos Basin, with total estimated oil reserves of approximately 30 billion barrels of oil (ANP, 2016, 2021).

The presalt carbonate reservoirs in the Santos Basin are represented by the coquinas of the Itapema Formation at the base and by the Barra Velha Formation, at the top (Moreira et al., 2007). The Barra Velha was deposited within an alkaline-lacustrine paleoenvironment during the late rift and sag phases of the Aptian (Wright and Barnett, 2015), and it has been suggested that precipitation occurred controlled by chemical processes (Wright, 2012; Wright and Barnett, 2015; Wright and Tosca, 2016; Wright and Barnett, 2017). Hydrothermal activity on rift faults and lixiviation of the surrounding terrains by meteoric water fed the lacustrine waters with alkalis and CO₂ (Szatmari and Milani, 2016). Diagenetic processes also affected these carbonates and either improved or diminished their reservoir properties depending on location (Wright and Barnett, 2020).

Barra Velha Formation is composed of different kinds of grains such as shrubs, spherulites, carbonate muds, and Mg-rich clays, and lithological definition changes depending on the origin and abundance of these grains. However, the carbonate rock types of this formation can be represented by three main groups: mudstones or laminites, in-situ carbonates, and reworked carbonates (Terra et al., 2010; Pereira et al., 2013; Rezende and Pope, 2015; Wright and Barnett, 2015; Farias et al., 2019; Gomes et al., 2020; Ferreira et al., 2021a). Proximal lacustrine facies are in-situ carbonates comprising lithologies such as shrubby carbonates and spherulitic carbonates. All these rocks could be reworked

by erosion. Distal or local structural low facies of the Barra Velha Formation can be represented by mudstones or laminites. There is also evidence that in some locations volcanic rocks occur intercalated with these lacustrine lithologies, such as suggested in the works of Fornero et al. (2019) and Penna et al. (2019).

Petrophysical reservoir characterization is usually hard for Barra Velha carbonates due to the formation's complex depositional history and facies heterogeneity that requires advanced modeling techniques and deep understanding of conceptual depositional models (Johann et al., 2012; Johann, 2013; Bruhn et al., 2017; Ferreira et al., 2019a; Ferreira et al., 2019b; Penna and Lupinacci, 2020; Ferreira et al., 2021a; Penna and Lupinacci, 2021).

Castro and Lupinacci (2019) perform a petrophysical evaluation of the reservoirs within the Barra Velha Formation in the Buzios Field and propose a division for it at its top into upper and lower sags, with the lower sag being characterized by a greater stevensite clay content, which diminishes reservoir properties, and an upper rift phase at its base. They suggest that upper sag and upper rift sections are the best reservoirs and that the mean effective porosity for the entire formation is approximately 8% in the studied well.

Dias et al. (2019) perform an acoustic inversion in the Buzios Field to infer the relationship between acoustic impedance and porosity. There is a strong correlation between these two properties for the Barra Velha Formation, and two main trends are observed: one corroborated with the observations of Castro and Lupinacci (2019) where for the upper sag and upper rift sections, low acoustic impedance is associated with high porosity, and the second trend, for the lower sag section, associated low acoustic impedance values with low porosity, due to the presence of stevensite clays.

Machine learning algorithms have also been applied for presalt reservoir characterization mostly for qualitative purposes related to seismic facies individualization such as in the works of Ferreira et al. (2019a), Ferreira et al. (2019b), Jesus et al. (2019), Ferreira et al. (2021b). The methodologies applied use a series of seismic attributes in unsupervised learning for classification, and petrophysical signatures for each of the classified seismic facies, such as porosity and permeability, were only inferred by some of these authors.

Ferreira et al. (2021b) performed an unsupervised seismic facies classification for the presalt carbonates from the Barra Velha Formation. in the Buzios Field. These authors discriminated three seismic classes: buildups, carbonate platforms, and debris, and further permeability and porosity distributions were inferred after basic statistical evaluation for each of these classes. The debris and carbonate buildup seismic classes were considered the best reservoirs with, respectively, average porosity from 0.11 to 0.12 v/v and average permeability from 600 to 704 md.

Penna and Lupinacci (2021) performed a volumetric estimation of porosity and permeability for the Mero Field presalt reservoirs, located in the Santos Basin. They used flow units and lithologies as constraints for this modeling, with both generated by Bayesian inference having as inputs elastic attributes. Later, the porosity and permeability volumes were estimated for each of the discrete property models, flow units and lithological units, by using regressions between the discrete property versus porosity and porosity versus permeability. These authors concluded that the estimation of permeability-porosity characteristics of the reservoirs was better achieved using flow units as constraints and also that there was a strong impedance-porosity relationship for presalt reservoirs. Another conclusion was that for the Barra Velha Formation, in general, permeability-porosity characteristics were good, except for some continuous layers in the uppermost section.

Classic geostatistical modeling for estimating petrophysical properties and reservoir characterization of facies are widely used with an extensive bibliography (Ziegel et al., 1998; Lantuéjoul, 2002; Caers, 2005; Pyrcz and Deutsch, 2014; Azevedo and Soares, 2017; Ferreira and Lupinacci, 2018). These methods have been successfully applied to the characterization of presalt Brazilian carbonate reservoirs (Peçanha et al., 2019; Ferreira et al., 2021a).

Ferreira et al. (2021a) used an integrated workflow for geostatistical facies reconstruction that included a truncated Gaussian simulation with the results of 4D sedimentary simulation as trends for the Barra Velha Formation in the Buzios Field. The lithotypes modeled were spherulitites and shrubby carbonate rocks, which dominated the structural highs; reworked facies, which were the byproduct of the erosion and transport of the previous lithologies and occurred in fault borders; and laminites, which occurred in both connected and isolated structural lows. Their model also suggested that the Barra

Velha Formation is muddier at the base transitioning to in-situ carbonates in the middle section, before becoming muddier again at the top.

It can be stated that even though geostatistical modeling is a powerful tool for the estimation of 3D reservoir properties and facies, it is based on a series of premises that if are not fulfilled prior to modeling, might cause a series of pitfalls (Caers, 2005; Sarma, 2009; Azevedo and Soares, 2017). Hirsche et al. (1998) reviewed the premises and pitfalls in geostatistical methods and pointed out that one of the main premises is the stationarity of the modeled continuous variable, which assumes that its mean and variance are constants throughout the modeled area. In practice, this is a very hard premise to be achieved since, geologically, nonstationarity can be caused by changes in lithology, facies, or fluid saturation. These geological trends must be removed prior to modeling, and this process usually requires division of data into stationary groups such as a facies model built for the area. However, in complex geological settings, this division into stationary groups cannot be associated solely to different lithologies, for example, there are cases such as secondary porosity generation through diagenetic processes.

Another important assumption is the linear correlation between the modeled property and the used secondary variable, usually a seismic attribute or a linear combination of those, when cokriging is applied. This correlation needs extensive data analysis to be proved, and different sampling rates between seismic and well data can diminish it. There are also limitations regarding the construction of the variograms, which represent the spatial correlation of the variable to be modeled when well data are sparse. For those cases, geological knowledge must be applied for a cohesive spatial correlation.

Envisioning the creation of a modeling methodology that can overcome classical geostatistics limitations and the usual extensive work for its precise parameterization., Daly (2020a) developed an algorithm, called EMBER, for nonstationary spatial modeling using multiple secondary variables that combines geostatistics with quantile random forests. It provides estimation and stochastic simulation results, which are produced by the nonlinear combination of embedded geostatistical models. Those outputs represent the spatial continuity of the modeled variable with additional variables, such as spatial trends and seismic attributes. Examples of this methodology application are shown in the works of Daly (2020b), Daly et al. (2020), and Daly (2021).

In this paper, we propose the use of the EMBER algorithm to perform effective porosity 3D modeling for the Barra Velha Formation in the Buzios Field, using well data information, a facies model and two seismic attributes as secondary variables, as well as permeability 3D modeling, using the resulting porosity model. By applying this methodology, we aim to improve the efficiency of the presalt reservoir characterization process within Buzios Field and address its potential by creating robust petrophysical property models without the extensive labor required by other advanced reservoir characterization techniques for complex sedimentary environments.

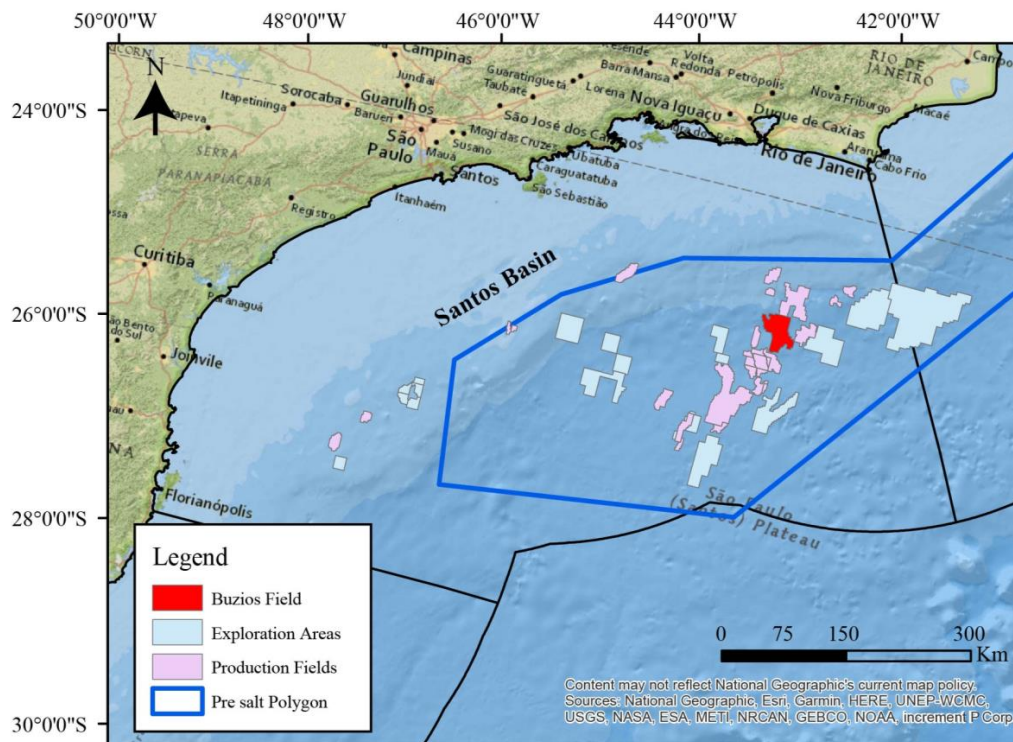


Figure 31: Location of the Buzios Field within the Santos Basin.

4.2. Method

The dataset available consisted of 770 km² of 3D poststack depth-migrated seismic (PSDM) data and effective porosity and permeability well logs from 13 wells within Buzios Field. We mapped the base of salt (of Upper Aptian age) and pre-Alagoas (of Lower Aptian age) unconformities which represent, respectively, the top and bottom limits of the Barra Velha Formation. Ages of the mapped unconformities were established by Moreira et al. (2007). Figure 32 shows the data coverage across the study area

including well location, depth contours of the base of salt unconformity, and the location of the seismic sections are presented in this study.

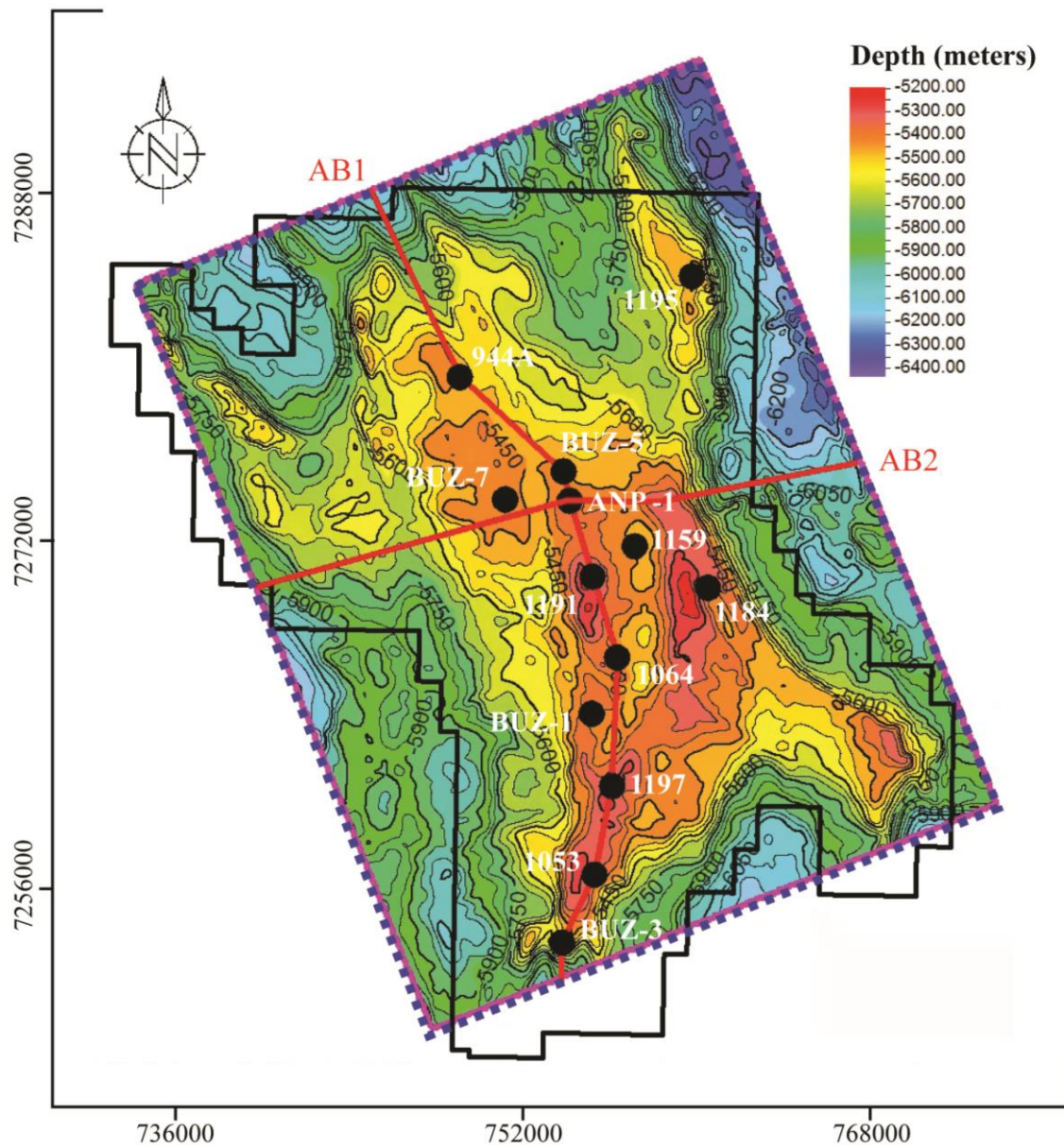


Figure 32: Map view of the base of salt interpreted seismic horizon (depth contours) across Buzios Field (black polygon) with the coverage of the 3D seismic data shown by the dashed blue rectangle and well locations shown by black circles. The red lines show the location of the arbitrary seismic lines (AB1 and AB2) presented in this study.

The workflow for property modeling is divided into two stages: (1) selection of secondary variables to be used as inputs for the (2) nonstationary spatial modeling of effective porosity and permeability using the EMBER algorithm.

Selection of the secondary variables for EMBER modeling

The selection of the secondary variables for modeling was done considering the evaluation of several seismic attributes based on amplitude, phase, and frequency or a combination of these components to identify stratigraphic and structural characteristics that could be conceptually correlated, linearly or nonlinearly, with the effective porosity and permeability distributions throughout the Barra Velha Formation within the area of Buzios Field. As discussed by Daly (2020a, 2021), EMBER algorithm rationale is based on the assumption that secondary variables, which might include seismic attributes and other types of data, might not explicitly contain information about the spatial correlation of the modeled property; therefore, linear correlation between secondary and primary variables is not required.

We chose as secondary variables one facies model, one stratigraphic seismic attribute, and one structural seismic attribute as inputs for EMBER effective porosity modeling:

- The geostatistical facies reconstruction property model was built via integration between geological process modeling and truncated Gaussian simulation by Ferreira et al. (2021a). We built this model considering the Barra Velha Formation conceptual geological information, such as inferred lacustrine base level curve, paleotopography, carbonate sedimentation, and erosion effects, with well log facies.
- The absolute acoustic impedance stratigraphic attribute, which usually correlates well with lithological signatures, was obtained using the inversion algorithm proposed by Russell and Hampson (1991, 2006) and Barclay et al. (2008). The used acoustic inverted seismic attribute was the one created by Dias et al. (2019) in the Barra Velha Formation interval for the Buzios Field.
- The local flatness structural attribute maps the flatness of reflectors, which are not necessarily horizontal, thus revealing vertical anomalies and faulted areas (Randen and Sønneland, 2005; Pereira, 2009).

For the EMBER permeability modeling, we used as a secondary variable the best resulting effective porosity simulated model. Before the simulation for each of the desired properties, the upscaling of both effective porosity and permeability logs from the available wells and the seismic attributes used as secondary variables for the effective

porosity modeling was performed. The grid in which the upscaling was done has a cell size of $100 \times 100 \times 10$ m (x, y, z) and was constructed between the base of salt and pre-Alagoas surfaces. Each of the secondary variables chosen for porosity modeling are shown in Figure 33 and Figure 34. The expression of these variables along an individual seismic trace extracted along the trajectory of the well ANP-1 is shown in Figure 35. As can be noted, there is no explicit linear correlation between any of the continuous secondary variables and either effective porosity or permeability upscaled well logs.

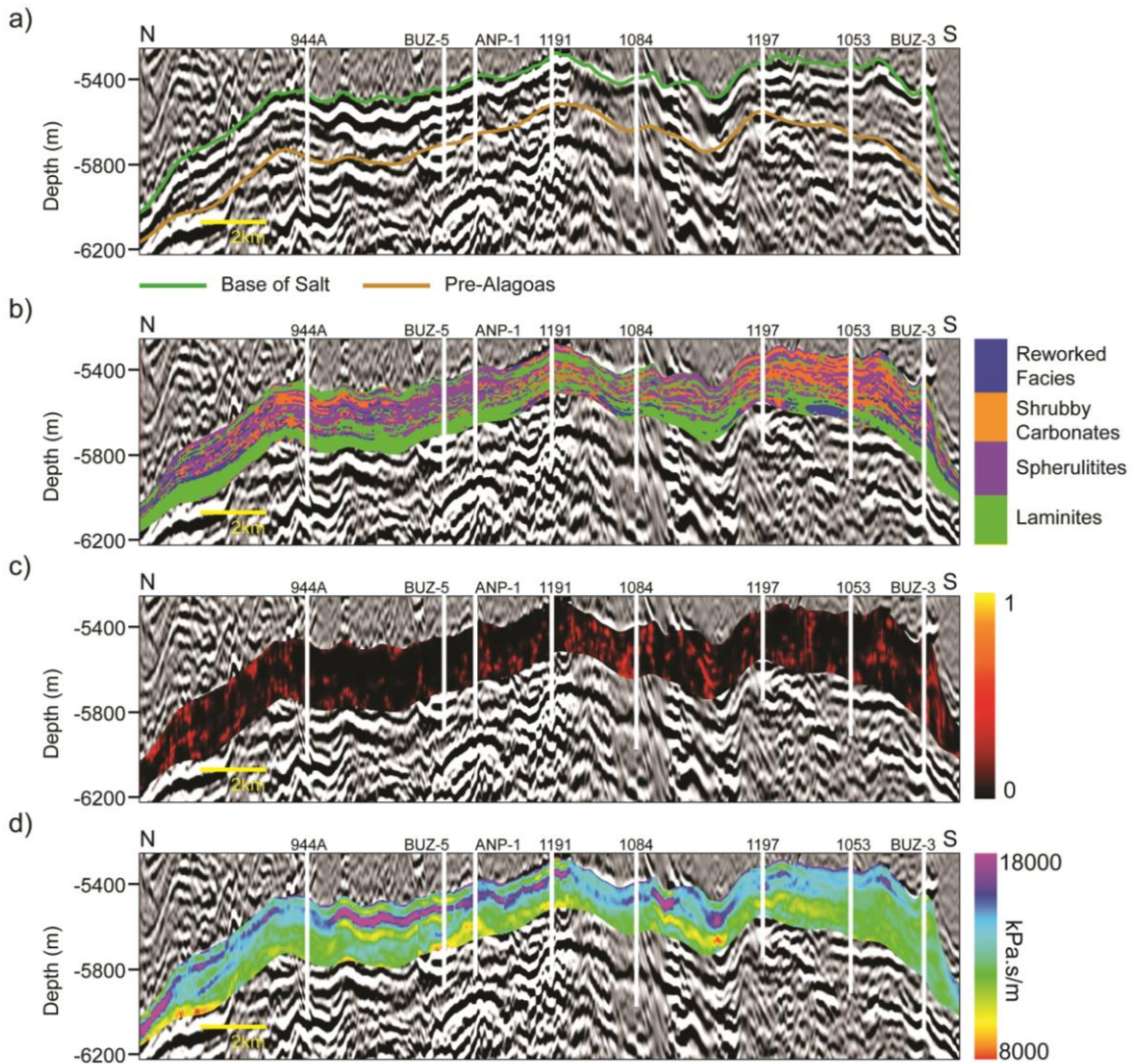


Figure 33: Arbitrary section 1 (AB1) with a) original seismic volume with Barra Velha Formation top and bottom unconformities, base of salt and pre-Alagoas, respectively, and secondary variables chosen for EMBER porosity modeling: b) facies model from Ferreira et al. (2021a), c) local flatness attribute, and d) acoustic impedance attribute from Dias et al. (2019).

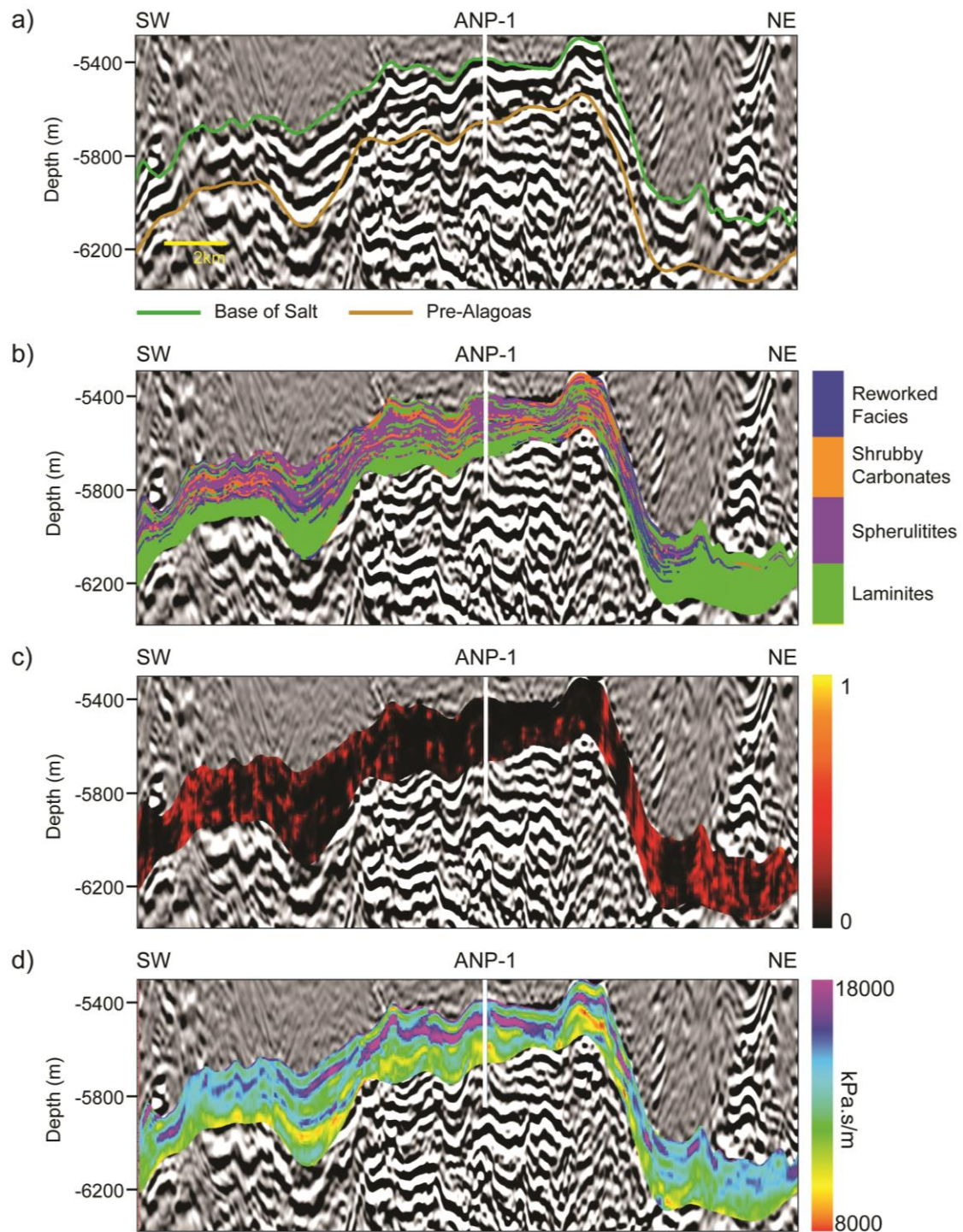


Figure 34: Arbitrary section 2 (AB2) with a) original seismic volume with Barra Velha Formation top and bottom unconformities, base of salt and pre-Alagoas, respectively, and secondary variables chosen for EMBER porosity modeling: b) facies model from Ferreira et al. (2021a), c) local flatness attribute, and d) acoustic impedance attribute from Dias et al. (2019).

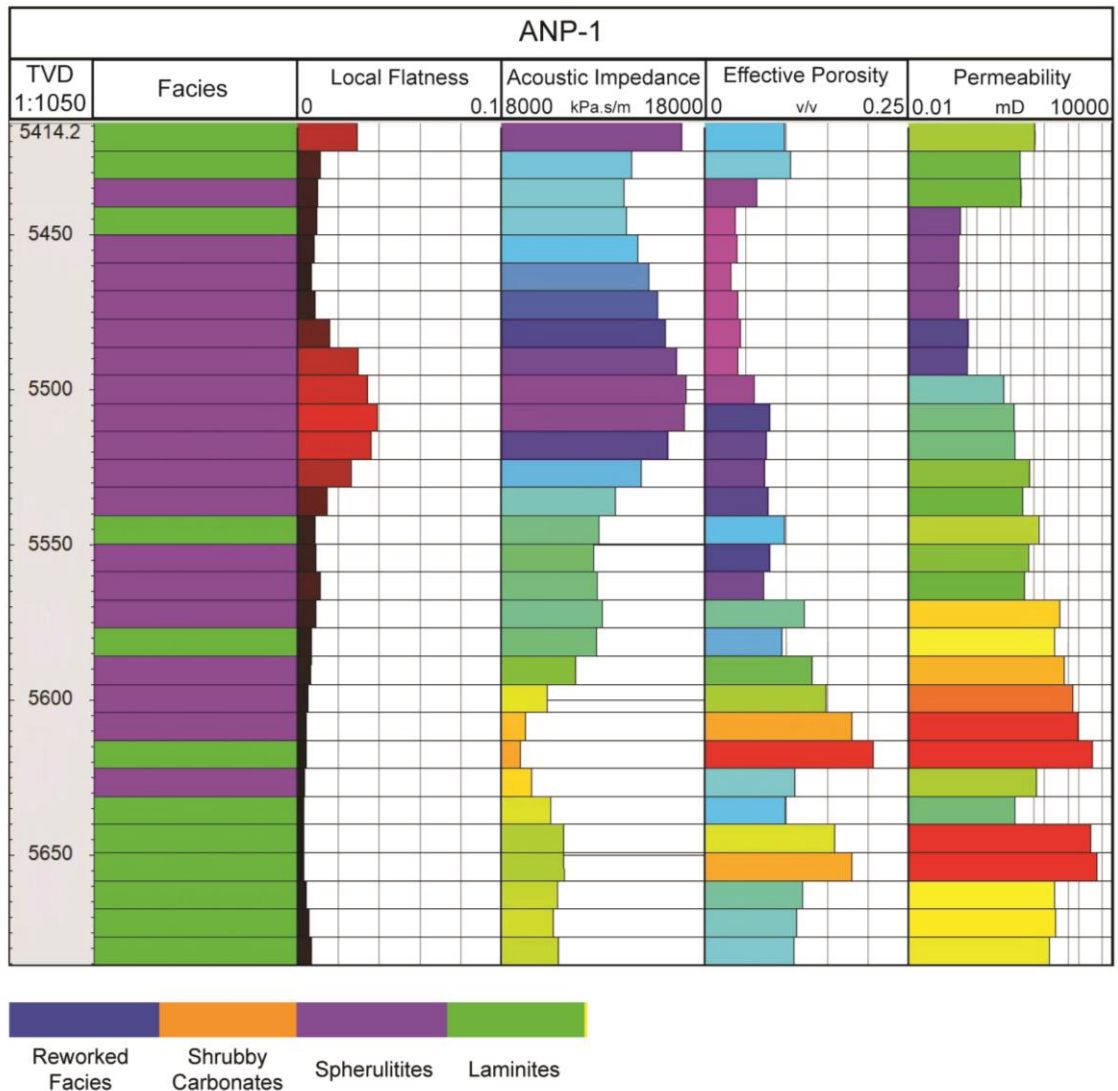


Figure 35: Expression for each of the secondary variables used for effective porosity EMBER modeling and effective porosity and permeability upscaled logs along the ANP-1 well trajectory within the Barra Velha Formation interval. From left to right, facies model, local flatness attribute, acoustic impedance attribute, and effective porosity and permeability well logs.

Spatial modeling of effective porosity and permeability using EMBER algorithm

EMBER property modeling algorithm developed by Daly (2020a) belongs to the class of conditional random fields (CRF) as defined by Lafferty et al. (2001). The CRF used by the methodology embeds prior spatial models using a Markovian hypothesis (Durrett, 2019). More specifically, as stated by Daly (2020b) and Daly et al. (2020) and further detailed by Daly (2020a) and Daly (2021), the CRF used in the EMBER algorithm works in the following manner for the estimation of the desired property:

Let $Z(x)$ be a target variable of interest at the location x and $\mathbf{Y}(x)$ be a vector of secondary variables observed at x . Let $\{Z_i, \mathbf{Y}_i\}$ be observations of the target and secondary variables observed in the field at the locations $\{x_i\}$, and finally let $\mathbf{Z}_e^*(x) = \mathbf{f}(\{Z_i, \mathbf{Y}_i\})$ be a vector of pre-existing estimators of $Z(x)$. Then the Markov hypothesis that is required is the conditional distribution of $Z(x)$ given all available data $F^{Z(x)|All}(z)$ satisfies as following:

$$F^{Z(x)|All}(z) = E[\mathbb{I}_{Z(x)<z} | \mathbf{Y}(x), \{Z_i, \mathbf{Y}_i\}] = E[\mathbb{I}_{Z(x)<z} | \mathbf{Y}(x), \mathbf{Z}_e^*(x)]. \quad 5.1$$

This states that the conditional distribution of $Z(x)$ given all the secondary values observed at x and given all the remote observations of $\{Z_i, \mathbf{Y}_i\}$ reduces to the far simpler conditional distribution of $Z(x)$ given all the secondary values observed at x and the vector of model predictions at x .

In this study, the target variables, $Z(x)$ are the effective porosity and permeability within Barra Velha Formation interval in the Buzios Field area. As previously mentioned, the seismic attributes acoustic impedance and local flatness as well as a facies model were used in the application for the effective porosity estimation, and the best resulting porosity model simulated was the only secondary variable used for the permeability estimation. In addition, two embedded simple kriging models are used as input variables, one with a long-range and one with a short-range, and the contribution of these models are determined together with that of the secondary variables during construction of $F^{Z(x)|All}(z)$. This is motivated by the empirical observation that the main contribution of embedded kriging in the algorithm is to provide information about lateral continuity of the target variable. This allows the EMBER process to be fully automated.

Also, as described in Lafferty et al. (2001), the CRF does not require stringent hypotheses such as the stationarity of the property of interest and the stationarity of the relationship between the modeled variables and the secondary variables. The embedded models $\mathbf{Z}_e^*(x)$ are constructed with these hypotheses; however, this influence is mitigated in two ways. First, the Markov hypothesis removes any direct influence of the construction of $\mathbf{Z}_e^*(x)$, instead symmetrically weighing its influence on the final estimate on the ability of secondary variables to predict the target distribution. Second, the mean impact of stationarity in a classic model is seen in stochastic realizations, which must bring the full multivariate distribution and therefore lean heavily on the hypotheses. This

can be avoided by the proposal made by Daly (2020a), in which a nonparametric paradigm is used for the estimation of $F^{Z(x)|All}(z)$. The inference problem is complicated by the dependency on the embedded models $Z_e^*(x)$. If these estimators made use of $Z(x)$ in the estimation of $Z(x)$, a bias would have been introduced. This could be solved by the simple expediency of training the decision forest on cross-validated estimates. Thus, the training data set for each tree is $\{Z_i; Y_i, Z_{CV_e}^*(x)\}$, where $Z_{CV_e}^*(x)$ are crossvalidated model estimates at x . With the estimates of $F^{Z(x)|All}(z)$ at all target locations x , conditional realizations of the reservoir model are produced. A modified conditional P field simulation is used, which honors data at the well locations, and the simulation follows the local heteroscedasticity observed in the conditional distribution as well as the spatially varying relationship between secondary variables and modeled variable.

In summary, some of the outputs of this methodology for both effective porosity and permeability modeled properties are the algorithm conditional distributions, such as P10 and P90, the uncertainty which is given by the subtraction of the P10 and P90 distributions, and properties stochastic simulations. As an additional quality control for the results, we used the ANP-1 well as a blind test; therefore, it was not included in the EMBER algorithm. Also, it is important to note that 30 simulation results were generated for effective porosity and for permeability and the ones illustrated in this study were the ones that presented the best linear correlations with upscaled well logs from the blind test well.

4.3. Results and Discussion

The evaluation of the effective porosity and permeability EMBER simulations are presented as arbitrary sections in Figure 36 and in map view projected over the base of salt surface in Figure 37. As can be observed, the two modeled reservoir properties are quite similar in behavior, probably due to the linear correlation between the effective porosity and permeability upscaled well logs, around 82%, which clearly influenced EMBER algorithm for permeability modeling using the effective porosity modeling results as a secondary variable. Also, it is important to highlight that even though a facies model was used as an input for EMBER effective porosity modeling, there was little influence from it in the observed results, most probably related to the lack of predictability of the facies model with respect to the porosity well logs distribution. However, if the

facies model had more influence on the results, they would be a scenario conditional to the facies model.

The mean effective porosity and permeability values for the Barra Velha Formation within Buzios Field are 0.10 v/v and 440 md, respectively, and this fact indicates that those reservoirs present a good quality. Both reservoir property models also present a clear vertical trend of high values at base of the Barra Velha Formation that become lower in the intermediate section and then high again in the uppermost section. This fact corroborates with the conclusions presented by Castro and Lupinacci (2019), Dias et al. (2019), and Penna and Lupinacci (2021) in which the best reservoirs for the Barra Velha Formation both at the Buzios Field and in other Fields are usually at its basal section due to better reservoir characteristics and continuity.

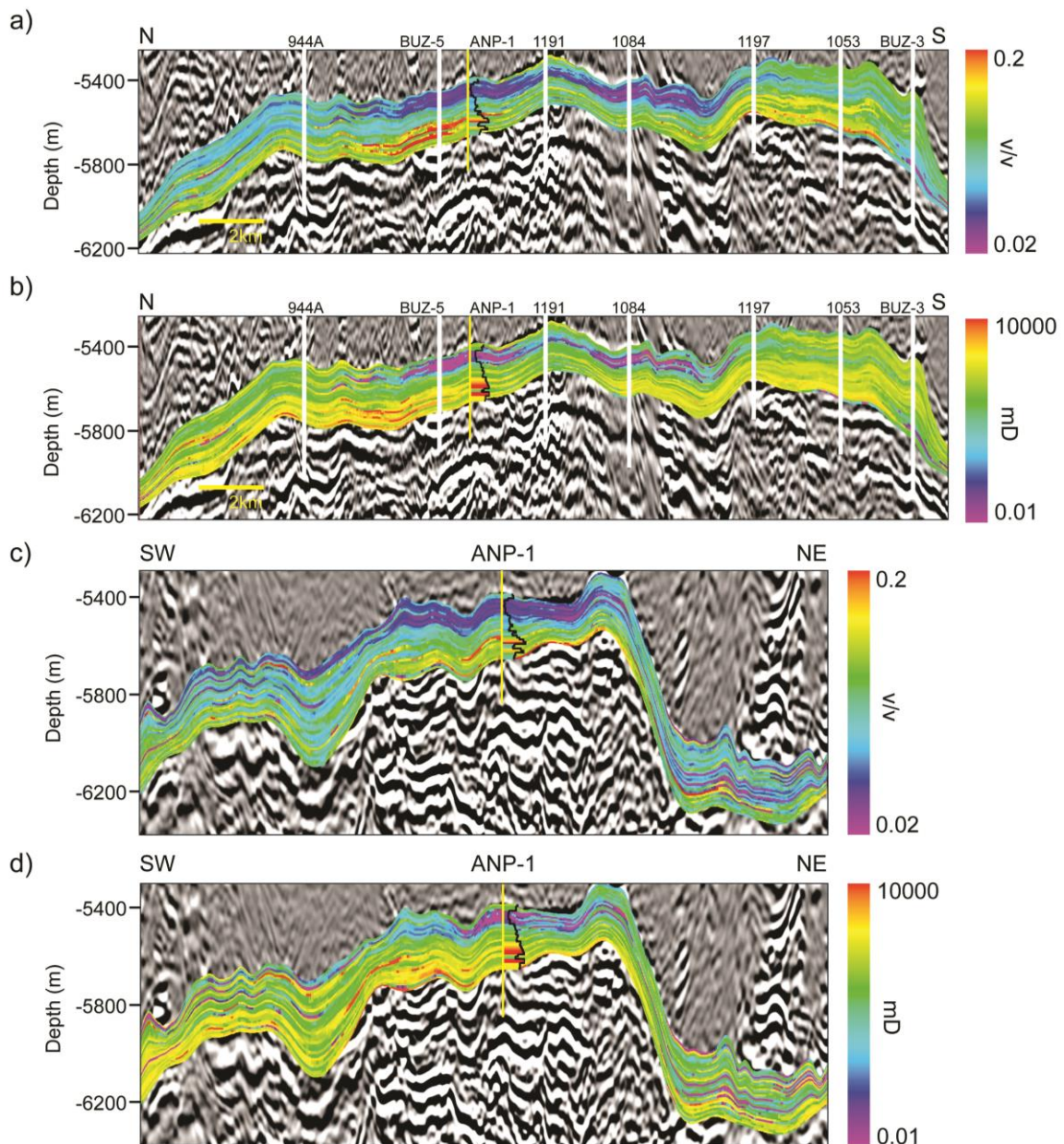


Figure 36: The resulting EMBER 3D property modeling volume along arbitrary line 1 (AB1) for a) effective porosity and b) permeability and along the arbitrary line 2 (AB2) for c) effective porosity and d) permeability. Well paths are shown by the white lines, except for ANP-1 well used as a blind test, which is presented with a yellow line and with the associated upscaled property.

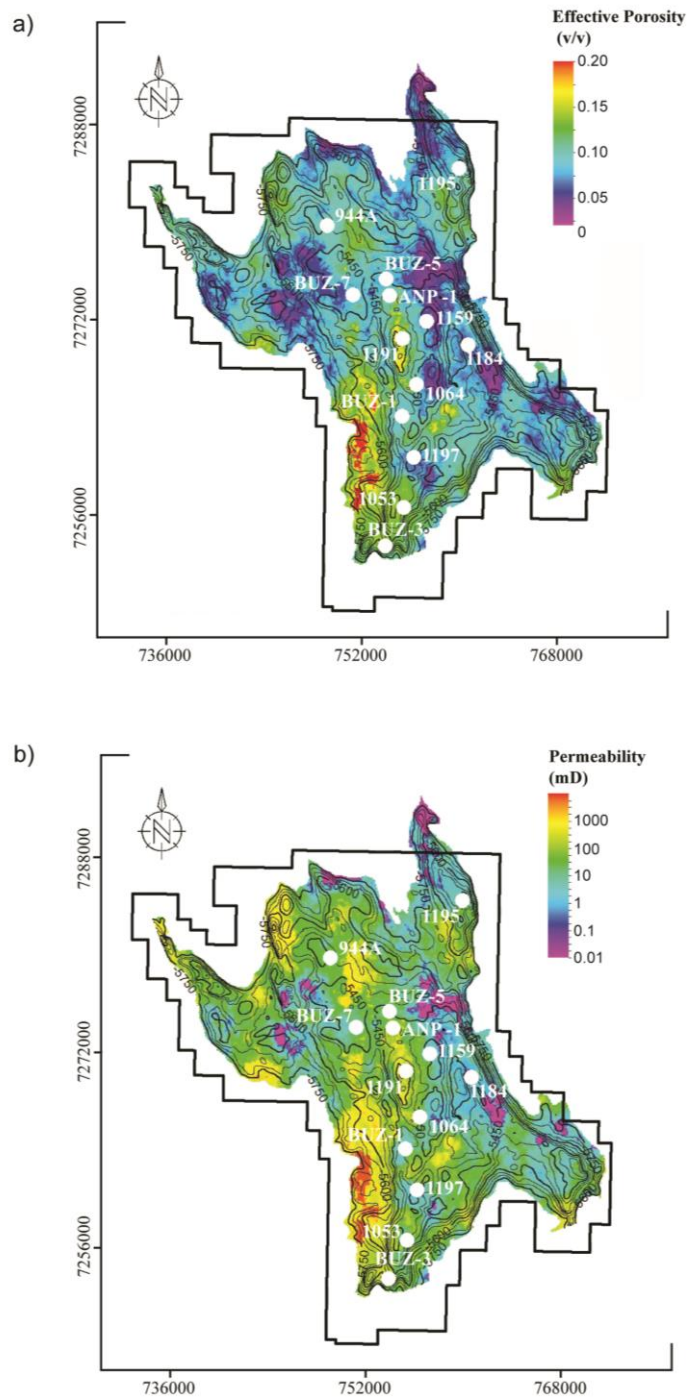


Figure 37: The results EMBER 3D property modeling presented in map view for a) effective porosity and b) permeability over the base of salt surface (top of the Barra Velha Formation) and restricted to the main structural highs. Well locations are represented by the white circles, and the black polygon shows the limits of the Buzios Field.

At the map view perspective, it is noticeable that at the structural highs, the highest effective porosities and permeability values occur, and those are aligned to a north-south trend. This is probably due to the presence of buildup-shaped seismic patterns formed at

fault borders, which, as suggested by Ferreira et al. (2021b), represent some of the best reservoirs within Buzios Field. These features can also be observed in Figure 33a and Figure 34a. Another tendency that can be recognized in both section and map views is the low effective porosity and permeability values within isolated structural lows within structural highs. This is probably due to the higher content of finer carbonate deposits, in these areas as suggested by some authors such as Neves et al. (2019) and Ferreira et al. (2021a), which diminishes reservoir properties.

An analysis of the effective porosity model with the secondary variables used in the EMBER algorithm for its simulation, shows that the model does not directly follow the behavior of any of the secondary variables across the modeled area. This is probably due to the nature of the methodology, which selects the weight of each of the secondary variables locally and based on their actual capacity to estimate the desired property. Nonetheless, some comparisons can be made, such as the tendency of the acoustic impedance volume, which presents lower values at the base of the Barra Velha Formation and that becomes higher in the intermediate section and then lower again at the top (Figure 33d and Figure 34d). This negatively correlates with the effective porosity modeling results and, consequently, the permeability results. However, the property modeling results present a much higher frequency than the acoustic impedance attribute. This is probably due to the consideration of other secondary variables and the embedded kriging models created by the algorithm to describe the spatial correlation of the modeled variable in the modeling process.

Also, there are several areas where acoustic impedance values are lower and should be correlated with high effective porosities and permeabilities or vice-versa; however, this is not the case in this study. This could be related to the occurrence of laminites in the facies model, which usually present lower acoustic impedance values; however, since they are composed of finer deposits, they are expected to have lower effective porosity and permeability values. Another inferred cause for this to happen could be diagenetic processes that could have increased or diminished those reservoir properties at different places. Correlation of the property modeling results with the local flatness attribute is trickier (Figure 33c and Figure 34c). It seems that the places that have higher local flatness attribute values, which indicates lower reflector flatness, usually present medium to high effective porosity and permeability values. This could be

indicative of good reservoir characteristics at faulted areas or areas where chaotic reflectors occur.

As discussed, the facies model (Figure 33b and Figure 34b) seems to have little influence on the effective porosity results. However some observations can be made such as that at the upper section of the Barra Velha Formation, the shrubby carbonates and spherulitites located at structural highs present medium to high effective porosity and permeability values. The same behavior can be noted for the reworked facies near fault borders. This fact confirms the suggestion made by Ferreira et al. (2021a) that these could be the best reservoirs within the Barra Velha Formation for the Buzios Field. For the lower section of this formation, the facies model presents mainly laminites which are composed of finer carbonate grains and classified as nonreservoir by these authors. However, both effective porosity and permeability simulation results showed medium to high values, which indicates good reservoir quality for the lower section of the Barra Velha Formation. This fact was also noted in other works such as Dias et al. (2019) and Penna and Lupinacci (2021). Therefore, this leads to the suggestion that probably the occurrence of laminites in the lower section of the Barra Velha Formation at structural highs was overestimated by Ferreira et al. (2021a). It is also important to highlight that the effective porosity and permeability models were built based on information from wells drilled at structural highs; therefore, caution should be used when using those models to evaluate reservoir quality at the structural lows within Buzios Field, due to any bias effect not evaluated.

For quality control purposes, the well ANP-1 was excluded from the EMBER simulations and, therefore, used as a blind test for both effective porosity and permeability models. Figure 36 and Figure 38a illustrate the comparison between the upscaled effective porosity and permeability logs for this well and the results of the simulations for each of these properties at section and well views, respectively. For both effective porosity and permeability, linear correlation between original and simulated data is high, 73% and 78% respectively, thus confirming the predictive capacity of the used methodology. Figure 38b and Figure 38c illustrate the histograms for both the well upscaled cells and the EMBER simulation results for both effective porosity and permeability, respectively. As can be noted, the modeled results also match quite well the initial properties distribution.

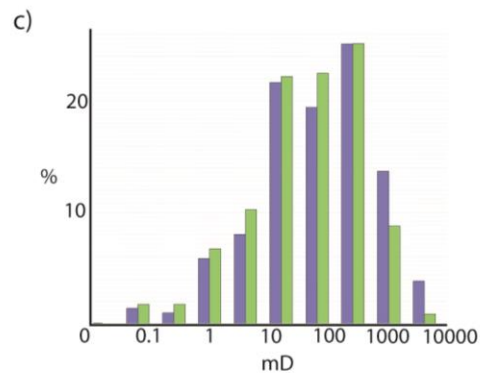
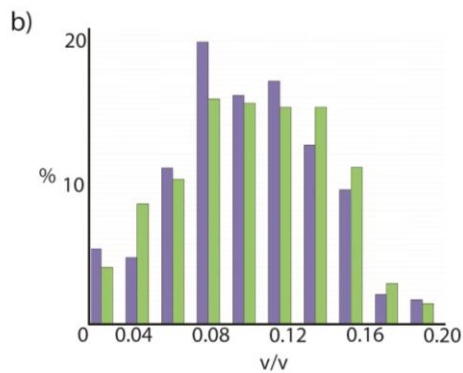
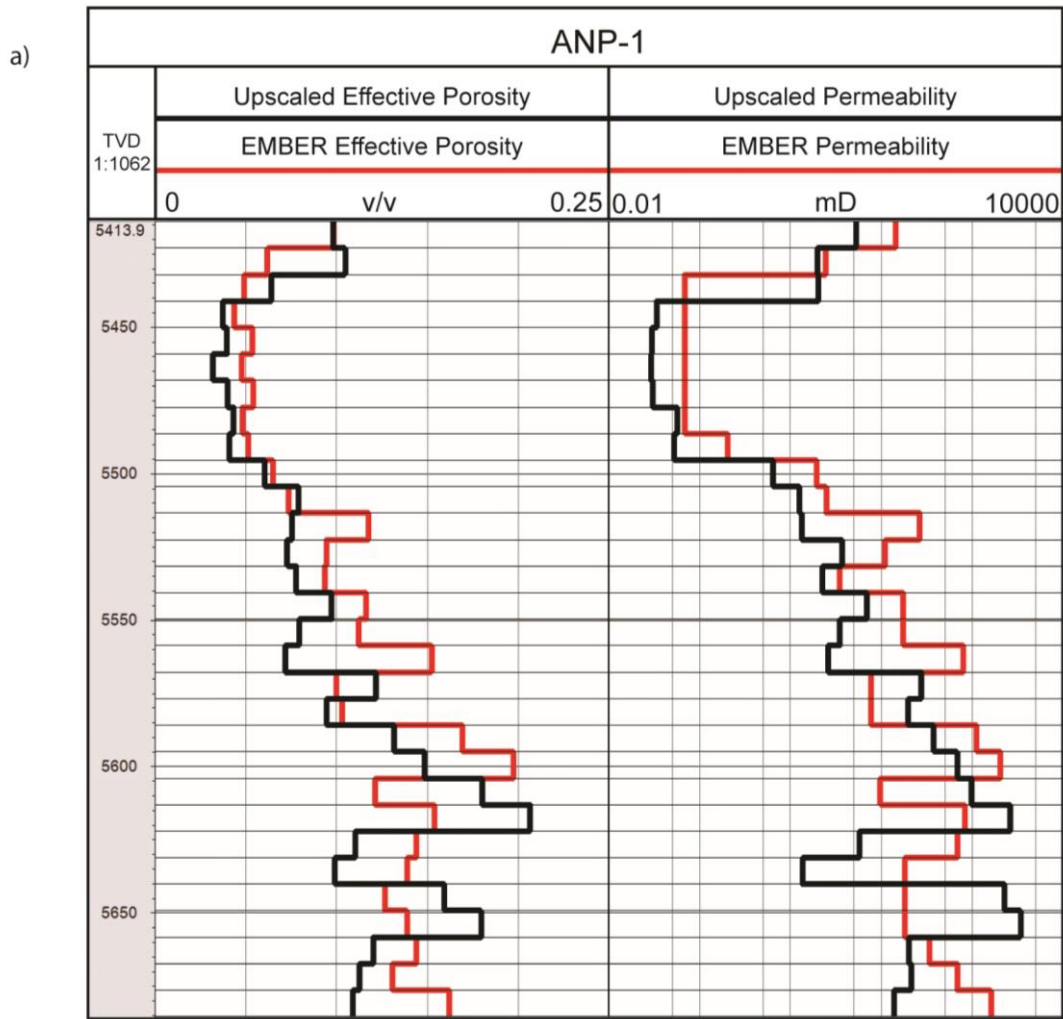


Figure 38: Comparison between the effective porosity and permeability upscaled well logs (black lines) and EMBER simulation results (red lines) for those properties are presented in a). In b) and c), effective porosity and permeability upscaled well log distributions (green histograms) and results distributions (blue histograms) are shown, respectively.

Finally, to address the simulation result uncertainties, the conditional EMBER distributions, P10 and P90, and the uncertainty volumes were evaluated for effective porosity (Figure 39) predictions. We highlight that higher uncertainties are concentrated in the lower section of the Barra Velha Formation. This fact indicates that even though the lower section of the Barra Velha Formation is considered to have the best reservoirs, it also presents higher level of uncertainty; therefore, conclusions and decisions should be made with caution for that section. Also, we highlight that uncertainty was not evaluated for permeability results since the effective porosity simulation was used as its input and, therefore, the uncertainty for permeability simulation would be biased by effective porosity uncertainty.

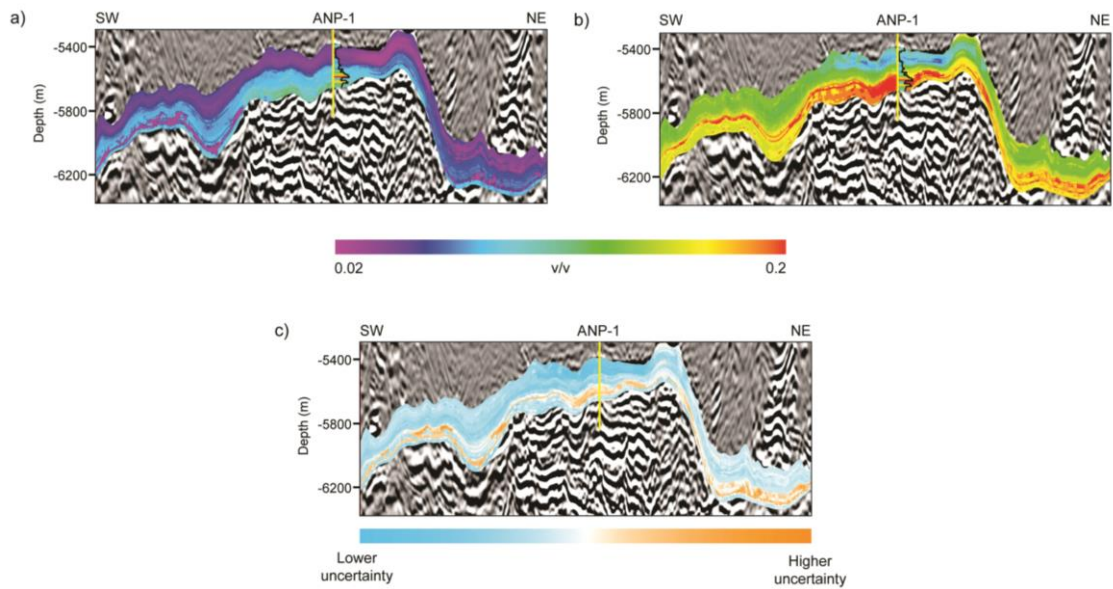


Figure 39: Illustrations at the arbitrary section 2 (AB2) for effective porosity P10 (a) and P90 (b) conditional distributions and uncertainty (c). Blind test ANP-1 well is represented by the yellow line, and its associated upscaled effective porosity well log is illustrated on the right side of the well trajectory.

4.4. Conclusions

We proposed a methodology using an EMBER algorithm for modeling of effective porosity and permeability using secondary variables within the Barra Velha Formation across Buzios Field. Effective porosity modeling results could only be associated at some locations with secondary variables used for the effective porosity simulation. However, a linear correlation between primary and secondary variables is not a requirement for the adopted methodology. Since the permeability simulation result was

generated using the effective porosity result as a secondary variable in the EMBER algorithm, they consequently have a high linear correlation and behave with the same patterns throughout Buzios Field.

Average effective porosity and permeability were 0.10 v/v and 440 md, respectively, indicating good reservoir quality within Barra Velha Formation. Also, they presented a vertical and general trend of a basal section with high effective porosities and permeabilities, an intermediate section with lower reservoir properties, and again an upper section of higher reservoir properties. The lower section of the formation presented more continuity and could be inferred as its best reservoir interval.

Two horizontal trends for effective porosity and permeability were observed at the base of salt surface, which represents the Barra Velha Formation top. One trend of higher values was aligned to the north-south direction and correlated to buildup seismic patterns at fault borders associated with spherulitites and shrubby carbonates from the facies model. And another trend of lower reservoir properties related to isolated structural lows within structural highs possibly associated to the occurrence of finer deposits, as suggested by the facies model.

High linear correlation between the simulation results for effective porosity and permeability and the upscaled well logs for the blind test well ANP-1 proved the predictive capacity of the used algorithm. Also, the upscaled well log distributions were generally preserved for both properties modeling results. Finally, conditional distributions analysis indicated that the basal section of the Barra Velha Formation presents higher uncertainty for the estimation of effective porosity; therefore, even though this interval is considered to have the best reservoir characteristics, decision making should be done with caution for this section.

6. Final Consideration

The proposed and applied advanced 3D reservoir characterization workflows and innovative algorithms in this thesis were able to provide important discussions regarding the geology of the Barra Velha Formation within the area of the Buzios Field. Those insights provided a better understanding regarding the origin and possible controls for the deposition of the Aptian presalt reservoirs for the Santos Basin and its impacts on their petrophysical characteristics and, consequently, reservoir quality.

Our results showed that the Barra Velha Formation throughout Buzios Field area presents mostly carbonate build-ups, aggradational/progradational carbonate platforms, and debris seismic facies. Those facies can be associated with a range of lithological facies and their respective sediments such as shrubby carbonates, spherulites, laminites, and reworked facies. The in-situ carbonate facies are located mostly at the structural highs and can be linked in occurrence usually with the carbonate platforms and build-up seismic facies. These can be considered the best quality reservoirs in the field for the studied interval and have effective porosities that range from 0.2 to 0.20 v/v and permeabilities that range from 0.01 to 10000 mD with average effective porosity of 0.10 v/v and average permeability of 440 mD. Such good reservoir characteristics can clearly explain why this field is so important in the Brazilian oil and gas scenario and, consequently corroborate to the relevance of the presalt reservoirs.

3D reservoirs characterization approaches were used for the papers published in journals and presented in this thesis. The first technique was based on the integrated application of 4D sedimentary modeling with geostatistical modeling methodology for facies reconstruction. One of the advantages of this integrated workflow is the capacity to create an individual conceptual geological model for each desired modeled area considering that the algorithm works as a digital sedimentary laboratory. It also allows the conceptualization of several different probable scenarios for the sedimentation processes and, consequently, expected lithological distributions considering paleotopography, base-level variations, tectonic activity, and, for carbonate rocks, even the carbonate factory production independently of biological, chemical, or mixed origin.

The main disadvantage of this method is in the high quantity of parameters to be adjusted for 4D sedimentary modeling which can allow the imagination of the geomodeler to go further than viable geological values for these parameters. Besides that,

the high quantity of parameters also makes it difficult to properly match the conceptual sedimentological results with facies data from wells, since the algorithm still cannot parametrize, itself considering real data from wells.

The second applied methodology was based on unsupervised seismic facies classification using neural networks algorithm and further qualitative inference of porosity and permeability associating seismic classification facies results with well data. One of the biggest advantages of this methodology is the quickness of its application and parametrization considering that it is only necessary to define the number of clusters to be classified from input data. This fact allows the interpreter to have a robust yet fast perspective of existing seismic facies in the study area and make a quick qualitative analysis regarding reservoir geology and properties.

The advantages of this machine learning methodology can also be considered its disadvantages by the detailed 3D reservoir characterization perspective, since the technique has its vertical resolution limited by seismic attribute resolution and, consequently, due to the known incompatibility between seismic data and well data its results can only provide means to infer about the petrophysical characteristics of the reservoir.

The methodology applied in the third paper presented in this thesis uses a machine learning algorithm that was built using geostatistical concepts to address the reservoir properties. From a practical perspective, the advantage of this methodology is undoubtedly its parametrization simplicity, accuracy, and quickness for the generation of multiple equiprobable stochastic results when compared to conventional geostatistical methodologies. Besides that, the possibility to use limitless secondary variables as inputs without the need of a previous combination amongst them, a known limitation from classical geostatistical algorithms, is very satisfactory.

The parametrization simplicity can be insufficient in some aspects since it does not allow the geomodeler to establish clearly and objectively the spatial correlation between the primary variable with each of the secondary variables, for example, by determination of weights per secondary variables.

In other words, all the technologies in this thesis can be applied to successfully characterize complex reservoirs such as the Brazilian presalt Aptian carbonates. However, the geomodeler and interpreter using them should consider their respective

advantages and limitations depending on the level of detail desired for the 3D reservoir model. This fact is intrinsically related to the time available for its construction and pertinent accuracy.

For the future of those 3D reservoir characterization methodologies in complex reservoirs, it would be interesting to develop a simpler parameterization approach for the geological process modeling. Possibly, machine learning algorithms could be a way to derive directly from well data the sedimentation rates and base level curves. This could dramatically decrease the level of uncertainty of the results which are based mostly on conceptual paleoenvironmental parametrization and increase the possibility of results matching well data better.

Regarding machine learning techniques, it is difficult to infer future developments considering the potential of the algorithms for automatizing processes and operations and its vast range of applicability in the oil and gas industry. However, recommendations for short-term developments in the unsupervised classification machine learning technologies could aim to diminish the limitations regarding vertical resolution, usually correlated to the input data of seismic origin. The automatized incorporation of filters that can help increase seismic data resolution can be a possible solution. Also, it can be expected the development of robust algorithms that can not only classify seismic facies but be used for automatized seismic horizon or fault interpretation which would help make the 3D reservoir characterization process a lot easier.

As for the algorithms using supervised machine learning for estimation of reservoir properties, much can be improved to incorporate more geomodeler oversight on the geological controls over the properties to be modeled. Also, it would be interesting to see those methods being available not only for the modeling of continuous reservoir properties, such as porosity and permeability, but also for discrete reservoir properties such as lithological facies.

Indeed, there is a whole world that can be expected in the next few years regarding the improvement of existing advanced 3D reservoir characterization techniques and the conceptualization and creation of new ones. The scenario for the future of this study area is expected to change rapidly and especially pushed by machine learning. This is the beauty of working with 3D geological modeling since all modeling processes are attempts to reproduce the factual geology and as such, they are always uncertain to some extent.

Uncertainty represents a range of possibilities and possibility is what drives constant evolution.

7. References

- Acevedo, A., A. Khramtsov, H. Madhoo, and D. Tetzlaff, 2016, Parameter Estimation and Sensitivity Analysis in Clastic Sedimentation Modeling, *in* N. J. Raju, ed., Geostatistical and Geospatial Approaches for the Characterization of Natural Resources in the Environment: Cham, Springer International Publishing, p. 89–93, doi:10.1007/978-3-319-18663-4.
- Alonso-Zarza, A. M., and L. H. Tanner (eds.), 2010, Carbonates in Continental Settings: Facies, Environments, and Processes: Amsterdam, Elsevier, 381 p.
- ANP, 2021, Boletim da Produção de Petróleo e Gás Natural: Rio de Janeiro, 40 p.
- ANP, 2016, Plano de Desenvolvimento do Campo de Buzios: Rio de Janeiro, 3 p.
- Ariza Ferreira, D. J., R. M. Dias, and W. M. Lupinacci, 2021, Seismic pattern classification integrated with permeability-porosity evaluation for reservoir characterization of presalt carbonates in the Buzios Field, Brazil: *Journal of Petroleum Science and Engineering*, v. 201, p. 108441, doi:10.1016/j.petrol.2021.108441.
- Azerêdo, A. C., L. V Duarte, R. Baptista, S. G. Vieira, and M. Olho-azul, 2011, Microbialites from Rift and Sag systems : new insights into terminological and classification issues ?, *in* Geophysical Research Abstracts: European Geosciences Union, p. 7473.
- Azevedo, L., and A. Soares, 2017, Geostatistical Methods for Reservoir Geophysics: Cham, Springer International Publishing, Advances in Oil and Gas Exploration & Production, 159 p., doi:10.1007/978-3-319-53201-1.
- Barclay, F., K. B. Rasmussen, A. Cooke, D. Cooke, D. Salter, D. Lowden, S. Pickering, A. Rasmussen, and R. Roberts, 2008, Seismic Inversion : Reading Between the Lines: *Oilfield Review*, p. 42–63.
- Berra, F., A. Lanfranchi, P. L. Smart, F. F. Whitaker, and P. Ronchi, 2016, Forward modelling of carbonate platforms: Sedimentological and diagenetic constraints from an application to a flat-topped greenhouse platform (Triassic, Southern Alps, Italy): *Marine and Petroleum Geology*, v. 78, p. 636–655, doi:10.1016/j.marpetgeo.2016.10.011.

- Beucher, H., and D. Renard, 2016, Truncated Gaussian and derived methods: *Comptes Rendus Geoscience*, v. 348, no. 7, p. 510–519, doi:10.1016/j.crte.2015.10.004.
- Borgomano, J., C. Lanteaume, P. Léonide, F. Fournier, L. F. Montaggioni, and J.-P. Masse, 2020, Quantitative carbonate sequence stratigraphy: Insights from stratigraphic forward models: *AAPG Bulletin*, v. 104, no. 5, p. 1115–1142, doi:10.1306/11111917396.
- Boyd, A., A. Souza, G. Carneiro, V. Machado, W. Trevizan, B. Coutinho, P. Netto, R. Azeredo, R. Polinski, and A. Bertolini, 2015, Presalt Carbonate Evaluation for Santos Basin, Offshore Brazil: *PETROPHYSICS*, v. 56, no. 6, p. 577.
- Bruhn, C. H. L., A. C. C. Pinto, P. R. S. Johann, C. C. M. Branco, M. C. Salomão, and E. B. Freire, 2017, Campos and Santos Basins: 40 Years of Reservoir Characterization and Management of Shallow- to Ultra-Deep Water, Post- and Pre-Salt Reservoirs - Historical Overview and Future Challenges, *in OTC Brasil: Offshore Technology Conference*, doi:10.4043/28159-MS.
- Buckley, J. P., D. Bosence, and C. Elders, 2015, Tectonic setting and stratigraphic architecture of an Early Cretaceous lacustrine carbonate platform, Sugar Loaf High, Santos Basin, Brazil: *Geological Society, London, Special Publications*, v. 418, no. 1, p. 175–191, doi:10.1144/SP418.13.
- Burgess, P. M., 2006, The Signal and the Noise: Forward Modeling of Allocyclic and Autocyclic Processes Influencing Peritidal Carbonate Stacking Patterns: *Journal of Sedimentary Research*, v. 76, no. 7, p. 962–977, doi:10.2110/jsr.2006.084.
- Caers, J., 2005, *Petroleum Geostatistics: Richardson*, Society of Petroleum Engineers, 88 p.
- de Castro, T., and W. Lupinacci, 2019, Evaluation of fine-grains in pre-salt reservoirs, *in Proceedings of the 16th International Congress of the Brazilian Geophysical Society&Expogef: Brazilian Geophysical Society*, p. 1–6, doi:10.22564/16cisbgf2019.299.
- Cerling, T. E., 1994, Chemistry of closed basin lake waters: a comparison between African Rift Valley and some central North American rivers and lakes, *in E. H. Gierlowski-Kordesch, and K. Kelts, eds., The Global Geological Record of Lake Basins: Cambridge, Cambridge University Press*, p. 29–30.

- Chang, H. K., M. L. Assine, F. S. Correa, J. S. E. Tinen, A. C. Vidal, and L. E. Koike, 2008, Sistemas petroliferos e modelos de acumulacao de hidrocarbonetos na Bacia de Santos: *Revista Brasileira de Geociências*, v. 38, no. 2, p. 29–46, doi:OSTI ID: 21131501.
- Chidsey, T. C., M. D. Vanden Berg, and D. E. Eby, 2015, Petrography and characterization of microbial carbonates and associated facies from modern Great Salt Lake and Uinta Basin's Eocene Green River Formation in Utah, USA: Geological Society, London, Special Publications, v. 418, no. 1, p. 261–286, doi:10.1144/SP418.6.
- Contreras, J., R. Zühlke, S. Bowman, and T. Bechstädt, 2010, Seismic stratigraphy and subsidence analysis of the southern Brazilian margin (Campos, Santos and Pelotas basins): *Marine and Petroleum Geology*, v. 27, no. 9, p. 1952–1980, doi:10.1016/j.marpetgeo.2010.06.007.
- Council, T. C., and P. C. Bennett, 1993, Geochemistry of ikaite formation at Mono Lake, California: Implications for the origin of tufa mounds: *Geology*, v. 21, no. 11, p. 971, doi:10.1130/0091-7613(1993)021<0971:GOIFAM>2.3.CO;2.
- Daly, C., 2021, An Application of an Embedded Model Estimator to a Synthetic Nonstationary Reservoir Model With Multiple Secondary Variables: *Frontiers in Artificial Intelligence*, v. 4, doi:10.3389/frai.2021.624697.
- Daly, Colin, 2020, An embedded model estimator for non-stationary random functions using multiple secondary variables: arXiv.
- Daly, C., 2020, Tight Integration of Decision Forests into Geostatistical Modelling, *in* First EAGE Digitalization Conference and Exhibition: European Association of Geoscientists & Engineers, p. 1–5, doi:10.3997/2214-4609.202032095.
- Daly, C., M. Hardy, and K. McNamara, 2020, Leveraging Machine Learning for Enhanced Geostatistical Modelling of Reservoir Properties, *in* 82nd EAGE Annual Conference & Exhibition: European Association of Geoscientists & Engineers, p. 1–5, doi:10.3997/2214-4609.202011723.
- Daly, C., S. Quental, and D. Novak, 2010, A Faster, More Accurate Gaussian Simulation Introduction to Gaussian Random Function Simulation, *in* GeoCanada: p. 1–5.

- Dias, R. M., T. M. Castro, M. A. C. Santos, and W. M. Lupinacci, 2019, Understanding the relationship between acoustic impedance and porosity in the presalt of the Buzios Field, Santos Basin, *in* First EAGE Workshop on Pre-Salt Reservoir: from Exploration to Production: European Association of Geoscientists & Engineers, p. 1–5, doi:10.3997/2214-4609.201982009.
- Dorobek, S., L. Piccoli, B. Coffey, and A. Adams, 2012, Carbonate Rock-Forming Processes in the Pre-salt “Sag” Successions of Campos Basin, Offshore Brazil: Evidence for Seasonal, Dominantly Abiotic Carbonate Precipitation, Substrate Controls, and Broader Geologic Implications, *in* AAPG Hedberg Conference: American Association of Petroleum Geologists, p. 4–5.
- Du, K., and M. N. S. Swamy, 2014, *Neural Networks and Statistical Learning*: London, Springer London, 824 p., doi:10.1007/978-1-4471-5571-3.
- Durrett, R., 2019, *Probability: Theory and Examples*: Cambridge University Press, 490 p., doi:10.1017/9781108591034.
- Farias, F., P. Szatmari, A. Bahniuk, and A. B. França, 2019, Evaporitic carbonates in the pre-salt of Santos Basin – Genesis and tectonic implications: *Marine and Petroleum Geology*, v. 105, no. November 2018, p. 251–272, doi:10.1016/j.marpetgeo.2019.04.020.
- Ferreira, D. J. A., H. P. L. Dutra, T. M. de Castro, and W. M. Lupinacci, 2021, Geological process modeling and geostatistics for facies reconstruction of presalt carbonates: *Marine and Petroleum Geology*, v. 124, no. February 2021, p. 104828, doi:10.1016/j.marpetgeo.2020.104828.
- Ferreira, D. J. A., and W. M. Lupinacci, 2018, An approach for three-dimensional quantitative carbonate reservoir characterization in the Pampe field, Campos Basin, offshore Brazil: *AAPG Bulletin*, v. 102, no. 11, p. 2267–2282, doi:10.1306/04121817352.
- Ferreira, D. J. A., W. M. Lupinacci, T. M. de Castro, N. L. Casado, M. Alvarenga, Y. Bezerra, J. F. Caparica Junior, and M. Antonio Cetale Santos, 2019, Neural network unsupervised classification as an advanced presalt reservoir characterization technique: a Buzios Field case study, *in* 16th International Congress of the Brazilian Geophysical Society and EXPOGEF: Brazilian

Geophysical Society, p. 6.

- Ferreira, D., W. Lupinacci, T. de Castro, N. Casado, M. Alvarenga, Y. Bezerra, J. Junior, and M. A. Santos, 2019, Neural network unsupervised classification as an advanced presalt reservoir characterization technique - a Buzios Field case study, *in* Proceedings of the 16th International Congress of the Brazilian Geophysical Society & Expogef: Brazilian Geophysical Society, p. 1–6, doi:10.22564/16cisbgf2019.217.
- Ferreira, D. J. A., W. M. Lupinacci, I. de A. Neves, J. P. R. Zambrini, A. L. Ferrari, L. A. P. Gamboa, and M. Olho Azul, 2019, Unsupervised seismic facies classification applied to a presalt carbonate reservoir, Santos Basin, offshore Brazil: AAPG Bulletin, v. 103, no. 4, p. 997–1012, doi:10.1306/10261818055.
- Ferreira, D. J. A., G. M. B. de Oliveira, T. M. Castro, R. M. Dias, and W. M. Lupinacci, 2021, Geostatistics assisted by machine learning for reservoir property modeling: A case study in presalt carbonates of Buzios Field, Brazil: The Leading Edge, v. 40, no. 12, p. 876–885, doi:10.1190/tle40120876.1.
- Figueiredo, L. P. De, B. B. Rodrigues, M. Roisenberg, and D. Grana, 2019, Bayesian elastic facies inversion (BELFI) applied to Lula field, *in* First EAGE Workshop on Pre-Salt Reservoir: from Exploration to Production: European Association of Geoscientists & Engineers, p. 1–4, doi:10.3997/2214-4609.201903439.
- Fornero, S. A., G. M. Marins, J. T. Lobo, A. F. M. Freire, and E. F. de Lima, 2019, Characterization of subaerial volcanic facies using acoustic image logs: Lithofacies and log-facies of a lava-flow deposit in the Brazilian pre-salt, deepwater of Santos Basin: Marine and Petroleum Geology, v. 99, no. 6, p. 156–174, doi:10.1016/j.marpetgeo.2018.09.029.
- Fornero, S. A., G. M. Marins, J. T. Lobo, A. F. M. Freire, and E. F. De Lima, 2019, Characterization of subaerial volcanic facies using acoustic image logs: Lithofacies and log-facies of a lava-flow deposit in the Brazilian pre-salt, deepwater of Santos Basin: Marine and Petroleum Geology, v. 99, p. 156–174, doi:10.1016/j.marpetgeo.2018.09.029.
- Gierlowski-Kordesch, E. H., 2010, Lacustrine Carbonates, *in* A. M. Alonso-Zarza, and L. H. Tanner, eds., Carbonates in Continental Settings: Facies, Environments, and

- Processes: Amsterdam, Elsevier, p. 1–101, doi:10.1016/S0070-4571(09)06101-9.
- Gomes, J. P., R. B. Bunevich, L. R. Tedeschi, M. E. Tucker, and F. F. Whitaker, 2020, Facies classification and patterns of lacustrine carbonate deposition of the Barra Velha Formation, Santos Basin, Brazilian Pre-salt: *Marine and Petroleum Geology*, v. 113, no. September 2019, p. 104176, doi:10.1016/j.marpetgeo.2019.104176.
- Gomes, P. O., B. Kilsdonk, J. Minken, T. Grow, and R. Barragan, 2008, The outer high of the Santos Basin, Southern São Paulo Plateau, Brazil: pre-salt exploration outbreak, paleogeographic setting, and evolution of the syn-rift structures, *in* AAPG International Conference and Exhibition: American Association of Petroleum Geologists, p. 26–29.
- Gomes, P. O., J. Parry, and W. Martins, 2002, The Outer High of the Santos Basin, Southern São Paulo Plateau, Brazil: Tectonic Setting, Relation to Volcanic Events and some Comments on Hydrocarbon Potential, *in* AAPG Hedberg Conference: American Association of Petroleum Geologists, p. 9.
- Guerra, J. N., 2016, Process Modelling of Carbonate Deposition , Miocene Northern and Southern Marion Platform: Imperial College London, 63 p.
- Hale, D., 2009, Structure-oriented smoothing and semblance: CWP Report, v. 635, p. 261–270.
- Haq, B. U., 2014, Cretaceous eustasy revisited: *Global and Planetary Change*, v. 113, p. 44–58, doi:10.1016/j.gloplacha.2013.12.007.
- Herlinger, R., E. E. Zambonato, and L. F. De Ros, 2017, Influence of Diagenesis On the Quality of Lower Cretaceous Pre-salt Lacustrine Carbonate Reservoirs from Northern Campos Basin, Offshore Brazil: *Journal of Sedimentary Research*, v. 87, no. 12, p. 1285–1313, doi:10.2110/jsr.2017.70.
- Hill, J., D. Tetzlaff, A. Curtis, and R. Wood, 2009, Modeling shallow marine carbonate depositional systems: *Computers & Geosciences*, v. 35, no. 9, p. 1862–1874, doi:10.1016/j.cageo.2008.12.006.
- Hirsche, K., S. Boerner, C. Kalkomey, and C. Gastaldi, 1998, Avoiding pitfalls in geostatistical reservoir characterization: A survival guide: *The Leading Edge*, v. 17, no. 4, p. 493–504, doi:10.1190/1.1437999.

- Hotelling, H., 1933, Analysis of a complex of statistical variables into principal components: *Journal of Educational Psychology*, v. 24, no. 6, p. 417–441, doi:10.1037/h0071325.
- Høye, T. H., R. Rouzairol, R. Basani, and E. W. M. Hansen, 2016, Sedimentary Process Modelling for Testing Depositional Hypothesis of the Peregrino Reservoir, Brazil, *in* Second Conference on Forward Modelling of Sedimentary Systems: European Association of Geoscientists & Engineers, p. 1–5, doi:10.3997/2214-4609.201600386.
- Huang, X., C. M. Griffiths, and J. Liu, 2015, Recent development in stratigraphic forward modelling and its application in petroleum exploration: *Australian Journal of Earth Sciences*, v. 62, no. 8, p. 903–919, doi:10.1080/08120099.2015.1125389.
- Huang, T., G. Yang, and G. Tang, 1979, A fast two-dimensional median filtering algorithm: *IEEE Transactions on Acoustics, Speech, and Signal Processing*, v. 27, no. 1, p. 13–18, doi:10.1109/TASSP.1979.1163188.
- Jesus, C., M. O. Azul, W. Lupinacci, and L. Machado, 2017, Mapping of carbonate mounds in the Brazilian presalt zone, *in* SEG Technical Program Expanded Abstracts 2017: Society of Exploration Geophysicists, p. 3298–3303, doi:10.1190/segam2017-17789870.1.
- Jesus, C., W. M. Lupinacci, P. Takayama, J. Almeida, and D. J. A. Ferreira, 2020, An approach to reduce exploration risk using spectral decomposition, prestack inversion, and seismic facies classification: *AAPG Bulletin*, v. 104, no. 5, p. 1075–1090, doi:10.1306/10161918065.
- Jesus, C., M. Olho Azul, W. M. Lupinacci, and L. Machado, 2019, Multiattribute framework analysis for the identification of carbonate mounds in the Brazilian presalt zone: *Interpretation*, v. 7, no. 2, p. T467–T476, doi:10.1190/INT-2018-0004.1.
- Johann, P., 2013, Challenges in Brazilian Pre-Salt Reservoirs Geophysical Characterization: doi:10.3997/2214-4609.20131228.
- Johann, P. R., A. F. Martini, A. Maul, and J. P. P. Nunes, 2012, Reservoir Geophysics in Brazilian Pre-Salt Oilfields, *in* Offshore Technology Conference: Offshore Technology Conference, p. 1–10, doi:10.4043/23681-MS.

- Kattah, S., and Y. Balabekov, 2015, Seismic facies/geometries of the pre-salt limestone units and newly-identified exploration trends within the Santos and Campos basins, Brazil, *in* 14th International Congress of the Brazilian Geophysical Society & EXPOGEF: Brazilian Geophysical Society, p. 288–293, doi:10.1190/sbgf2015-057.
- Lafferty, J., A. McCallum, and F. C. N. Pereira, 2001, Conditional Random Fields: Probabilistic Models for Segmenting and Labeling Sequence Data, *in* 18th International Conference on Machine Learning 2001: p. 282–289, doi:10.29122/mipi.v11i1.2792.
- Lanteaume, C., F. Fournier, M. Pellerin, and J. Borgomano, 2018, Testing geologic assumptions and scenarios in carbonate exploration: Insights from integrated stratigraphic, diagenetic, and seismic forward modeling: *The Leading Edge*, v. 37, no. 9, p. 672–680, doi:10.1190/tle37090672.1.
- Lantuéjoul, C., 2002, *Geostatistical Simulation*: Berlin, Heidelberg, Springer Berlin Heidelberg, 232 p., doi:10.1007/978-3-662-04808-5.
- Liechoscki de Paula Faria, D., A. Tadeu dos Reis, and O. Gomes de Souza, 2017, Three-dimensional stratigraphic-sedimentological forward modeling of an Aptian carbonate reservoir deposited during the sag stage in the Santos basin, Brazil: *Marine and Petroleum Geology*, v. 88, p. 676–695, doi:10.1016/j.marpetgeo.2017.09.013.
- Logan, B. W., G. R. Davies, J. F. Read, and D. E. Cebulski, 1970, *Carbonate Sedimentation and Environments, Shark Bay, Western Australia*: American Association of Petroleum Geologists, doi:10.1306/M13369.
- Lupinacci, W. M., L. de M. S. Gomes, D. J. A. Ferreira, R. Bijani, and A. F. M. Freire, 2020, An integrated approach for carbonate reservoir characterization: a case study from the Linguado Field, Campos Basin: *Brazilian Journal of Geology*, v. 50, no. 4, doi:10.1590/2317-4889202020190103.
- Lupinacci, W. M., R. P. C. Viana, D. J. A. Ferreira, I. de A. Neves, J. P. R. Zambrini, M. O. Azul, A. L. Ferrari, and L. A. P. Gamboa, 2019, IMPACTS OF HALOKYNESES IN SEISMIC INTERPRETATION AND GENERATION OF THE TOP SALT SURFACE IN A DISTAL PORTION OF THE SANTOS

BASIN: Brazilian Journal of Geophysics, v. 37, no. 2,
doi:10.22564/rbgf.v37i2.1997.

Madhoo, H. A., A. Acevedo, D. Tetzlaff, and J. Tveiten, 2016, Combining Forward Stratigraphic Modelling with Seismic Reconstruction to Improve Reservoir Characterization, *in* ACM SIGCOMM Computer Communication Review: p. 521–522, doi:10.3997/2214-4609.201600382.

McCulloch, W. S., and W. Pitts, 1943, A logical calculus of the ideas immanent in nervous activity: *The Bulletin of Mathematical Biophysics*, v. 5, no. 4, p. 115–133, doi:10.1007/BF02478259.

Mercedes-Martín, R., A. T. Brasier, M. Rogerson, J. J. G. Reijmer, H. Vonhof, and M. Pedley, 2017, A depositional model for spherulitic carbonates associated with alkaline, volcanic lakes: *Marine and Petroleum Geology*, v. 86, p. 168–191, doi:10.1016/j.marpetgeo.2017.05.032.

Merriam, D. F., and J. C. Davis (eds.), 2001, *Geologic Modeling and Simulation*: Boston, MA, Springer US, Computer Applications in the Earth Sciences, doi:10.1007/978-1-4615-1359-9.

Moreira, J. L. P., C. V. Madeira, J. A. Gil, and M. A. P. Pinheiro, 2007, Bacia de Santos: *Boletim de Geociencias da Petrobras*, v. 15, no. 2, p. 531–549.

Muniz, M. C., and D. W. J. Bosence, 2015, Pre-salt microbialites from the Campos Basin (offshore Brazil): image log facies, facies model and cyclicity in lacustrine carbonates: *Geological Society, London, Special Publications*, v. 418, no. 1, p. 221–242, doi:10.1144/SP418.10.

Neves, I. de A., W. M. Lupinacci, D. J. A. Ferreira, J. P. R. Zambrini, L. O. A. Oliveira, M. Olho Azul, A. L. Ferrari, and L. A. P. Gamboa, 2019a, Presalt reservoirs of the Santos Basin: Cyclicity, electrofacies, and tectonic-sedimentary evolution: *Interpretation*, v. 7, no. 4, p. SH33–SH43, doi:10.1190/INT-2018-0237.1.

Neves, I. de A., W. M. Lupinacci, D. J. A. Ferreira, J. P. R. Zambrini, L. O. A. Oliveira, M. Olho Azul, A. L. Ferrari, and L. A. P. Gamboa, 2019b, Presalt reservoirs of the Santos Basin: Cyclicity, electrofacies, and tectonic-sedimentary evolution: *Interpretation*, v. 7, no. 4, p. SH33–SH43, doi:10.1190/INT-2018-0237.1.

- Peçanha, A. A., W. M. Lupinacci, D. J. A. Ferreira, and A. F. M. Freire, 2019, A workflow for reservoir characterization applied to presalt coquinas from the Linguado Field, Campos Basin, Brazil: *Journal of Petroleum Science and Engineering*, v. 183, p. 106451, doi:10.1016/j.petrol.2019.106451.
- Penna, R., S. Araújo, A. Geisslinger, R. Sansonowski, L. Oliveira, J. Rosseto, and M. Matos, 2019, Carbonate and igneous rock characterization through reprocessing, FWI imaging, and elastic inversion of a legacy seismic data set in Brazilian presalt province: *The Leading Edge*, v. 38, no. 1, p. 11–19, doi:10.1190/tle38010011.1.
- Penna, R., and W. M. Lupinacci, 2020, Decameter-Scale Flow-Unit Classification in Brazilian Presalt Carbonates: *SPE Reservoir Evaluation & Engineering*, v. 23, no. 04, p. 1420–1439, doi:10.2118/201235-PA.
- Penna, R., and W. Moreira Lupinacci, 2021, 3D modelling of flow units and petrophysical properties in brazilian presalt carbonate: *Marine and Petroleum Geology*, v. 124, p. 104829, doi:10.1016/j.marpetgeo.2020.104829.
- Pereira, L. A., 2009, *Seismic Attributes in Hydrocarbon Reservoirs Characterization*: Universidade de Aveiro, 183 p.
- Pereira, A. D. F., E. C. Dos Santos, E. P. Silva, K. D. S. Leite, J. De Tritlla, H. F. Ayres, and J. De Machin, 2013, Santos Microbial Carbonate Reservoirs: A Challenge, *in* OTC Brasil: Offshore Technology Conference, p. 1–3, doi:10.4043/24446-MS.
- Della Porta, G., 2015a, Carbonate build-ups in lacustrine, hydrothermal and fluvial settings: comparing depositional geometry, fabric types and geochemical signature: Geological Society, London, Special Publications, v. 418, no. 1, p. 17–68, doi:10.1144/SP418.4.
- Della Porta, G., 2015b, Carbonate build-ups in lacustrine, hydrothermal and fluvial settings: comparing depositional geometry, fabric types and geochemical signature: Geological Society, London, Special Publications, v. 418, no. 1, p. 17–68, doi:10.1144/SP418.4.
- Pozo, M., and J. Calvo, 2018, An Overview of Authigenic Magnesian Clays: *Minerals*, v. 8, no. 11, p. 520, doi:10.3390/min8110520.
- Pyrzcz, M. J., and C. V. Deutsch (eds.), 2014, *Geostatistical Reservoir Modeling*: New

York, Oxford University Press, 448 p.

- Randen, T., E. Monsen, C. Signer, A. Abrahamsen, J. O. Hansen, T. Sæter, and J. Schlaf, 2000, Three-dimensional texture attributes for seismic data analysis, *in* SEG Technical Program Expanded Abstracts 2000: Society of Exploration Geophysicists, p. 668–671, doi:10.1190/1.1816155.
- Randen, T., and L. Sønneland, 2005, Atlas of 3D Seismic Attributes: p. 23–46, doi:10.1007/3-540-26493-0_2.
- Rezende, M. F., and M. C. Pope, 2015, Importance of depositional texture in pore characterization of subsalt microbialite carbonates, offshore Brazil: Geological Society, London, Special Publications, v. 418, no. 1, p. 193–207, doi:10.1144/SP418.2.
- Riccomini, C., L. G. Sant’Anna, and C. C. G. Tassinari, 2012, Pré-sal: geologia e exploração: Revista USP, v. 0, no. 95, p. 33, doi:10.11606/issn.2316-9036.v0i95p33-42.
- Rogerson, M. et al., 2017, Are spherulitic lacustrine carbonates an expression of large-scale mineral carbonation? A case study from the East Kirkton Limestone, Scotland: Gondwana Research, v. 48, p. 101–109, doi:10.1016/j.gr.2017.04.007.
- Russell, B., and D. Hampson, 1991, Comparison of poststack seismic inversion methods, *in* SEG Technical Program Expanded Abstracts 1991: Society of Exploration Geophysicists, p. 876–878, doi:10.1190/1.1888870.
- Russell, B., and D. Hampson, 2006, The old and the new in seismic inversion: Canadian Society of Exploration Geophysics Recorder, v. 31, no. 10, p. 5–10.
- Russell, S. J., and P. Norvig (eds.), 2010, Artificial Intelligence: A Modern Approach: New Jersey, Pearson, 1095 p.
- Sabato Ceraldi, T., and D. Green, 2016, Evolution of the South Atlantic lacustrine deposits in response to Early Cretaceous rifting, subsidence and lake hydrology: Petroleum Geoscience of the West Africa Margin, v. 438, no. 2012, p. 22pp, doi:10.1144/SP438.10.
- Saller, A., S. Rushton, L. Buambua, K. Inman, R. McNeil, and J. A. D. (Tony) Dickson, 2016, Presalt stratigraphy and depositional systems in the Kwanza Basin, offshore

- Angola: AAPG Bulletin, v. 100, no. 07, p. 1135–1164, doi:10.1306/02111615216.
- Sancevero, S. S., A. Z. Remacre, and R. de S. Portugal, 2006, O papel da inversão para a impedância acústica no processo de caracterização sísmica de reservatórios: Revista Brasileira de Geofísica, v. 24, no. 4, p. 495–512, doi:10.1590/S0102-261X2006000400004.
- Sarma, D. D., 2009, Geostatistics with Applications in Earth Sciences: Dordrecht, Springer Netherlands, 1–205 p., doi:10.1007/978-1-4020-9380-7.
- Szatmari, P., and E. J. Milani, 2016, Tectonic control of the oil-rich large igneous-carbonate-salt province of the South Atlantic rift: Marine and Petroleum Geology, v. 77, p. 567–596, doi:10.1016/j.marpetgeo.2016.06.004.
- Taner, M. T., F. Koehler, and R. E. Sheriff, 1979, Complex seismic trace analysis: Geophysics, v. 44, no. 6, p. 1041–1063, doi:10.1190/1.1440994.
- Terra, J. G. S. et al., 2010, Classificações Clássicas De Rochas Carbonáticas: Boletim de Geociencias da Petrobras, v. 18, no. 1, p. 9–29.
- Tetzlaff, D. M., 1987, A simulation model of clastic sedimentary processes: Stanford University, 345 p.
- Tetzlaff, D., and G. Priddy, 2001, Sedimentary Process Modeling: From Academia to Industry, in D. F. Merriam, and J. C. Davis, eds., Geologic Modeling and Simulation: Springer US, p. 45–69, doi:10.1007/978-1-4615-1359-9_4.
- Tetzlaff, D. M., and M.-T. Schafmeister, 2007, Interaction among sedimentation, compaction, and groundwater flow in coastal settings, in Coastline Changes: Interrelation of Climate and Geological Processes: Geological Society of America, p. 65–87, doi:10.1130/2007.2426(05).
- Tetzlaff, D. M., J. Tveiten, P. Salomonsen, A. Christ, and W. Athmer, 2014, Geologic process modeling, in IX Congreso De Exploración Y Desarrollo De Hidrocarburos: Instituto Argentino del Petroleo y del Gas, p. 155–174.
- Whitaker, F., and M. Frazer, 2018, Process-based Modelling of Syn-depositional Diagenesis, in Reactive Transport Modeling: Chichester, UK, John Wiley & Sons, Ltd, p. 107–155, doi:10.1002/9781119060031.ch3.

- Wright, V. P., 2012, Lacustrine carbonates in rift settings: the interaction of volcanic and microbial processes on carbonate deposition: Geological Society, London, Special Publications, v. 370, no. 1, p. 39–47, doi:10.1144/SP370.2.
- Wright, V. P., and A. J. Barnett, 2015, An abiotic model for the development of textures in some South Atlantic early Cretaceous lacustrine carbonates: Geological Society, London, Special Publications, v. 418, no. 1, p. 209–219, doi:10.1144/SP418.3.
- Wright, V. P., and A. Barnett, 2017, Classifying Reservoir Carbonates When the Status Quo Simply Does Not Work : A Case Study from the Cretaceous of the South Atlantic, *in* AAPG Annual Conference and Exhibition: American Association of Petroleum Geologists, p. 108–121.
- Wright, V. P., and A. Barnett, 2017, Critically Evaluating the Current Depositional Models for the Pre-Salt Barra Velha Formation , Offshore Brazil *, *in* AAPG Annual Conference and Exhibition: Search and Discovery, p. 1–40.
- Wright, V. P., and A. J. Barnett, 2020, The textural evolution and ghost matrices of the Cretaceous Barra Velha Formation carbonates from the Santos Basin, offshore Brazil: *Facies*, v. 66, no. 1, p. 7, doi:10.1007/s10347-019-0591-2.
- Wright, V. P., and N. Tosca, 2016, A Geochemical Model for the Formation of the Pre-Salt Reservoirs , Santos Basin, Brazil : Implications for Understanding Reservoir Distribution, *in* AAPG Annual Convention and Exhibition: American Association of Petroleum Geologists, p. 32.
- Zalán, P., K. Rodriguez, and M. Cvetkovic, 2019, Extraordinary Remaining Potential in the Pre-Salt of Santos Basin, *in* Proceedings of the 16th International Congress of the Brazilian Geophysical Society&Expogef: Brazilian Geophysical Society, p. 1–8, doi:10.22564/16cisbgf2019.128.
- Zhao, T., V. Jayaram, A. Roy, and K. J. Marfurt, 2015, A comparison of classification techniques for seismic facies recognition: *Interpretation*, v. 3, no. 4, p. SAE29–SAE58, doi:10.1190/INT-2015-0044.1.
- Ziegel, E. R., C. V. Deutsch, and A. G. Journel, 1998, Geostatistical Software Library and User's Guide: *Technometrics*, v. 40, no. 4, p. 357, doi:10.2307/1270548.